WEARABLE ANTENNA DESIGN FOR MICROPOWER GENERATION

M.Sc. Thesis by
Cem ÖZLEM

Department : **Electronics and Communication Engineering**

Programme : **Telecommunication Engineering**

Thesis Supervisors: Prof. Dr. Alessandra COSTANZO
Prof. Dr. İbrahim AKDUMAN

JUNE 2009

İSTANBUL TECHNICAL UNIVERSITY ★ INSTITUTE OF SCIENCE AND TECHNOLOGY

WEARABLE ANTENNA DESIGN FOR MICROPOWER GENERATION

M.Sc. Thesis by
Cem ÖZLEM
(504071304)

Date of submission :	**04 May 2009**
Date of defence examination:	**04 June 2009**

Supervisor (Chairman) :	**Prof. Dr. İbrahim AKDUMAN (ITU)**
Members of the Examining Committee :	**Assoc. Prof. Dr. Ali YAPAR (ITU)**
	Assis. Prof. Dr. Lale TÜKENMEZ ERGENE (ITU)

JUNE 2009

İSTANBUL TEKNİK ÜNİVERSİTESİ ★ FEN BİLİMLERİ ENSTİTÜSÜ

ÇOK DÜŞÜK SEVİYELERDEKİ GÜÇ ÜRETİMİ İÇİN GİYİLEBİLİR ANTEN TASARIMI

YÜKSEK LİSANS TEZİ
Cem ÖZLEM
(504071304)

Tezin Enstitüye Verildiği Tarih :   04 Mayıs 2009
Tezin Savunulduğu Tarih :   04 Haziran 2009

Tez Danışmanı :   Prof. Dr. İbrahim AKDUMAN (İTÜ)
Diğer Jüri Üyeleri :   Doç. Dr. Ali YAPAR (İTÜ)
Yrd. Doç. Dr. Lale TÜKENMEZ ERGENE (İTÜ)

HAZİRAN 2009

FOREWORD

First and foremost, I would like to express my appreciation to all people that supported and helped me with my Masters Thesis.

May 2009   Cem Özlem

                                                   Telecommunication Engineering

TABLE OF CONTENTS

ABBREVIATIONS

AC	**:**	Alternating Current
ACMSA	**:**	Aperture Coupled Microstrip Antenna
BW	**:**	Bandwidth
CMOS	**:**	Complementary Metal Oxide Semiconductor
CP	**:**	Circular Polarization
DC	**:**	Direct Current
GHz	**:**	Gigahertz
GSM	**:**	Global System for Mobile Communications
IC	**:**	Integrated Circuit
ISM	**:**	Industrial, Scientific and Medical
LAN	**:**	Local Area Network
LHCP	**:**	Left Hand Circular Polarization
MHz	**:**	Megahertz
OFDM	**:**	Orthogonal Frequency Division Multiplex
PCS	**:**	Personal Communication Service
RF	**:**	Radio Frequency
RFID	**:**	Radio Frequency Identification
RHCP	**:**	Right Hand Circular Polarization
VSWR	**:**	Voltage Standing Wave Ratio

x

LIST OF TABLES

LIST OF FIGURES

WEARABLE ANTENNA DESIGN FOR MICROPOWER GENERATION

SUMMARY

Electronic devices such as cell phone, Wi-Fi hardware and radio-TV receiver and transmitters, which are frequently used, and have an important part in daily life, continuously emit electromagnetic energy. Even though the power of this energy is low, it can open a door to us to charge our mobile devices such as cell phones or iPods without any need for a cable. It would be a pity to restrict the use of this application with storing energy for cell phones and iPods. The concept of supplying energy for electronic devices without cables or batteries may be applied to many areas to be used as supportive devices.

In order to convert the electromagnetic energy in the environment to electrical energy, a proper antenna and a rectifier are needed. Since the application does not include particular information about the direction or the amount of the incoming signal, the antenna-rectifier system should be designed very carefully. Considering this, the antenna was designed to be a circularly polarized microstrip antenna with multi-resonance, including GSM 900, GSM 1800 and W-LAN bands, in which the electromagnetic energy is intensively found in the environment. For the rectifier circuit which is supposed to convert the sinusoidal signal collected by the antenna into direct current, Schottky diode, whose threshold voltage is lower than the others, was preferred. The rectifier circuit, which consists of capacitors and Schottky diodes, was chosen as simple as possible in order to minimize the loss occurring in the circuit elements.

At the next step of the application, in order the antenna to be carried comfortably on human body, it was redesigned using wearable, flexible, conducting and dielectric fabric. It may seem awkward to imagine an antenna to be placed or integrated on a dress as if it is an ordinary piece of cloth, but the studies on wearable conducting and dielectric fabric in the last a few years let us know that electronic devices can be carried on human body as comfortable as any normal fabric, without restricting the mobility of the user. The flexible fabric also allows us to place it anywhere such as arms or legs. Bending the antenna with an angle obviously changes the parameters of the antenna. Therefore, the measurements should be carried out very sensitively and carefully. The effect of human tissue to the antenna characteristics should be also considered. In this study, researching the kinds of wearable fabric, different alternatives were discussed. The simulations were carried out for two different kinds of fabric. The antenna was bent considering the rib cage profile, and the effects of the human body to the antenna parameters were investigated.

ÇOK DÜŞÜK SEVİYELERDEKİ GÜÇ ÜRETİMİ İÇİN GİYİLEBİLİR ANTEN TASARIMI

ÖZET

Günlük hayatta büyük bir önemi olan ve sıkça kullanılan elektronik aletler, örneğin; cep telefonu, Wi-Fi donanımlar ve radyo-televizyon alıcı vericileri, ortama devamlı olarak elektromanyetik enerji yaymaktadırlar. Bu enerji her ne kadar çok düşük miktarlarda olsa da, bize kullanılabilir enerji adı altında, cep telefonu ya da ipod gibi taşınabilir aletlerimizi, pil ya da kabloya ihtiyaç duymadan şarj etmemize olanak verebilir. Bu uygulamayı sadece cep telefonu ve ipod için enerji depolamakla kısıtlamak acımasızlık olur. Elektronik aygıtlara kablosuz ve pilsiz enerji sağlama kavramı, ileride birçok alanda uygulama bularak, kişisel yardımcı cihazlar gibi kullanılabilir.

Ortamdaki elektromanyetik enerjiyi kullanılabilir elektrik enerjisine dönüştürmek için anten ve doğrultucu devreye ihtiyaç vardır. Uygulama, gelen sinyalin yönü ve miktarı hakkında belirli bir bilgi içermediğinden, anten ve doğrultucudan oluşan sistem çok dikkatli tasarlanmalıdır. Bu amaç doğrultusunda anten tasarımı ele alınırken; elektromanyetik enerjinin ortamda en yoğun bulunduğu GSM 900, GSM 1800 ve W-LAN bantlarını kapsayan, çok rezonanslı, dairesel polarizasyonlu mikroşerit anten tasarımı gerçekleştirildi. Antenin topladığı sinüzoidal sinyali doğru akıma çevirecek doğrultucu devre için, eşik değeri diğer diyotlara göre çok düşük, Schottky diyot tercih edildi. Kapasiteler ve Schottky diyotlardan oluşan doğrultucu devre, devre elemanlarında oluşan kayıpları en aza indirgemek için en basit şekilde seçildi.

Uygulamanın bir sonraki adımında, antenin kolayca insan vücudu üzerinde rahatsızlık vermeden taşınabilmesi için; anten, giyilebilir, esnek, iletken ve iletken olmayan kumaşlarla yeniden tasarlandı. Antenin herhangi bir kumaş gibi kıyafet üzerine konulması yada kıyafete entegre edilmesi kulağa tuhaf gelebilir, ancak son yıllarda, giyilebilir iletken ve iletken olmayan kumaşlar üzerinde yapılan yoğun çalışmalar, elektronik cihazların normal kumaş rahatlığında, kullanıcının hareket yeteneğini kısıtlamadan vücut üzerinde taşınmasına olanak vermektedir. Esnek kumaş aynı zamanda, antenin vücut üzerinde herhangi bir yere; kol veya bacak gibi, yerleştirilmesine de olanak sağlamaktadır. Antenin belirli bir açı ile bükülmesi, tabii ki anten parametrelerini değiştirmektedir. Bunun için çok dikkatli ve hassas ölçümler gerekmektedir. Aynı zamanda, insan dokusunun anten karakteristiğine etkisi de göz önüne alınmalıdır. Bu çalışmada, giyilebilir kumaşlar araştırılırken farklı seçenekler ele alındı. Ölçümler, iki farklı özellikte iki çeşit kumaş için yapıldı. Aynı zamanda anten, göğüs kafesi profili göz önüne alınarak büküldü ve insan vücudunun anten parametrelerine etkisi araştırıldı.

1. INTRODUCTION

The trends in technology allow the decrease in both size and power consumption of complex digital systems. This decrease in size and power gives rise to new models of computing and use of electronics, with many small devices working collaboratively or at least with strong communication capabilities. Examples of these new models are wearable devices and wireless sensor networks. Currently, these devices are powered by batteries. However, batteries present several disadvantages: the need to either replace or recharge them periodically and their big size and weight compared to high technology electronics. One possibility to overcome these power limitations is to extract (harvest) energy from the environment to either recharge a battery, or even to directly power the electronic device [1].

Energy is everywhere in the environment surrounding us — available in the form of thermal energy, light (solar) energy, wind energy, and mechanical energy. However, the energy from these sources is often found in such minute quantities that it cannot supply adequate power for any viable purpose. In fact, until recently, it has not been possible to capture such energy sufficiently to perform any useful work [2].

This scenario is about to change.

Energy harvesting (also known as power harvesting or energy scavenging) is the process by which ambient energy is captured from one or more of these naturally-occurring energy sources, converted into electricity and used to drive small autonomous electronic, electrical and combined devices or storing them for later use. When compared with the energy stored in ordinary storage elements, such as batteries and the like, the environment represents a fairly infinite source [2-5].

This thesis will focus on Radio Frequency (RF) energy harvesting, whose magnitude of the available energy is the least among all these energy sources. Figure 1.1 shows the approximate amount of energy per unit available from harvesting sources [6].

1

Energy Source	Harvested Power
Vibration/Motion	
Human	4 µW/cm²
Industry	100 µW/cm²
Temperature Difference	
Human	25 µW/cm²
Industry	1–10 mW/cm²
Light	
Indoor	10 µW/cm²
Outdoor	10 mW/cm²
RF	
GSM	0.1 µW/cm²
WiFi	0.001 mW/cm²

Figure 1.1: Energy harvesting estimates [6]

Most people do not realize that there is a plenty of energy all around us at all times. We are being exposed with energy waves every second of the day. Radio and television towers, satellites orbiting earth, and even the cellular phone antennas are continuously transmitting energy. What if there was a way we could harvest the energy that is being transmitted and employ it as a source of power? If it could be possible to collect the energy and store it, we could potentially use it to power other circuits. The first type of application of using wasted power is in cellular phone, this power could be used to recharge a battery that is constantly being depleted. The potential exists for cellular phones, and even more complicated devices - i.e. pocket organizers, person digital assistants (PDAs), and even notebook computers - to become completely wireless [7]. The second type of application in using harvesting power, which in some cases can also help decrease health hazards. For instance, the rooftops of buildings in city centers are often rented to a number of wireless suppliers and technical workers have reported healthiness problems when servicing a transmitter in the presence of other operating transmitters. In this location, a variety of output powers, frequencies, and polarizations are existing, and interference between a numbers of antennas in each other's near fields alters their radiation properties, accounting for more wasted power. This power can be received, rectified, and stored for further use [8]. An example of another employable application is wireless LAN (shortly WLAN) that links two or more computers or devices using modulation technology based to enable communication between devices in a limited area [9], where devices simultaneously connect each others by using radio frequencies. This indoor area where in plenty of RF energy can find is very convenient for harvesting applications. However, it is mentioned that use of existing

electromagnetic radiation, like the one generated by cell phones, radio transmitters, Wi-Fi equipment is in principle possible, but this solution is not viable except in specific locations. First the available energy density is low (typically µW/cm2), and second it is not always desirable, or even legally allowed, to block radiation (e.g. for emergency calls) [10].

In order to realize these applications, we need a concept named energy harvesting. The concept needs an efficient antenna along with a circuit capable of converting alternating-current (AC) voltage to direct-current (DC) voltage. The efficiency of an antenna is related to the shape and impedance of the antenna and the impedance of the circuit. If the two impedances are not matched then there is reflection of the power back into the antenna meaning that the circuit was unable to receive all the available power. Matching of the impedances means that the impedance of the antenna is the complex conjugate of the impedance of the circuit [7]. These antenna and AC-DC rectifier circuit characteristics will be discussed in detail further.

Another important aim of the thesis is to present the designed antenna as a part of garment (piece of clothing), in this way making it mobile. As we know the existing antennas can not operate effectively when they are used in the vicinity of a human body due to the reduction of impedance characteristics [11], but nevertheless the development of wearable intelligent textile systems offer very effective solutions. Wearable antennas (also known as textile antenna) presented by Locher [12] and Ouyang [13] are designed from the combination of the conductive threads and the non-conductive threads. Integration of an antenna into a garment can be achieved by making the antenna itself out of textile material. Textile antennas provide so many benefits with the availability of conductive textile materials, known as electro-textiles, which are conductive fabrics constructed by interpolating conductive metal/polymer threads with normal fabric threads or conductive threads, enables the manufacturing of textile antennas and makes them an unobtrusive part of the wearable textile system, and also these fabrics are considered a strong candidate to be integrated into clothing for distributed body-worn electronics because they are washable, durable and flexible [13,14]. Selection criteria for conductive fabrics and methods of creating will be explained in details further.

In this thesis, the whole system consists of an antenna to pick up the power present in the media, an impedance matching network to ensure the maximum power transfer in the system, and the rectifier circuit to convert the RF signal to a DC voltage.

The antenna design is critical in the RF-DC power conversion system since it must extract the power radiated by the radio waves. The antenna performs best when its impedance matched to the rectifier circuit at the operating frequency to reduce transmission losses [15]. Moreover, the antenna must have an area small enough to be put on clothing, and also a bandwidth large enough to cover the frequency bands of GSM, PCS and Wi-Fi protocols, which are the most intensive ones in the environment, therefore, which promise more available energy when captured.

A matched network between the antenna and the rectifier is necessary in order to fine-tune the impedance match between the antenna and the rectifier for further reduction of the transmission loss, and to increase the voltage gain [15].

Due to the low incident power densities between $10^{-5} - 10^{-1} mW/cm^2$, the rectifier circuit must be designed to reduce the threshold voltage (V_{th}) and the internal losses of the devices as much as possible, simply to improve the efficiency of the RF-DC power conversion system.

This thesis also presents textile antenna technology, which allows a wearable and a mobile antenna. For our purpose, the most convenient model of such is a microstrip antenna, with a microstrip feed line, for it yields many advantages such as lightweight and have a small volume and a low-profile planar configuration, can be made conformal to the host surface, their ease of mass production using printed-circuit technology leads to a low fabrication cost, they allow both linear and circular polarization, can be made compact for use in personal mobile communication, they allow for dual and triple frequency operations. Microstrip antennas suffer from some disadvantages as compared to conventional microwave antennas such as narrow bandwidth, and lower gain [16]. Increase the bandwidth can be achieved by a suitable choice of feeding technique and impedance matching network. In this thesis, 90° broadband balun which is presented by Guo [17] will be used in order to enhance the wideband circular polarization performance. For further information, various models of broadband microstrip antennas

4

for different purposes are described in [16]. Moreover, for the proposed antenna, microstrip antenna structures are generally favored in wearable applications since they can easily be integrated in clothing due to its compact geometry and planar profile [12, 18].

Rectification of microwave signals for supplying dc power through wireless transmission has been proposed and researched in the context of high-power beaming since the 1950s, a good review of which is given [8]. Applications for this type of power transfer have been proposed for power transmission and detection, long distance power beaming [19], helicopter powering, intersatellite power transmission [8], and short-range wireless power transfer, e.g., between two parts of satellite. In all of these cases, the polarization, continuous wave frequency, and power of the incoming RF field were not time varying, well defined, or known a priori. In this thesis, it is investigated that the prospect of efficiently capturing power contained in fields with unknown and arbitrary time varying spectral distribution and polarization [19].

1.1 Receiving Antenna

In order to capture electromagnetic waves and convert the energy into a current, the proposed design will require an antenna. The goal of this thesis is to maximize the harvested energy of time varying signals, with a very small power level and an arbitrary polarization, in the environment. In order to achieve this, it is obvious that the circularly polarized (CP) microstrip antennas, which compared to linear polarized antennas, allows for greater flexibility in orientation angle between transmitter and receiver, better mobility and weather penetration, and reduction in multi-path reflections and other kinds of interferences [17]. An antenna is usually regarded to be CP when its axial ratio stays below 3 dB for a given direction of propagation. CP is particularly useful for a number of radar, communication, and navigation systems because the rotational orientations of the transmitter and the receiver antennas are unimportant in relation to the received signal strength. With linearly polarized signals, on the other hand, there will be only very weak reception if the transmitter and receiver antennas are nearly orthogonal. Also, the circularly polarized wave reverses its sense of polarization from right hand to left hand CP and vice versa after reflection from regular objects [16]. Many designs of

single-feed, circularly polarized microstrip antennas with square or circular patches are presented in [20]. Circular polarization can be obtained if two or more orthogonal linearly modes, of equal amplitude and 90^0 time-phase difference, are independently excited. This can be accomplished by adjusting the physical dimensions of the patch and using either single, or two or more feeds. For microstrip antennas of the single-fed type, circular polarization can be generated without the need of an external polarizer. For microstrip antennas of the dual-fed type, circular polarization can be generated with the use of an external polarizer, resulting in a larger footprint beneath the patch. However, compared to the single-fed type, wider impedance and axial-ratio bandwidths can be achieved, even with a single-element configuration. Feed network configurations comprising Wilkinson power dividers, a log periodic balun, and a three-stub 90^0 hybrid coupler, have been investigated in the open literature. The conventional two-stub ($\sim 25\%$ bandwidth) or three-stub ($\sim 40\%$ bandwidth) branch-line hybrid couplers have been commonly used to obtain circular polarization. A quadruple L-probe circular patch antenna utilizing a pair of two-stub 90^0 hybrid couplers was shown to deliver a measured impedance bandwidth ($S_{11} < -10dB$) of 45% and axial ratio-bandwidth (AR<3dB) of 45%. The conventional 90^0 hybrid coupler, commonly used as an external polarizer for dual-fed type CP antennas. This symmetrical 3-dB directional coupler provides balanced power splitting and 90^0 phase shifting between its output ports [17].

A novel feed network configuration, namely the 90^0 broadband balun, which exhibits a wide impedance bandwidth ($S_{11} < -10dB$) of 187.6%, from 0.09 to 2.81 GHz, while regular 90^0 hybrid coupler exhibits a much narrower impedance bandwidth ($S_{11} < -10dB$) of 30.9% from 1.53 to 2.09 GHz, was accomplished by Guo [17]. In order the performance of this new feed line over the entire antenna structure to be observed, the circular patch fed by the L-probe, is combined into the structure. The proposed antenna exhibits considerably wide simulated and measured impedance bandwidth ($S_{11} < -10dB$) of 59.52 %, from 1.18 to 2.18 GHz, and 60.24%, from 1.16 to 2.16 GHz, respectively. It is also mentioned that the L-probe single-element rectangular patch antenna has a typical impedance bandwidth ($S_{11} < -10dB$) of around 30%. The

simulated and measured axial ratio of the dual L-probe antenna exhibits rather wide 3dB axial-ratio bandwidths of 39%, from 1.26 to 1.87 GHz, and 37.7%, from 1.25 to 1.83 GHz, respectively. In addition, geometry, radiation pattern, axial-ratio, and gain simulations and measurements results of the circularly polarized quadruple L-probe circular patch antenna can be seen at the same reference [17]. In this research [17], it was shown that for the quadruple L-probe patch antennas, the use of the proposed 90^0 broadband balun, in place of the conventional 90^0 hybrid coupler, allows for significantly improved impedance and axial-ratio bandwidths. Figure 1.2 (a) and (b) show the conventional 90^0 hybrid and the proposed 90^0 broadband balun.
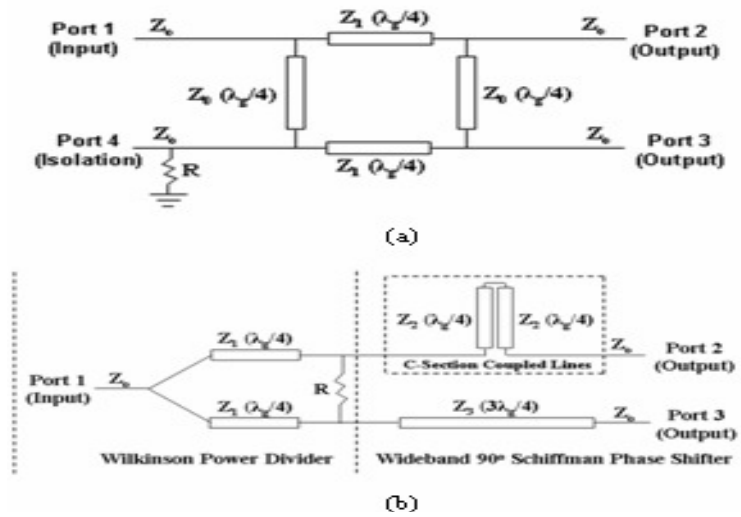
Figure 1.2: (a) The conventional 90^0 hybrid and **(b)** The proposed 90^0 broadband balun [17]

An another significant study of reception and rectification of arbitrarily polarized broadband time-varying low-power-density (between $10^{-5} - 10^{-1} mW/cm^2$) microwave radiation is presented in [8], which develops a 64-element dual circularly-polarized spiral rectenna array over a frequency range of 2-18 GHz with single-tone and multitone incident waves. The remarkable point in this study is that the integrated design of antenna and rectifier, which eliminates the matching and the filtering circuits, allowing a compact element design. In addition, the increase in rectenna efficiency for multitone input waves is presented.

As it was previously mentioned, the difficulty in these kinds of low-power-density research is that the nonlinear decrease in the efficiency due to the low input power levels when compared to power-beaming applications. The research also indicates that at microwave frequency band (1 GHz and higher), Schottky diodes (GaAs or Si) with shorter transmit times is required as a rectifier. Moreover, it is particularly emphasized that for low-power applications, there is generally not enough power to drive the diode in a high-efficiency mode. Therefore, it is important to use a diode with low turn-on voltage. Different kinds of Schottky diodes were tested, and the rectification performance was seen to depend most significantly on saturation current, junction capacitance, built-in potential, and series resistance. Measurement results for various incident power levels show that the conversion efficiency is highly dependent on an incident power levels, for instance the efficiency is 0.1% for an incident power density of $5.10^{-5} mW/cm^2$, and 20% for an incident power density of $0.07 mW/cm^2$. Concluding the research, it should be highlighted that if one of the requirements, such as high-power, narrow-band, linear polarization, and/or the transmission of time-constant power, is relaxed, higher efficiencies up to 60% at the X-band can be expected [8].

The similar studies were done by Hagerty and Popovic, for in details info please see [19] and [22].

Since the first aperture coupled microstrip antenna was proposed, a large number of variations in geometry have been suggested by workers around the world. The fact that the aperture coupled antenna geometry lends itself so well to such modifications is due in part to the nature of printed antenna technology itself, but also to the multi-layer structure of the antenna. The aperture coupled microstrip antenna involves over a dozen material and dimensional parameters, and Pozar summarized in [23] the basic trends with variation of these parameters. Researchers have been engaged in removing bandwidth limitations of this kind of antennas for the past 20 years, and have been successful in achieving an impedance bandwidth of up to 90% and gain bandwidth up to 70% in separate antennas. Most of these innovations utilize more than one mode, give rise to increase in size, height, or volume, and are accompanied by degradation of the other characteristics of the antenna. As mentioned above, increase the bandwidth can be achieved by a suitable choice of feeding technique and impedance matching network.

A considerable part of the (open) literature shows interest in the broadbanding aspect of microstrip antennas, which can be reviewed basically in [23].

In addition, analytical models for microstrip antennas can be used for simplification of the microstrip antenna model to an equivalent circuit model in which the patch is characterized by the admittance Y_{patch} and the aperture by $Y_{ap.}$, since it shortens the duration of the antenna simulation. For further information, please see the book Microstrip Antenna Design Handbook.

1.2 Advanced Rectification Circuitry

This component of the proposed design will principally be responsible for converting the alternating current captured by the antenna into a useful direct current form. This direct current will then be used to eventually recharge the wireless device's battery as mentioned above. Due to the incredible reduction in power requirements for electronic devices, it has become possible to harvest electromagnetic energy for the purpose of recharging a portable wireless device's battery. In order to minimize, or even eliminate, the energy needed to power this circuitry, passive circuit elements will be used whenever possible. The design of this circuitry will be heavily dependent on the frequencies that are harvested [24]. A highly efficient passive power conversion circuit is needed in order to extract as possible as more power output gate of the rectifier. It is also mentioned above; the circuit efficiency extremely depends on incident wave power density. Rectification circuits for such systems must be optimized to improve on the minimum power-threshold it takes for the system to operate. In order to overcome this power-threshold, the system requires significantly more efficient circuit and system level design [15]. It was shown that a Schottky diode can work with a 15 mV (1μWatt) alternating voltage without an additional energy supply [25]. Schottky diodes are preferable in such applications due to their low forward-voltage drop between approximately 0.15V-0.45V, while a normal diode has between 0.7-1.7 volt drops. This lower voltage drop translates into higher system efficiency. A Schottky diode uses a metal-semiconductor junction as a Schottky barrier (instead of a semiconductor-semiconductor junction as in conventional diodes). This Schottky barrier results in both

very fast switching times and low forward voltage drop [26]. An important invention was presented by Siemens Semiconductor (now Infineon): a silicon carbide Schottky diode, please see the reference [27] for more info. In addition to Schottky diodes, alternative solutions are available. For example, CMOS technology is proposed as a rectifier at very low-received power applications. As presented in [15], a $0.25\,\mu m$ CMOS technology is used for reducing the threshold voltage of the rectifier circuit. Simulations and the measurements were obtained using a rectifier with a single structure and N cascade stages in order to boost the voltage gain by each stage. The results demonstrate that a novel rectifier circuit works with signals as low as 50mV, and has a maximum measured efficiency of 60%. However, since it allows high Quality factor, this rectifier operates at narrowband, which is clearly out of our purpose of broadband applications. The increased number of diodes in multistage rectifier will also vary the input resistance of the rectifier, as well as the input capacitance; hence, mismatches can occur between the antenna and the rectifier. In order to compensate circuit mismatches, low cost impedance matching by using just strap inductor between the antenna and the rectifier IC presented in [28], also, tradeoffs between device sizes and the number of rectification stages were investigated. The number of stages is essentially directly proportional to the amount of voltage obtained at the output of the system. Generally, the voltage of the output increases as the number of stages increases [7].

A set of criteria is successfully presented by De Vita and Iannaccone [29], for the optimization of the voltage multiplier, the power-matching network. Furthermore, they have shown that radio frequency identification (RFID) transponders, which require a dc power of $1\mu W$, can operate larger than 4 and 11m at the 2.45 GHz and 868 MHz ISM frequency bands, respectively.

Electronic technology will continue its evolution of decreasing energy consumption thanks to continuing scaling down of devices, nanotechnology and eventually, molecular electronics. New processing and communication techniques will also help reducing power consumption [1].

1.3 Textile Antenna Design

Wearable computing is a fast growing field in application- oriented research. Steadily progressing miniaturization in microelectronics along with other new technologies enables integration of functionality in clothing allowing entirely new applications. The vision of wearable computing describes future electronic systems as an integral part of our everyday clothing serving as intelligent personal assistants [12]. Electro-textiles are conductive fabrics constructed by interpolating conductive metal/polymer threads with normal fabric threads or conductive threads. There are three methods of creating conductive fibers:

1) The filling of fibers with carbon or metal particles;

2) The coating of fibers with conductive polymers or metal;

3) The use of fibers that are completely made of conductive material.

The state-of-the-art conductive fibers are highly conductive metal wires and plated fibers, which are superior to other alternatives in terms of conductivity. Many alternatives in the construction of the fibers exist; however, silver plated nylon fibers and thin silver plated copper fibers are the ones preferred [13]. The choice criteria of thread were investigated in the references [12] and [13]. In addition, requirements from conductive threads are listed in [12], mainly; low electrical resistance ($\leq 1\Omega/\square$), the resistance must be homogeneous over the antenna area, the fabric should be flexible, and a stretchable. Furthermore, it is mentioned that an electrically conductive fabrics are needed for the ground planes as well as for the antenna patches, while a fabric substrate, which provides the dielectric between the antenna patch and the ground plane, is required with constant thickness and stable permittivity. From an electrical point of view, they recommended using copper foils. However, such foils lack of drapability and elasticity that limits their use in clothing. Moreover, three kinds of fabrics are proposed; 1) *no-name nickel-platted fabric*, 2) *a silver- platted knitted fabric*, and 3*) a silver-copper-nickel-platted woven fabric*, in order to simulations results, third fabric was chosen as the most appropriate one among of others. *Nickel-platted woven fabric* was not chosen due to the sheet resistance of about

$5 \Omega / \square$. Additionally, measurements showed that the sheet resistance is inhomogeneous over the area. On the other hand, *Silver-Plated Knitted Fabric* is bendable and, therefore, it can comfortably be integrated into clothing since the fabric elongates where necessary. Regarding the affects of bending were presented that the warpage and bending have, of course, influence on the antenna characteristics, i.e., S_{11}. Second, they affect the sheet resistance due to strain stress. The conclusion statement regarding this material is that it satisfies all the stated requirements but homogeneity in resistance when bent. Regarding *3) a silver-copper-nickel-platted woven fabric:* Compared to the knitted fabric 2), fabric 3) features low elasticity due to its woven structure. In contrast to fabric 1), the fibers of fabric 3) are plated before weaving resulting in a low electrical resistance. Its shape can be manufactured precisely, but bending of such an antenna is then limited. Additionally, the edges of this fabric tend to fray easily due to the nature of woven fabric. This effect can be minimized by using manufacturing techniques explained in same research. In conclusion, the woven fabric possesses the best electrical properties among the three fabrics to build well-behaved antennas with geometrical accuracies. As a textile substrate they chose a woolen felt with a thickness of 3.5mm and a polyamide spacer fabric with a thickness of 6mm. The felt with a density of 1050 g/m^2 is dimensionally more stable and harder to bend, whereas the spacer fabric with 530 g/m^2 is lighter and elastic due to its knitting-based structure. Furthermore, the spacer fabric can easily be compressed. Nevertheless, the fabric totally recovers after release of the load. Such a fabric can be integrated in jackets and function as thermal insulation simultaneously. Finally, the permittivity and the loss tangent values are measured; a permittivity $\in_r = 1.45 \pm 0.02$ for the felt and $\in_r = 1.14 \pm 0.025$ for the spacer fabric was extracted at a frequency of 2.4GHz, and the loss tangent of the felt is $\tan \delta = 0.02$, whereas the loss tangent of the spacer is negligible. In contrast, flexible substrates such as polyamide and liquid crystalline polymers (LCP) are foils. Therefore, they lack drapabilty and are only bendable in one direction at a time. This textile-atypical behavior of foils is a major drawback for integration into clothing. In the section V. of the research, antenna manufacturing process is investigated. It is expressed that the critical points of the composition of the conductive antenna patch with the dielectric substrate are that; firstly the dimensions of the patch must be retained while being attached to the substrate, and

12

secondly, the attachment procedure must not affect the electrical properties of the patch, e.g., the sheet resistance. For composition, they evaluated the following four methods:

1) Liquid textile adhesive (brand: Golden Fix), 2) Point-wise application of conductive adhesives, 3) Sewing, 4) Adhesive sheets, which are activated by ironing.

The adhesive sheets 4) show the best results. It evenly deposits as a thin layer on the conductive textile by ironing. Moreover, the adhesive only penetrates the surface of the conductive textile such that patch sheet resistance and substrate permittivity are not changed. Finally, simulations were conducted with using the woven fabric for both the antenna patch and the ground plane in the case of the circularly polarized antenna with spacer fabric substrate by utilization of adhesive sheets for composition. The results; however, not surprising concerning circularly polarized antenna. Bending of the antenna changes the amplitude and the phase relations between the two orthogonal current modes present in the circularly polarized antenna. Bending pushes the axial ratio curve towards lower frequencies by about 80 MHz in the situation of antenna bent around its x-axis and abolishes circular polarization in the situation of antenna bent around its y-axis [12].

It is also emphasized on circular polarized rectangular patch antennas; the antenna bending can destroy the antenna's circular polarization characteristics. This happens with patch antennas, since they commonly employ structures, where both the antenna's length and width are in resonance with $+90^0$ phase shift. One possible solution to this problem is that one should design the antenna having an elliptical polarization. When this kind of antenna is bent along its longer dimensions, the result would be circular polarized characteristics. Of course, the extra length in one dimension should have a relation with the bending radius [30].

The organization of the thesis is as follows: In section 2, the antenna design with conventional materials and simulation results are presented. After, the matching network and the rectifier circuit with simulation results are given in the section 3, detailed explanation of wearable textile is presented in section 4, redesign of the antenna with wearable materials and the antenna performance are given in section 5, and a conclusion is presented in section 6.

2. ANTENNA DESIGN with CONVENTIONAL MATERIALS and SIMULATION RESULTS

2.1 The Aperture Coupled Microstrip Antenna (ACMSA)

A typical aperture coupled patch antenna is shown in Figure 2.1. The radiating microstrip patch element is etched on the top of the antenna substrate, and the microstrip feed line is etched on the bottom of the feed substrate. The thickness and dielectric constants of these two substrates may thus be chosen independently to optimize the distinct electrical functions of radiation and circuitry [23].

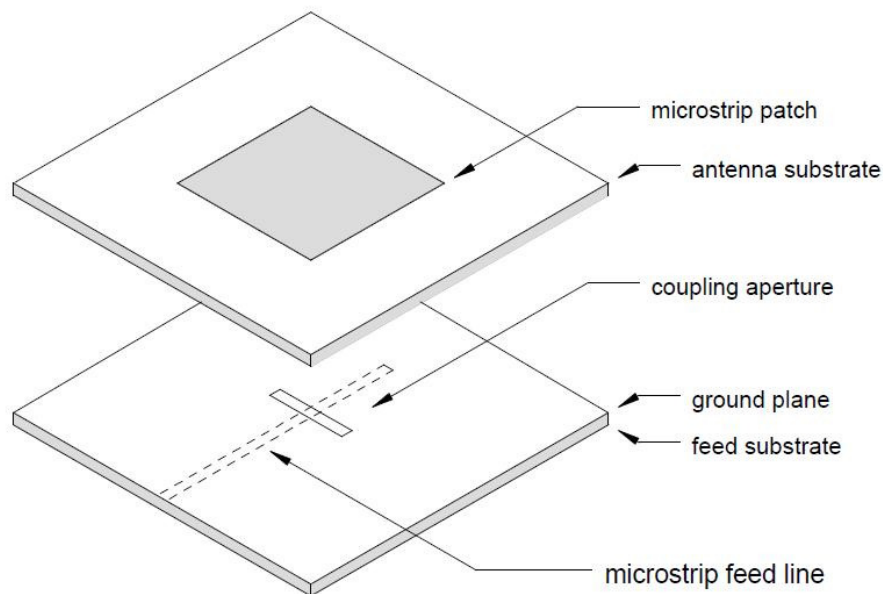**Figure 2.1:** Geometry of the basic aperture coupled microstrip antenna [23]

Although the original prototype antenna used a circular coupling aperture, it was quickly realized that the use of a rectangular slot would improve the coupling, for a given aperture area, due to its increased magnetic polarizability. Most aperture coupled microstrip antennas now use rectangular slots, or variations thereof. The aperture

coupled microstrip antenna involves over a dozen material and dimensional parameters, and the basic trends with variation of these parameters are summarized below:

Antenna substrate dielectric constant:

This primarily affects the bandwidth and radiation efficiency of the antenna, with lower permittivity giving wider impedance bandwidth and reduced surface wave excitation.

Antenna substrate thickness:

Substrate thickness affects bandwidth and coupling level. A thicker substrate results in wider bandwidth, but less coupling for a given aperture size.

Microstrip patch length:

The length of the patch radiator determines the resonant frequency of the antenna.

Microstrip patch width:

The width of the patch affects the resonant resistance of the antenna, with a wider patch giving a lower resistance. Square patches may result in the generation of high cross polarization levels, and thus should be avoided unless dual or circular polarization is required.

Feed substrate dielectric constant:

This should be selected for good microstrip circuit qualities, typically in the range of 2 to 10.

Feed substrate thickness:

Thinner microstrip substrates result in less spurious radiation from feed lines, but higher loss. A compromise of $0.01\,\lambda$ to $0.02\,\lambda$ is usually good.

Slot length:

The coupling level is primarily determined by the length of the coupling slot, as well as the back radiation level. The slot should therefore be made no larger than is required for impedance matching.

Slot width:

The width of the slot also affects the coupling level, but to a much less degree than the slot width. The ratio of slot length to width is typically 1/10.

Feed line width:

Besides controlling the characteristic impedance of the feed line, the width of the feed line affects the coupling to the slot. To a certain degree, thinner feed lines couple more strongly to the slot.

Feed line position relative to slot:

For maximum coupling, the feed line should be positioned at right angles to the center of the slot. Skewing the feed line from the slot will reduce the coupling, as will positioning the feed line towards the edge of the slot.

Position of the patch relative to the slot:

For maximum coupling, the patch should be centered over the slot. Moving the patch relative to the slot in the H-plane direction has little effect, while moving the patch relative to the slot in the E-plane (resonant) direction will decrease the coupling level.

Length of tuning stub:

The tuning stub is used to tune the excess reactance of the slot coupled antenna. The stub is typically slightly less than $\lambda g/4$ in length; shortening the stub will move the impedance locus in the capacitive direction on the Smith chart [23].

The ACMSA has several advantages:

· The top patch could be fabricated on a thick low dielectric substrate to enhance the bandwidth, and the feed network on the other side of the ground plane could be on a thin high dielectric substrate to reduce radiation losses.

· Radiation from the feed network does not interfere with the main radiation pattern, since the ground plane separates the two substrates.

· The excess reactance of the antenna can be compensated for by varying the length of the feed line of the open-circuited microstrip stub.

· The input impedance is easily controlled by the size, shape, and position of the aperture.

The ACMSA also has certain disadvantages. The total thickness of the antenna is large as compared to a probe-fed microstrip antenna. Also, the back radiation occurs more through the coupling aperture in the ground plane, which can be reduced by using a small aperture [16].

Several techniques have been used to analyze the ACMSA. These techniques include the transmission line model, the cavity model, and the integral equation method. All these techniques predict the performance of the antenna reasonably well [16].

A typical radiation pattern plot for an ACMSA can be seen in Figure 2.2, the forward radiation patterns are typical obtained with microstrip antenna elements, while the back radiation lobe is caused by radiation from the coupling slot [23].

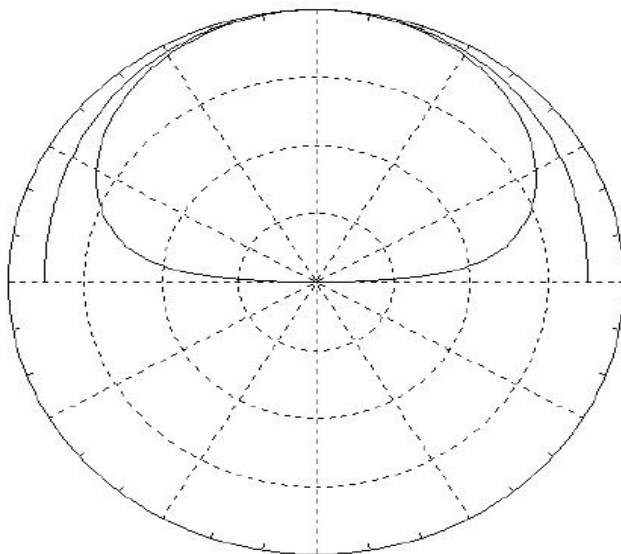**Figure 2.2:** Principal plane patterns for an aperture coupled microstrip antenna [23]

Since the first aperture coupled microstrip antenna was proposed, a large number of variations in geometry have been suggested by workers around the world. The fact that the aperture coupled antenna geometry lends itself so well to such modifications is due in part to the nature of printed antenna technology itself, but also to the multi-layer

18

structure of the antenna. Below some of the modified designs that have evolved from the basic aperture coupled antenna geometry are categorized:

Radiating elements:

The original aperture coupled antenna used a single rectangular patch. Since then, workers have successfully demonstrated the use of circular patches, stacked patches, parasitically coupled patches, patches with loading slots, and radiating elements consisting of multiple thin printed dipoles. Most of these modifications are intended to yield improved bandwidth.

Slot shape:

The shape of the coupling aperture has a significant impact on the strength of coupling between the feed line and patch. Thin rectangular coupling slots have been used in the majority of aperture coupled microstrip antennas, as these give better coupling than round apertures. Slots with enlarged ends, such as "dogbone", bow-tie, or H-shaped apertures can further improve coupling.

Type of feed line:

The microstrip feed line can be replaced with other planar lines, such as stripline, coplanar waveguide, dielectric waveguide, and similar. The coupling level may be reduced with such lines, however. It is also possible to invert the feed substrate, inserting an additional dielectric layer so that the feed line is between the ground plane and the patch element.

Polarization:

Besides linear polarization, it has been demonstrated that dual polarization and circular polarization can be obtained with aperture coupled elements.

Dielectric layers:

As with other types of microstrip antennas, it is easy to add a radome layer to an aperture coupled antenna, either directly over the radiating element, or spaced above the element. It is also possible to form the antenna and feed substrates from multiple layers, such as foam with thin dielectric skins for the etched conductors [23].

Losses:

The antenna is a resonant circuit therefore; energy will be stored in the system. This energy stored is inversely proportional to the dielectric height h. We can also describe the energy stored by the parameter Q (known as Quality Factor). Losses in the antenna will allow energy to leak away and such an antenna will have a lower Q factor.

The Q factor can be calculated from the following equation:

$$Q = \frac{2\pi f_r W_t\left(\frac{1}{h}\right)}{P_r + P_c + P_d + P_{sw}} \qquad (2.1)$$

f_r = resonant frequency

$W_t\left(\frac{1}{h}\right)$ = stored energy in the cavity

P_r = energy lost through radiation

P_d = dielectric loss

P_c = conductor loss

P_{sw} = surface wave loss (very small)

The antenna efficiency is given by;

$$\eta(\%) = \frac{P_r}{P_d + P_c + P_r}.\%100 \qquad (2.2)$$

Typically η can be between 80 to 90% for a patch antenna with a dielectric constant of 2.3 at 10GHz. Losses reduce the Q factor, which results in an increased bandwidth and reduced efficiency.

Typical Q factors are in the range 20-200 and the band-width is given by:

$$BW = \frac{100(s-1)}{Q\sqrt{s}} \qquad (2.3)$$

s=VSWR [31]

2.1.1 Circularly polarized antenna

A circularly polarized (CP) microstrip antenna (MSA) can be realized by exciting two orthogonal modes with equal magnitudes, which are in phase quadrature. The sign of the relative phase determines the sense of polarization (LHCP or RHCP). The simplest way to obtain CP is to use two feeds at orthogonal positions that are fed by 0° and 90° as shown in Figure 2.3. For a square or circular patch operating in the fundamental mode, when the two feeds are placed orthogonal to each other, the input impedance and resonance frequency of the antenna remain unaffected as the two feeds are at the null location of the orthogonal mode. Equal power with 90° phase difference to the feeds can be obtained either by using an external two-way 0° and 90° power divider or it can be integrated along with the antenna itself [16].
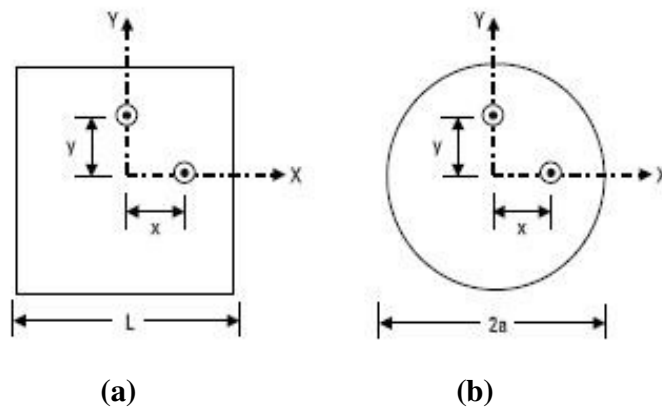

(a)   **(b)**

Figure 2.3: (a) Dual-feed square MSA and **(b)** circular MSA [16]

The CP operation of microstrip antennas can be achieved by using either single-feed or two-feed designs. The single-feed design has the advantage of a simple feed structure, and in addition, no external phase shifter is required. However, single-feed designs usually have a narrow CP bandwidth (3-dB axial ratio) of about 1% for a microstrip antenna with a dielectric substrate. For two-feed designs, single-layer, broadband CP microstrip antennas with a large CP bandwidth greater than 20% have been reported by some researches. These broadband CP designs mainly have a thick foam or air substrate; to achieve good impedance matching, feed methods using two three-dimensional microstrip transition feed lines and two aperture-coupled feeds have been used. Recently, two-feed designs using two gap-coupled probe feeds and two capacitively

coupled feeds have been presented. To achieve a much larger CP bandwidth, one should use a two-feed design incorporating a thick air substrate and an external phase shifter or power divider. It has been reported that, by using two gap-coupled or capacitively coupled feeds with a Wilkinson power divider to provide good equal-power splitting for the two feeds, the obtained 3-dB axial-ratio bandwidths can be as large as about 46% and 34%, respectively. One can also use a branch-line coupler as the external phase shifter, and the obtained 3-dB axial-ratio bandwidth can reach 60% referenced to a center frequency at 2.2 GHz. A four-feed design with $0^0 - 90^0 - 180^0 - 270^0$ phase shifts for a single-patch microstrip antenna has also been implemented, and very good CP quality has been obtained. The 2-dB axial-ratio bandwidth is 38%, and the 3-dB axial-ratio beam width for frequencies within the obtained CP bandwidth can be greater than 100^0. Relatively very slow degradation of the axial ratio from the antenna's broadside direction to large angles can be obtained compared to a corresponding broadband circularly polarized microstrip antenna with two-feed design [20].

2.1.2 Feed network configuration

Feed network configurations comprising Wilkinson power dividers, a log periodic balun, and a three-stub 90^0 hybrid coupler, have been investigated in the open literature. The conventional two-stub ($\sim 25\%$ bandwidth) or three-stub ($\sim 40\%$ bandwidth) branch-line hybrid couplers have been commonly used to obtain circular polarization. A quadruple L-probe circular patch antenna utilizing a pair of two-stub 90^0 hybrid couplers was shown to deliver a measured impedance bandwidth ($S_{11} < -10dB$) of 45% and axial ratio-bandwidth (AR<3dB) of 45%. The conventional 90^0 hybrid coupler, commonly used as an external polarizer for dual-fed type CP antennas. This symmetrical 3-dB directional coupler provides balanced power splitting and 90^0 phase shifting between its output ports [17].

A novel feed network configuration, namely the 90^0 broadband balun, which exhibits a wide impedance bandwidth ($S_{11} < -10dB$) of 187.6%, as it can be seen in Figure 2.4, from 0.09 to 2.81 GHz, while regular 90^0 hybrid coupler exhibits a much narrower impedance bandwidth ($S_{11} < -10dB$) of 30.9% from 1.53 to 2.09 GHz, was

accomplished by Guo [17]. This new balun comprises, as shown in Figure 2.5, a cascade of a 3-dB Wilkinson power divider, for wideband impedance matching and balanced power splitting, and a novel broadband 90^0 Schiffman phase shifter, for wideband consistent 90^0 phase shifting. The characteristic impedances are given by $Z_1 = 70.71$, $Z_2 = 50$, and $Z_3 = 50$.
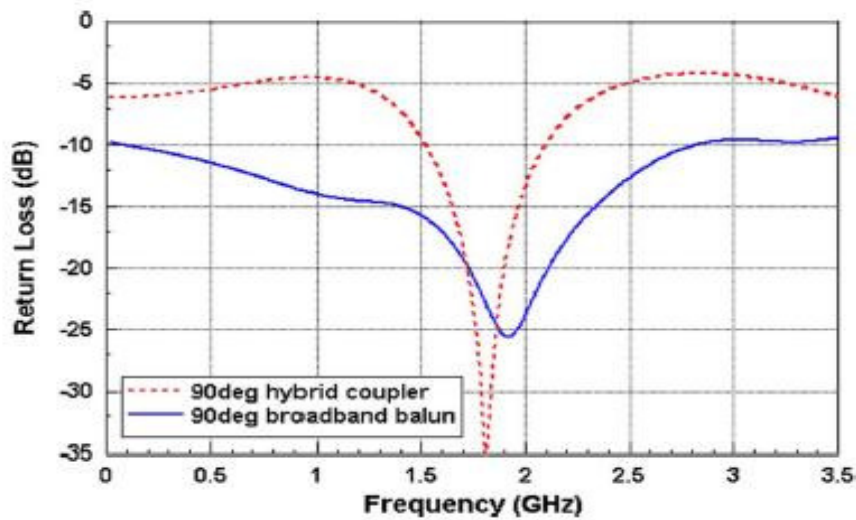

Figure 2.4: Simulated return loss comparison between the conventional 90^0 hybrid coupler and the proposed 90^0 broadband balun [17]
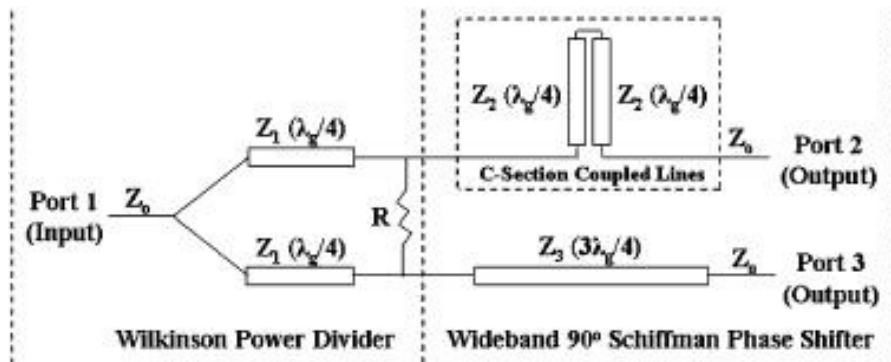

Figure 2.5: Schematics of the proposed 90^0 broadband balun [17]
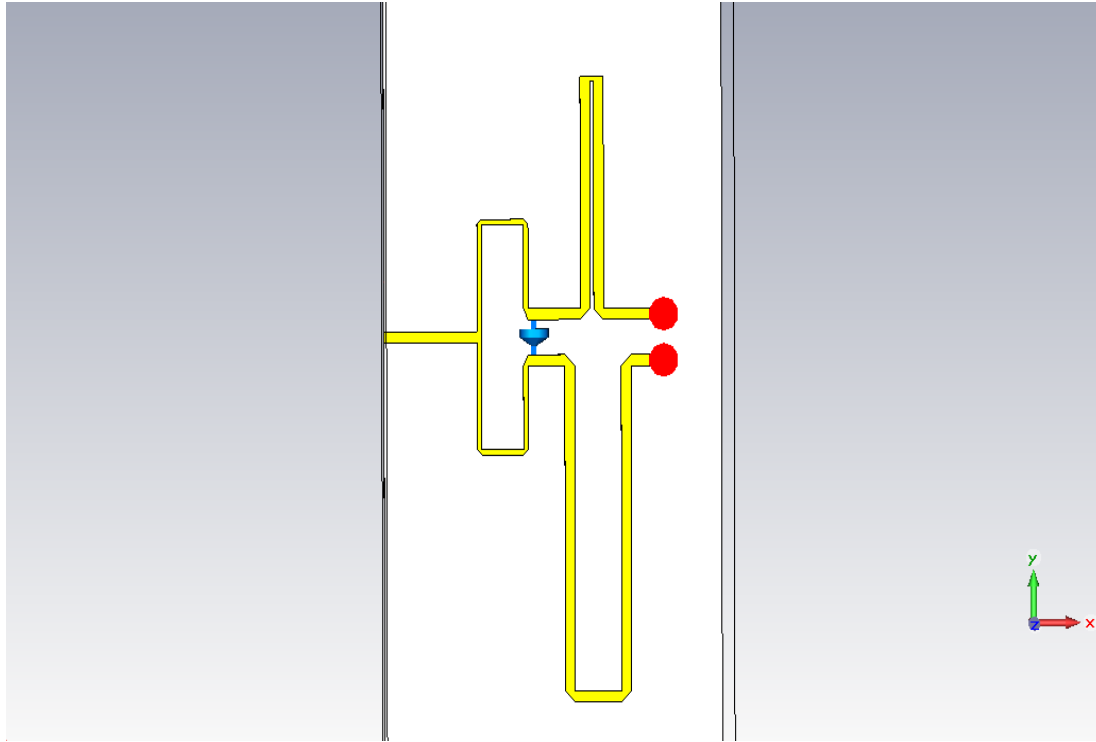
2.2 Design

2.2.1 Phase shifter

Figure 2.6: 90^0 broadband balun configuration [32]

Figure 2.6 shows the 90^0 broadband balun which comprises a cascade of a 3-dB Wilkinson power divider, for wideband impedance matching and balanced power splitting, and a novel broadband 90^0 Schiffman phase shifter, which is proposed by Guo [17], for wideband consistent 90^0 phase shifting. In order to generate circular polarization, this phase shifter was added before feed line ports. The characteristic impedances are $50\,\Omega$ for primary strip, $70.7\,\Omega$ for Wilkinson power divider strip which seems thinner in the same figure, and $50\,\Omega$ for 90^0 Schiffman phase shifter strip. As it can be seen in Figure 2.7, 90^0 broadband balun exhibits a wide impedance bandwidth (S_{11}<-10dB) from 0.6 GHz to 3GHz, which covers targeted bandwidth. Figure 2.8 shows the simulated output ports phase difference of wideband external polarizer.
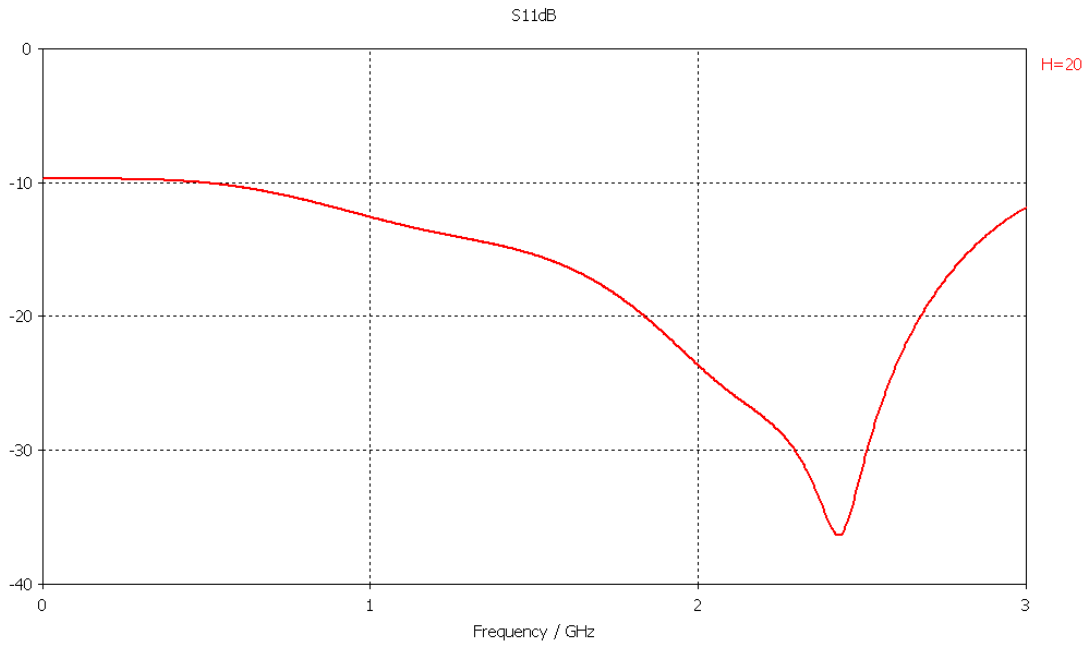
Figure 2.7: Simulated return loss (S_{11}) in the frequency range of 0-3 GHz [32]
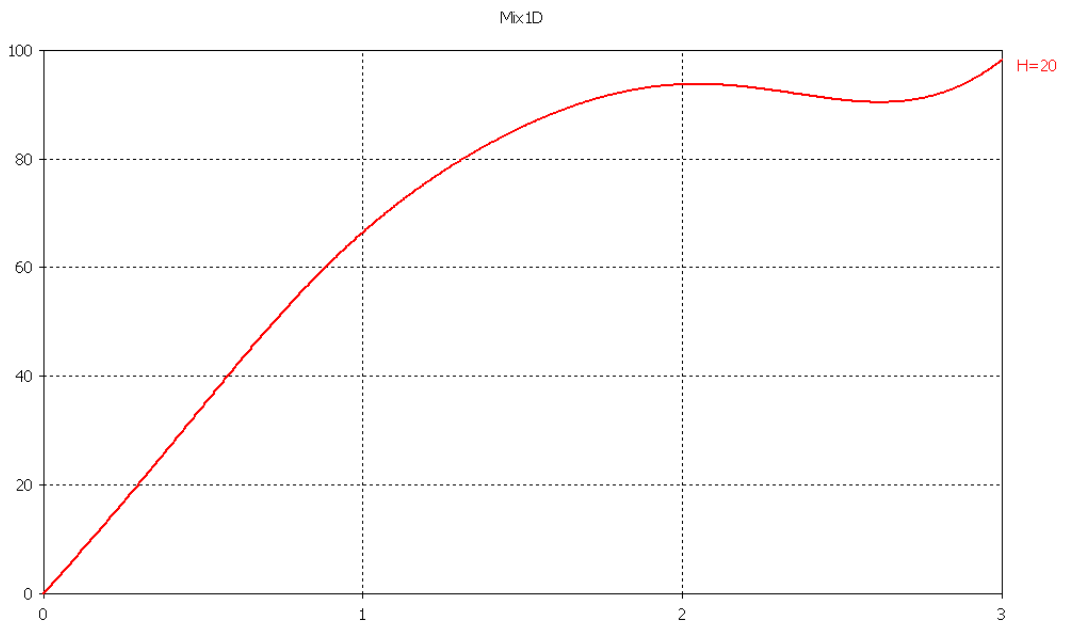

Figure 2.8: Simulated output ports phase difference [32]

The 90^0 broadband balun exhibits consistent 90^0 ($\pm 5^0$) output ports phase difference over a considerably wide band of from 1.6 to 2.7 GHz [32].

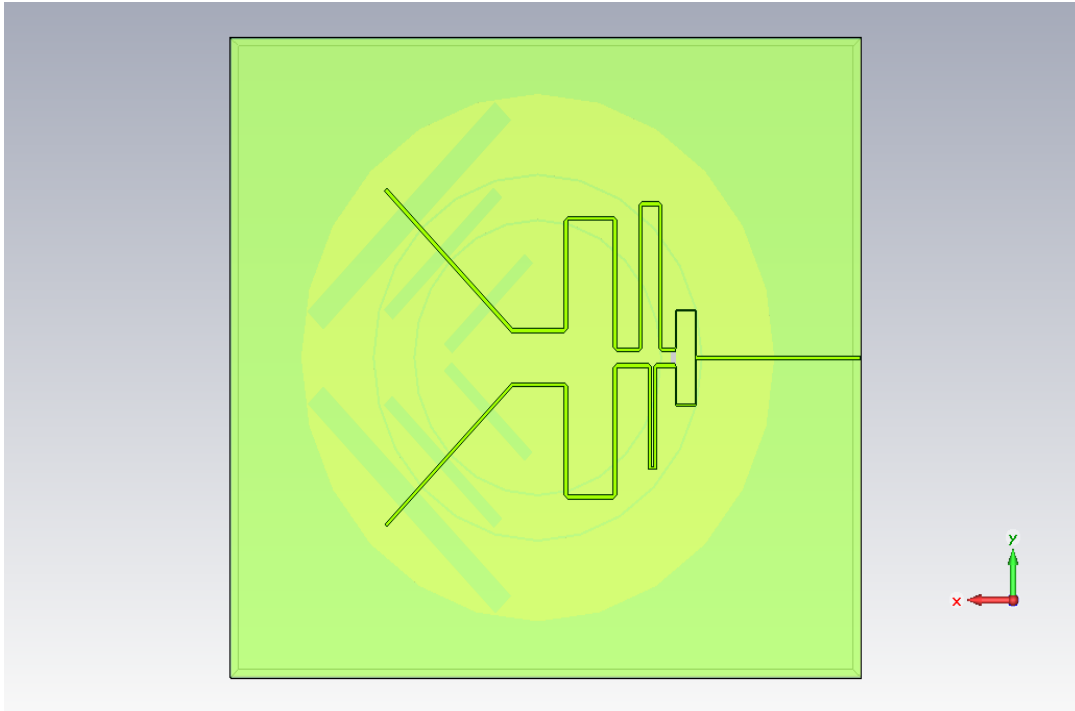## 2.2.2 Multi resonant circularly polarized patch antenna

Figure 2.9: Back view of the antenna [32]

The proposed antenna, illustrated in Figure 2.9 and 2.10, consists of 6 apertures in the ground plane fed by a microstrip line and three radiated patches, one being inner circular patch and two annular rings. The 6 apertures are located in group of two for each particular patch, the dimension of each group being the same within each particular patch. This antenna is printed on a substrate, polyhuretanic foam, of 4mm thickness with relative dielectric constant $\in_r$ =1.25, and the apertures in the ground plane and the feed line under the ground plane were printed on the same dielectric substrate, taconic, of height h =0.635mm, and relative permittivity $\in_r$ =6.15. By changing the radius of the inner patch and annular rings, resonant frequencies can be controlled.

This structure can excite three resonant frequencies by using the outer annular-ring, the inner annular-ring, and the circular patch, which decreases the Q-factor and increases bandwidth of the antenna, also the structural size becomes larger.

The resonant frequency of the lower band (890-915 MHz), which covers GSM-900 uplink band, is mainly determined by the larger outer ring radius. On the other hand,

inner circular patch excites the higher band (2410-2485 MHz), which covers W-LAN band while the resonant frequency of the middle mode (1710-1785 MHz), which covers GSM-1800 uplink band, is dependent on the inner-annular ring radius [32].
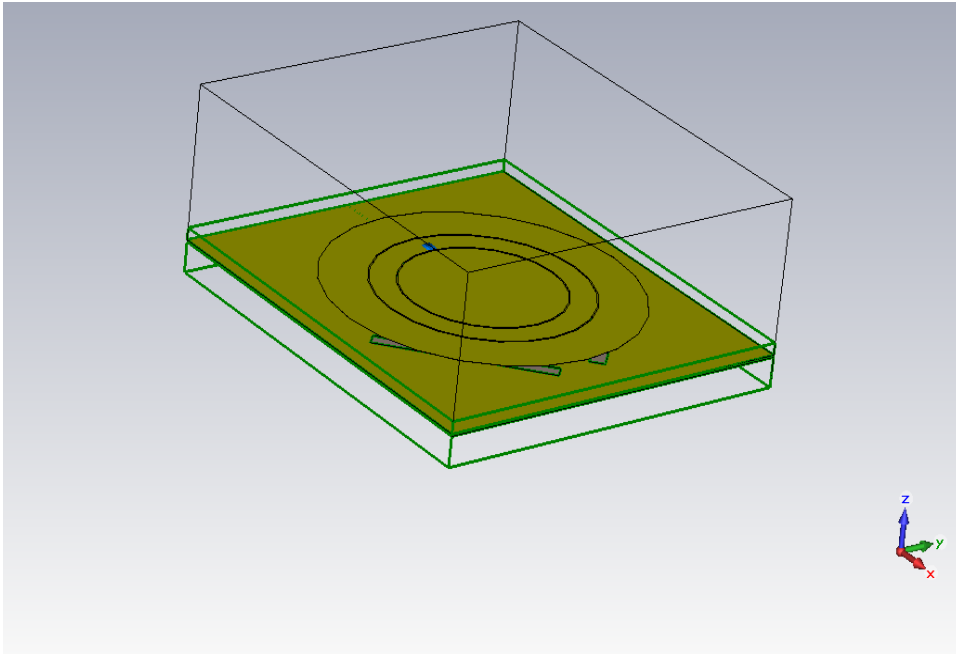

Figure 2.10: Perspective view of the antenna [32]

Return Loss

The return loss is defined as the ratio between the power reflected back from the antenna at the feed point and the power fed to the antenna. If the entire power is reflected back, S_{11} will be 0 dB. If the power is completely absorbed by the antenna, the value will be $-\infty$ dB. A low return loss value corresponds to a good matching at a specific frequency.

Figure 2.11 shows the simulated S_{11} characteristic of the proposed antenna in the frequency range of 0 to 15 GHz. It is clearly observed that wideband operation is achieved. Figures 2.12, 2.13, and 2.14 show the return loss of the antenna at purposed bandwidths in detail [32].
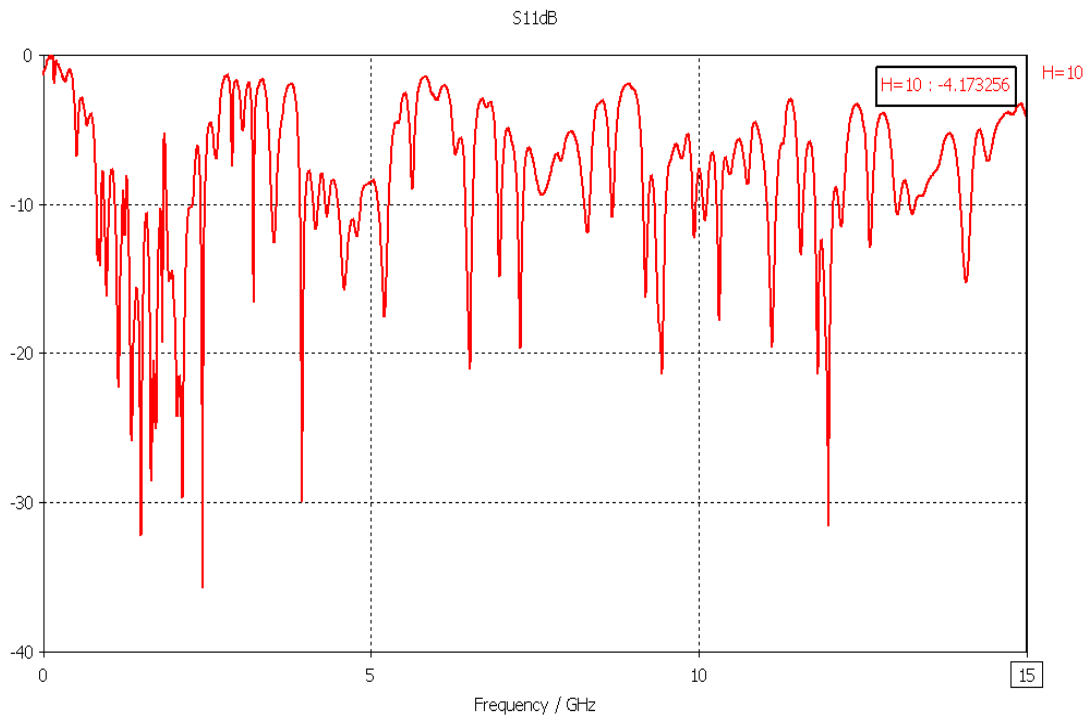
Figure 2.11: Simulated return loss (S_{11}) of the antenna [32]
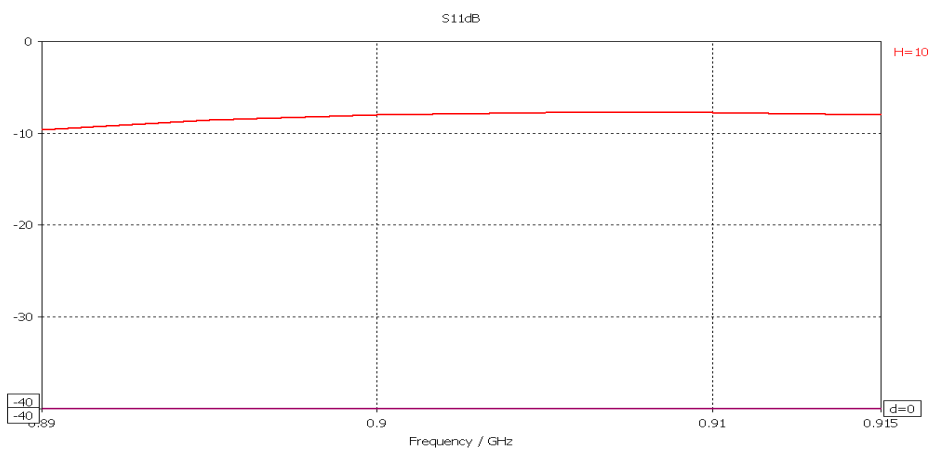
Figure 2.12: Simulated return loss (S_{11}) at the GSM-900 band [32]
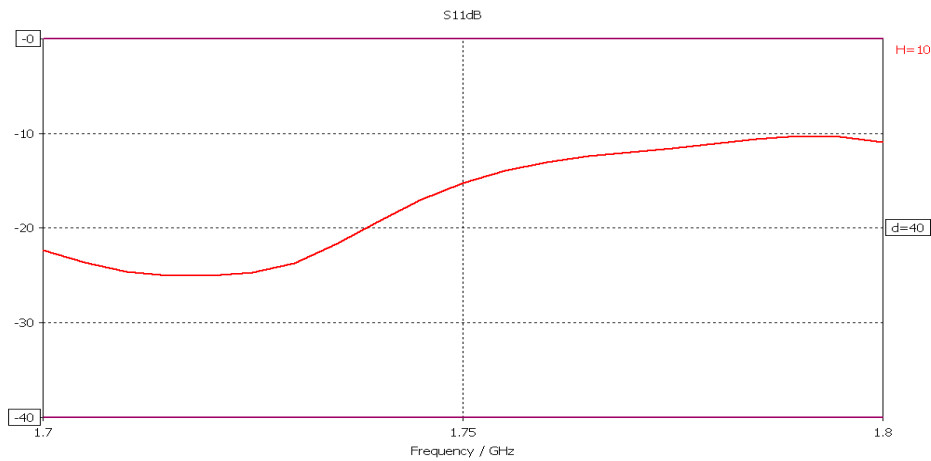
Figure 2.13: Simulated return loss (S_{11}) at the GSM-1800 band [32]
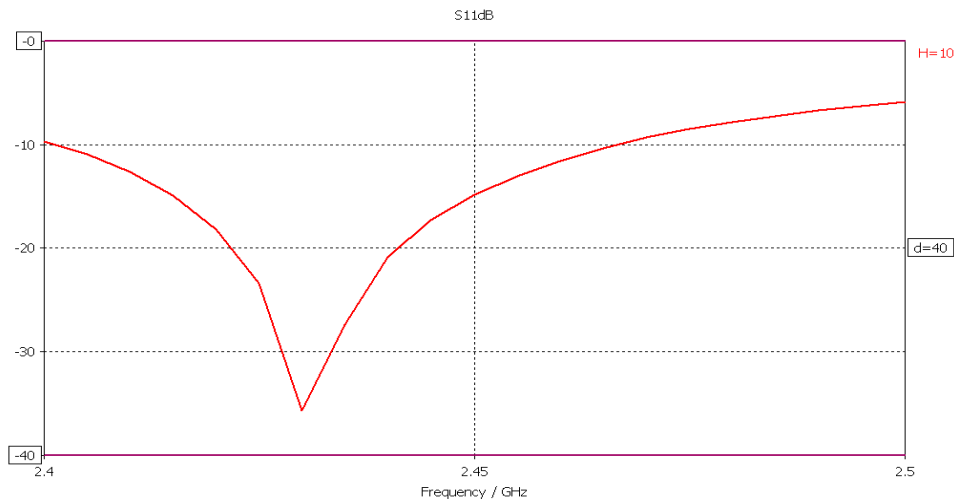
Figure 2.14: Simulated return loss (S_{11}) at the W-LAN band [32]

Axial Ratio

The axial ratio is a parameter to describe either elliptical or circular polarization. It is defined as the ratio of the major to the minor axis of the polarizations ellipse of an antenna. To achieve circular polarization, the field vector (electric or magnetic) must fulfill the following conditions:

1) The field must have two orthogonal linear components;

2) The two components must have the same magnitude;

3) The two components must have a time-phase difference of odd multiples of 90 [12].

29

In our case, simulated result of the axial ratio below 6 is purposed rate for effective circular polarization [32].
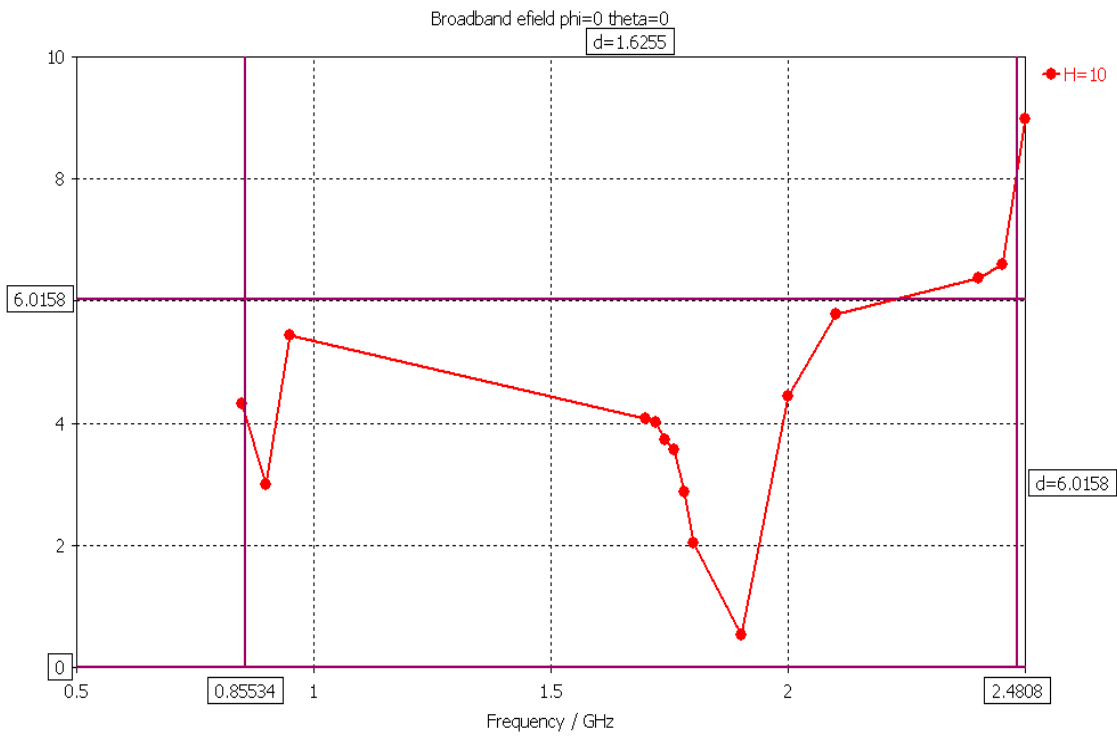
Figure 2.15: Simulated axial ratio of the antenna [32]

Radiation pattern

A radiation pattern characterizes the variation of the radiated far-field intensity of an antenna as an angular function at a specific frequency. Figures 2.16, 2.17, and 2.18 show the simulated radiation patterns in the E-plane for the proposed antenna at 900, 1760, and 2400 MHz, respectively. Very good broadside radiation patterns are observed for each three bands [32].

Type   Farfield
Approximation   enabled (kR >> 1)
Monitor   ff_00.9000 [1]
Component   Abs
Output   E-Field(r=1m)
Frequency   0.9
Rad. effic.   0.1008
Tot. effic.   0.08476
Emax   4.737 V/m

Figure 2.16: Simulated radiation pattern in the E-plane of the antenna at 900 MHz [32]

Type   Farfield
Approximation   enabled (kR >> 1)
Monitor   ff_01.7600 [1]
Component   Abs
Output   E-Field(r=1m)
Frequency   1.76
Rad. effic.   0.2499
Tot. effic.   0.2374
Emax   5.096 V/m

Figure 2.17: Simulated radiation pattern in the E-plane of the antenna at 1760 MHz [32]

31

Figure 2.18: Simulated radiation pattern in the E-plane of the antenna at 2400 MHz [32]

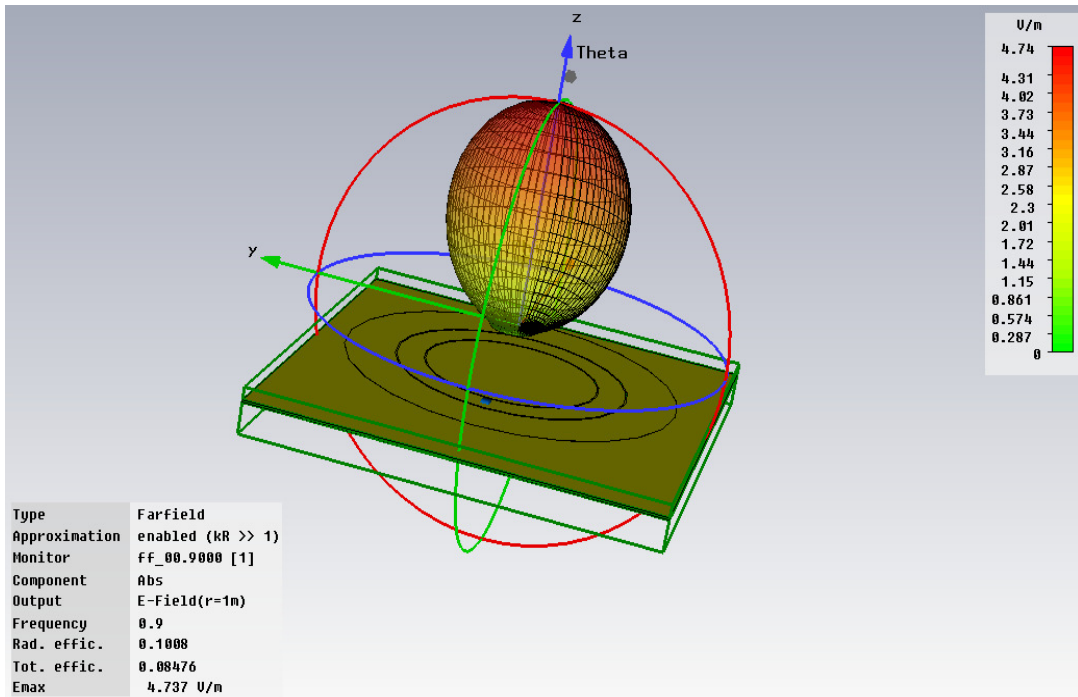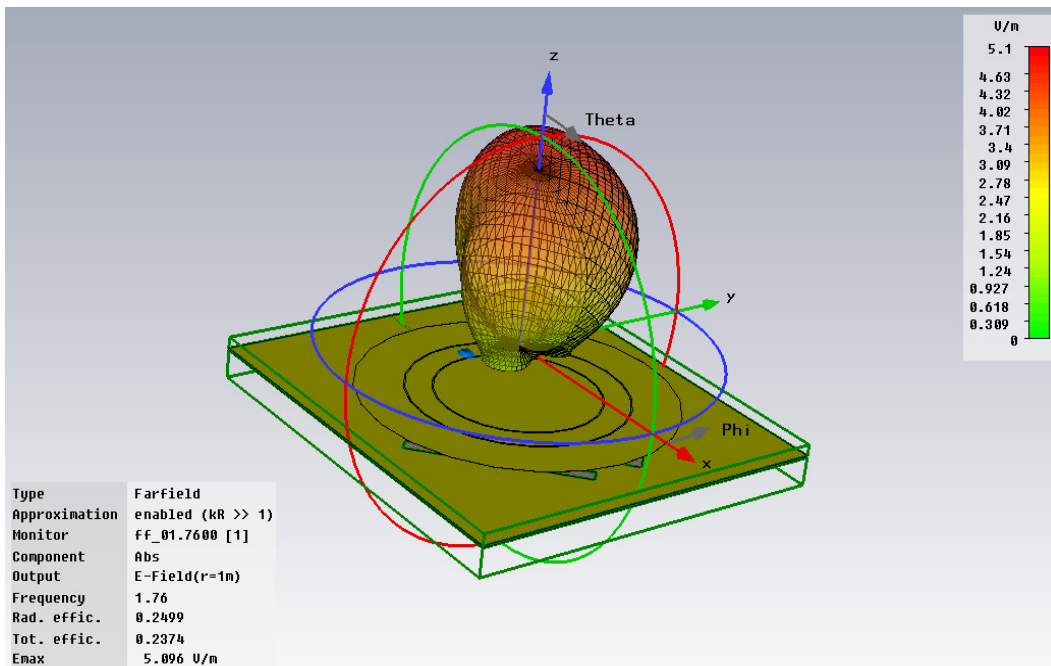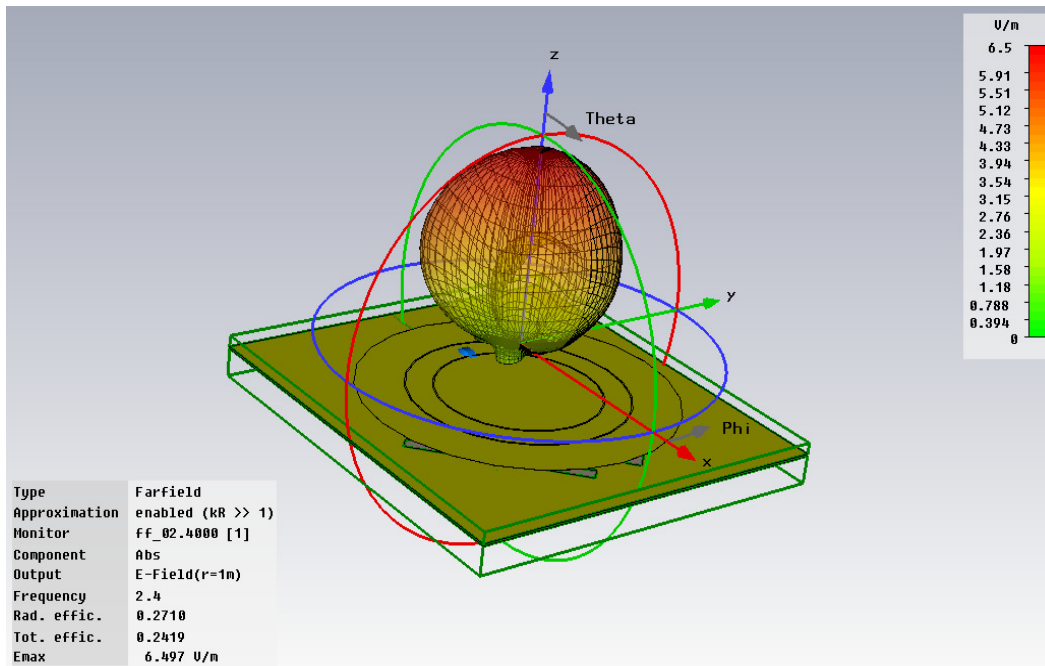## 3. RECTIFIER CIRCUIT and MATCHING NETWORK

In a far field RF energy harvesting system, RF energy must be extracted from the air at very low power density since the propagation energy drops off rapidly as distance from the source is increased. In free space, the electric field and power density drop off at the rate of $1/d^2$, where is the distance from the radiating source. The available power to the receiver decreases by 6 dB for every doubling of distance from the transmitter. With multi-path fading, the power density drops off at a much faster rate than $1/d^2$, it is therefore critical that the power conversion circuit operate at very low receive power to achieve longer operating distance. Rectification circuits for such systems must be optimized to improve on the minimum power-threshold it takes for the system to operate. To overcome this power-threshold, the system requires significantly more efficient circuit and system level design. One of the major challenges to achieving this goal is the relatively high voltage requirement of rectifying circuits currently employed. When the available RF power to the receiver is under 100μW, the available voltage for rectification in the RF to DC conversion system falls below 0.3V, much too low to overcome the threshold voltage (V_{th}) of conventional rectifier circuits. Alternative solutions must be found to circumvent or diminish the "dead-zone" in voltage rectification and otherwise reduce the effective threshold voltage in standard CMOS rectifier designs [15]. Some remarks on the solution of the highly sensitive and efficient rectifier circuit techniques as well as system level design issues for RF to DC power conversion can be found in [15]. In this research, fully passive rectifier circuits are designed in a 0.25μm CMOS technology optimized to operate at very low received power. A receive antenna is designed in a 4-layer FR4 board to maximize power transfer in the system. Furthermore, the system overview of the far-field RF power conversion system and the importance of each of the major blocks and design issues in the system

are described in detailed. The circuit level design of the far-field RF-DC power conversion system where the different rectifier designs are also shown.

High efficiency, low cost impedance match between the antenna and the rectifier, low output resistance for the rectifier and low input capacitance for the rectifier are all important goals in the design of the rectifier circuit. In order to fine tune the impedance match between the antenna and the rectifier to further reduce transmission loss and increase the voltage gain, a matching network between the receive antenna and rectifier is necessary [15]. It is mentioned in the research [28] that three methods of impedance matching can be used achieve high RF to DC conversion efficiency; they are transformer matching, L-matching and shunt inductor tuning. Transformer matching is cost prohibitive for the retail RFID tag targeted for only a few cents. L-matching uses a series inductor, and possibly additional elements, to resonate out the input capacitance of the IC. This type of match may provide Q voltage boosting if the antenna impedance is low and the rectifier impedance is relatively high. The shunt inductance tuning method only requires a simple strap inductor and is the least costly in terms of components. However, this requires an accurate estimation of the rectifier input shunt resistance. For RFID applications, a multistage rectifier is generally required to achieve a reasonable DC output voltage level. The increased number of diodes in multistage rectifier will also vary the input resistance of the rectifier, as well as the input capacitance. In same research, using the linear region model, the input resistance of both diode doublers and multi-stage rectifiers were derived. In addition, the input capacitance and output resistance of rectifiers were analyzed. These analyses make it possible to achieve higher efficiency in RF to DC conversion with low cost impedance matching by using just a strap inductor between the antenna and the rectifier IC [28].

The system, shown in Figure 3.1, consists of an antenna to pick up the power radiated by the RF waves, an impedance matching network to ensure maximum power transfer in the system, and a rectifier circuit to convert the RF signal to a DC voltage. The passive amplification of voltage is done by matching the impedances between the receive antenna and the rectifier circuit [15].
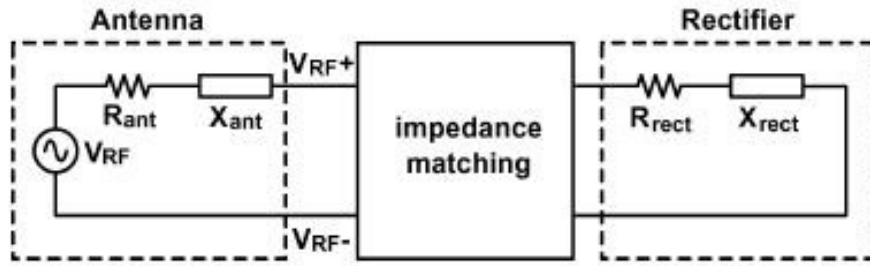
Figure 3.1: Passive RF-DC conversion circuit showing the equivalent circuit representation for the antenna and rectifier [15]

Power convertors that are used for many electronic devices today typically are much more complex than the rectifier used in this thesis. Power converter circuits have a lot of protective circuitry along with circuitry to reduce noise. In fact, it is a safety regulation that any power-conversion circuits use a transformer to isolate the input from the output. This prevents overload of the circuit and user injury by isolating the components from any spikes on the input line [7]. For this thesis, however, such a low power level is being used that a circuit this complex would require more power than is available, and it would therefore be very inefficient and possibly not function. In that case, it is necessary to use a simple design.

The simplest design that can be used is a half wave peak rectifier. This circuit requires only a capacitor and a diode to function. The schematic is shown in Figure 3.2. The explanation of how this circuit works is quite simple. The AC wave has two halves, one positive and one negative. On the positive half, the diode turns on and current flows, charging the capacitor. On the negative half of the wave, the diode is off such that no current is flowing in either direction. Now, the capacitor has voltage built up which is equal to the peak of the AC signal, hence the name. Without the load on the circuit, the voltage would hold indefinitely on the capacitor and look like a DC signal, assuming ideal components. With the load, however, the output voltage decreases during the negative cycle of the AC input, shown in Figure 3.3. This figure shows the voltage decreases exponentially. This is due to the RC time constant. The voltage decreases in relation to the inverse of the resistance of the load, R, multiplied by the capacitance C.

This circuit produces a lot of ripple, or noise, on the output DC of the signal. With more circuitry, that ripple can be reduced [7].
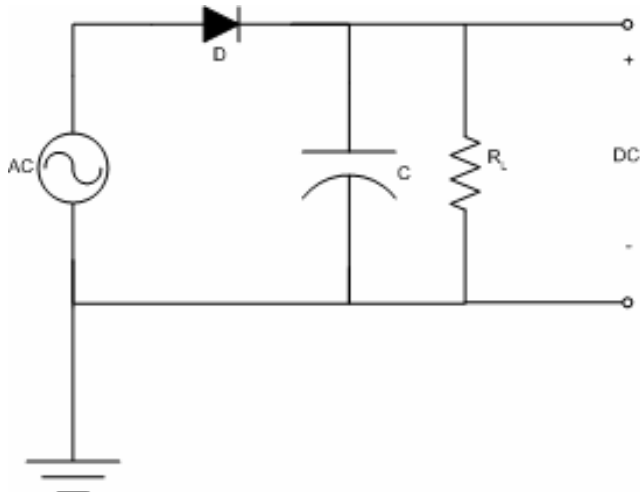

Figure 3.2: Half wave peak rectifier [7]
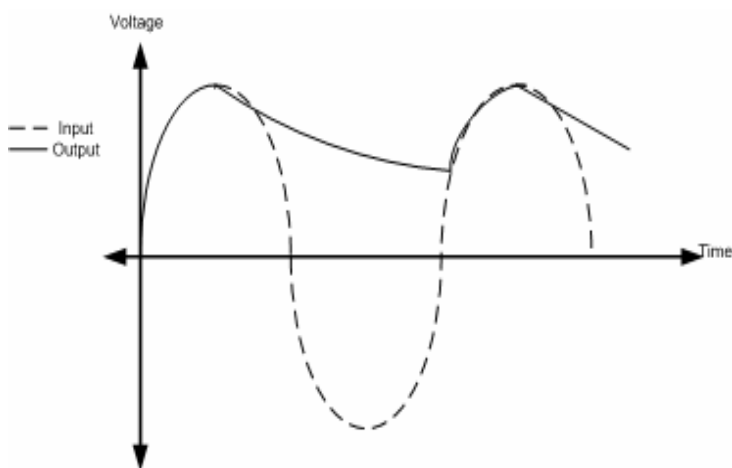
Figure 3.3: Half-wave Peak Rectifier Output Waveform [7]

The circuit that was chosen to be used is presented in Figure 3.4. This circuit is called a voltage doubler because in theory, the voltage that is received on the output is twice that at the input. The RF wave is rectified by D2 and C2 in the positive half of the cycle, and then by D1 and C1 in the negative cycle. But, during the positive half-cycle, the voltage stored on C1 from the negative half-cycle is transferred to C2. Thus, the voltage on C2 is roughly two times the peak voltage of the RF source minus the turn-on voltage of the

diode, hence the name voltage doubler. Therefore, the voltage at the output V_{out} is

$2V_{amp} - V_{th2} - V_{th1}$ [7].
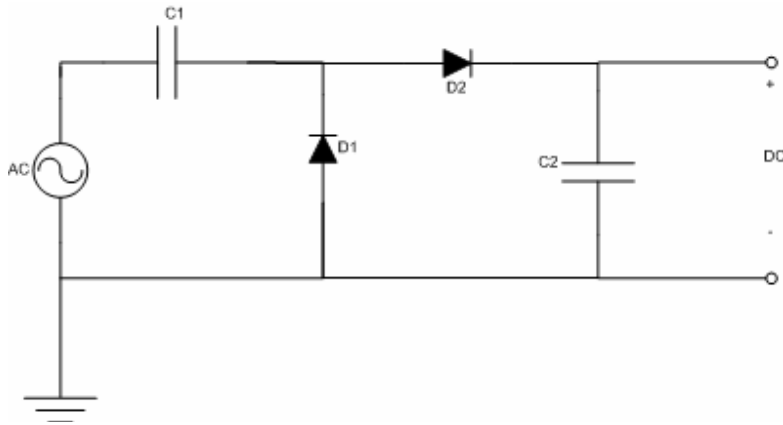
Figure 3.4: Voltage Double Schematic [7]

The output and the input waveforms of voltage doubler can be seen in Figure 3.5.
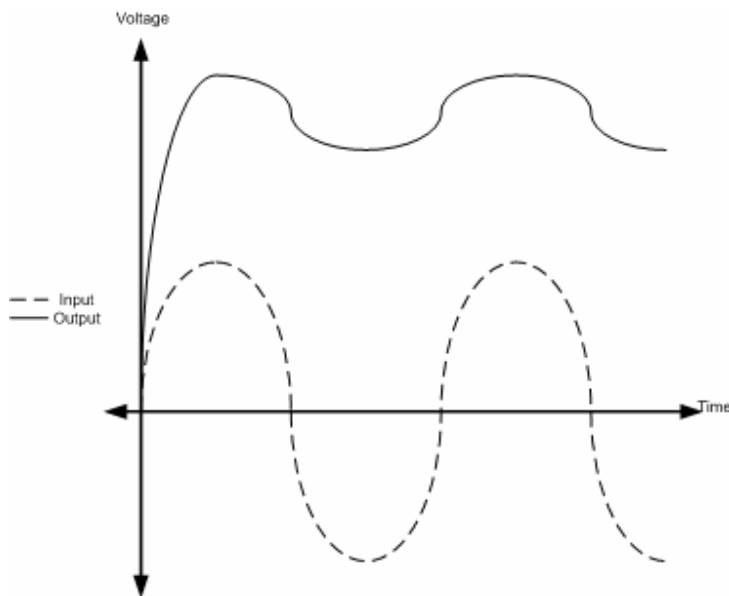
Figure 3.5: Voltage Doubler Waveform [7]

The most interesting feature of this circuit is that by connecting these stages in series, we can essentially stack them, like stacking batteries to get more voltage at the output. In order to further increase the supply voltage, an N-stage voltage multiplier is typically used, providing a DC output voltage, at constant input power, roughly N times larger

37

than that achievable with a single stage. The number of stages, as shown in Figure 3.6, in the system has the greatest effect on the output voltage. The capacitance, both in the stages and at the end of the circuit, affects the speed of the transient response and the stability of the output signal. The number of stages is essentially directly proportional to the amount of voltage obtained at the output of the system. Generally, the voltage of the output increases as the number of stages increases. This is due to how the voltage doubler works as explained previously [7, 29].

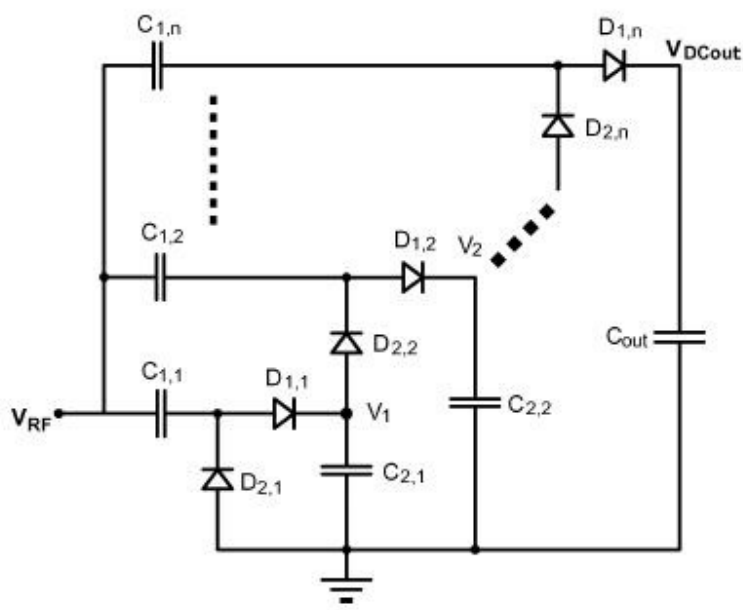**Figure 3.6:** Rectifier with N gain stages in cascade [15]

A set of criteria is successfully presented by De Vita and Iannaccone [29], for the optimization of the voltage multiplier, the power-matching network. It is worth to mention that one significant result in this research is that the maximum power efficiency is obtained by using the minimum number of stages as can be seen in Figure 3.7.
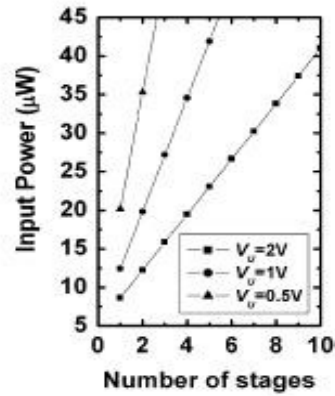
Figure 3.7: Required input power versus the number of stages for an output power of 5μW, for an I_s of $10^{-17} A$ [29]

3.1 Matching Network and Rectifier Design

In order to obtain a high power at the output ports of the rectifier, the impedance mismatch between the antenna and rectifier must be minimized. Figure 3.8 shows the matching network attached to the antenna's feed line port. This matching network comprises microstrip transmission lines which is the most straightforward approach for matching between two complex impedances. Attaching of matching network on the antenna feed substrate layer enables us to use the antenna surface effectively [32].

Figure 3.8: Picture of the attached matching network to the feed line [32]

Conventional design strategies of micro-power rectifiers are based on two assumptions. First, maximum output voltage yields maximum efficiency. Second, fewer stages, and thus fewer power-dissipating devices, give higher efficiency. This assumption does not take transistor sizing, parasitic, and leakage into consideration. Consider one rectifier stag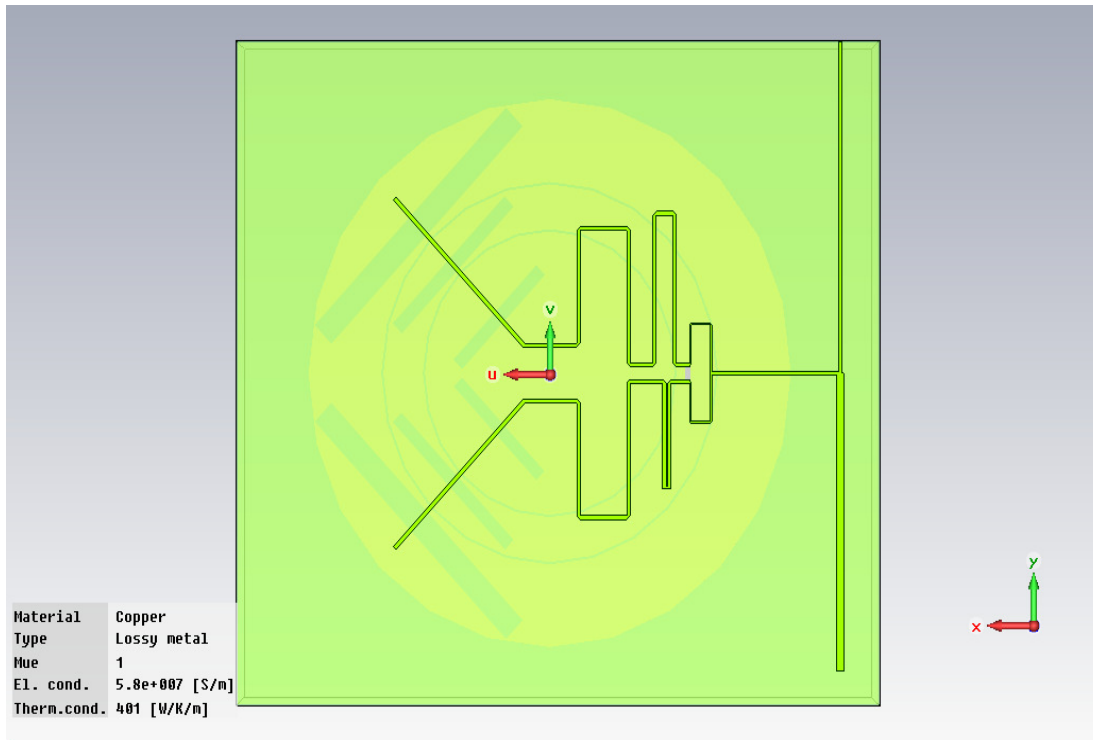e with the capacitor values fixed. To achieve a higher voltage, the resistances of the transistors have to be small, and large transistors have to be used, leading to larger parasitic loss and leakage. On the other hand, if the transistors are too small, then the charge transfer is incomplete, leading to a low output voltage and, thus, low efficiency. Hence, an optimal size of transistors is considered to achieve the maximum efficiency [33]. From the system point of view, the rectifier circuit must be designed to reduce threshold voltage loss as much as possible to improve the efficiency of the RF-DC power conversion system. In this research, one stage conventional voltage doubler rectifier, which comprises Schottky diodes and capacitors, is used, thus, increased losses due to increased stages were reduced. Schottky diodes are employed due to their shorter transmit times, low turn-on voltage, and low cost. The antenna, the circuit equivalent of matching network and the rectifier are shown in Figure 3.9.
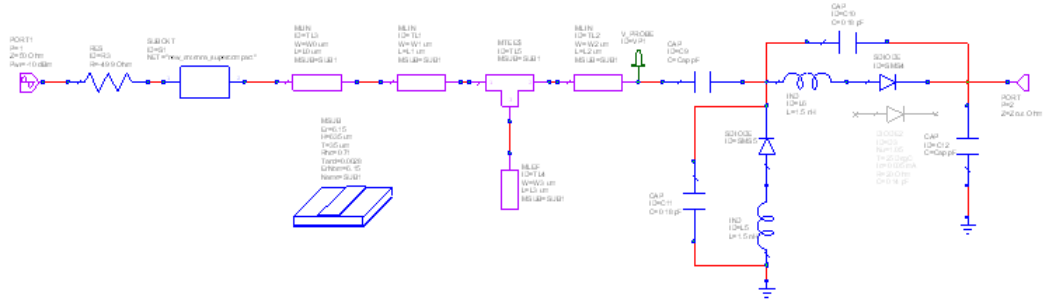
Figure 3.9: The equivalent circuit representation for the antenna, the matching network and the rectifier

The voltage doubler rectifier structure is considered for the design of the RF-DC power conversion system because it rectifies the full-wave peak-to-peak voltage of the incoming RF signal. The voltage doubler rectifier in Figure 3.10 consists of a peak rectifier formed by D_2 and C_2 and a voltage clamp formed by D_1 and C_1. The voltage clamp and the peak rectifier are arranged in cascade configuration to provide a passive level shift in voltage before rectification. In the negative phase of the input, current flows through D_1 diode while D_2 is cutoff. The voltage across diode D_1 stays constant around its threshold voltage and the voltage at node is charged to $-V_{th1}$. At the negative peak, the voltage across capacitor C_1 is $V_{amp} - V_{th1}$ (where V_{amp} is the amplitude of the input signal.) In the positive phase of the input, current flows through diode D_2 while D_1 is in cutoff. The voltage across capacitor C_1 remains the same as the previous phase because it has no way to discharge. At the positive peak, the voltage across D_1 is $2V_{amp} - V_{th1}$. Since D_2 is conducting current to charge C_2, the voltage at the output is a threshold voltage below that across D_1, i.e., the voltage at the output V_{out} is $2V_{amp} - V_{th2} - V_{th1}$ [15]. The parasitic components that affect performance of the RF-DC power conversion also can be seen in same figure (Figure 3.10).
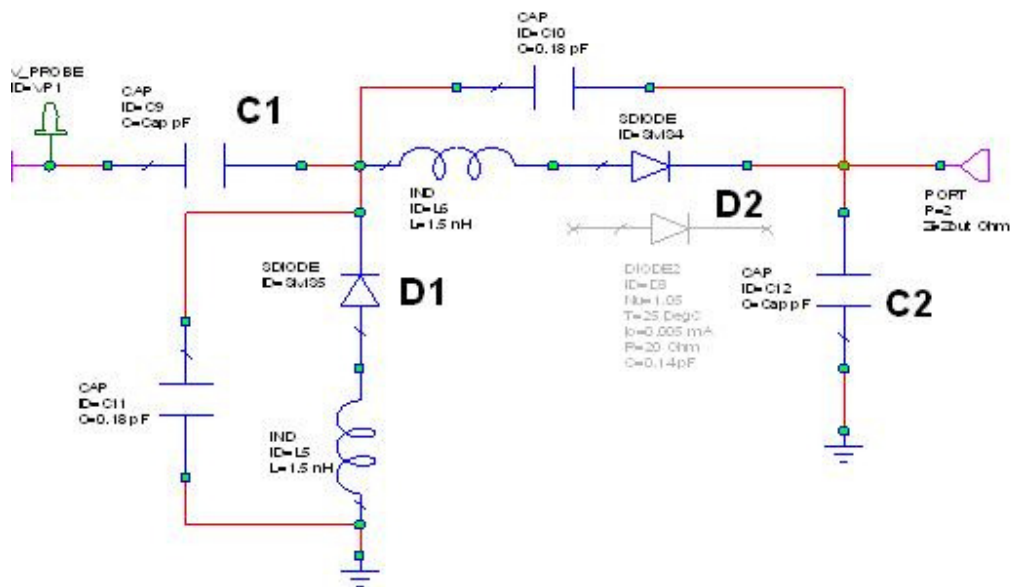
Figure 3.10: Conventional voltage doubler rectifier and parasitic components of diodes

Figure 3.11 (a)-(b) show the simulated real and imaginary of impedances of the antenna without matching network, the antenna with matching network and the rectifier around the operating frequency band. From the simulation data, the impedance of the antenna with matching network and rectifier match well in comparison to the antenna without matching network at the intended bandwidth. In order to maximize the power transfer from antenna to rectifier, the antenna and the rectifier input impedances should be complex conjugates of each other.

(a)

Frequency [GHz]
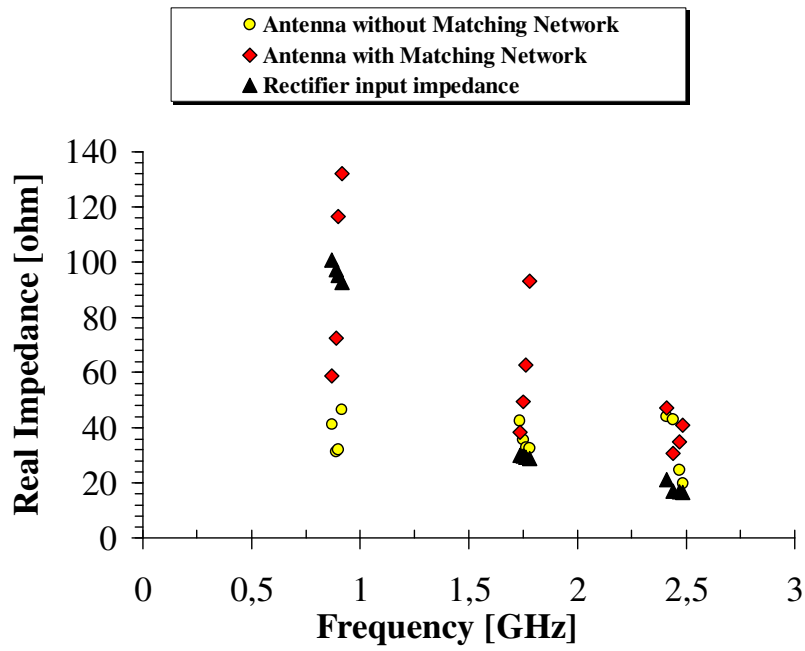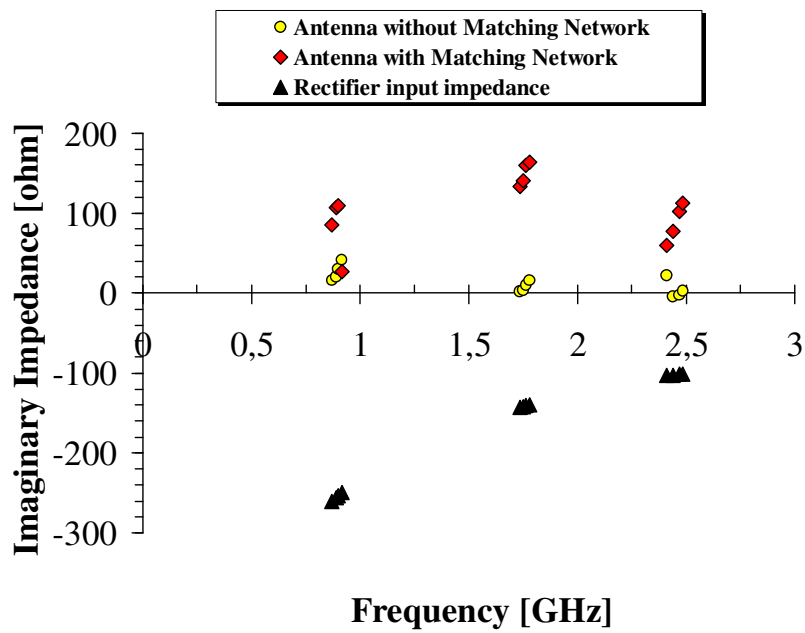
(b)

Figure 3.11: **(a)** Real and **(b)** Imaginary parts of the impedances of the antenna, the antenna with matching network, and the rectifier

43

In figure 3.12 (a)-(b)-(c), simulated results are shown for RF received power at the rectifier input ports versus DC power at the rectifier output ports for the intended frequency bands of 0.9GHz, 1.76GHz, and 2.45GHz. In same figure, incident power density in the environment also presented. As it can be seen in the same figure, DC power conversion is more efficient at lower frequency band since the antenna effective area, which is increased by longer wavelength, is related to antenna gain.
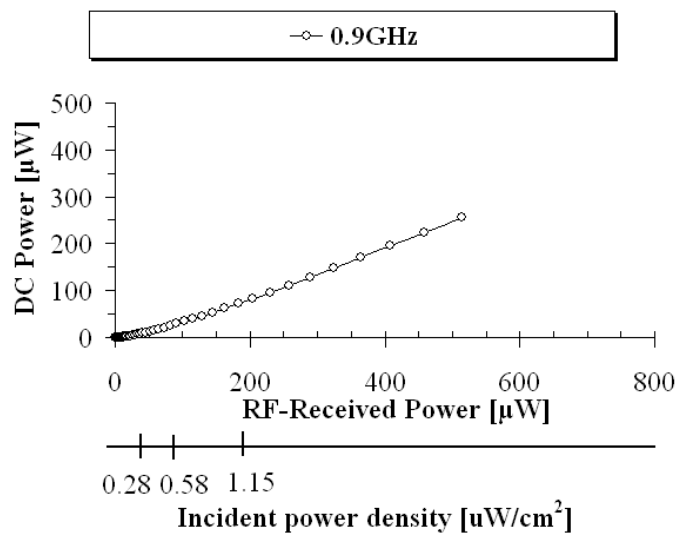
(a)
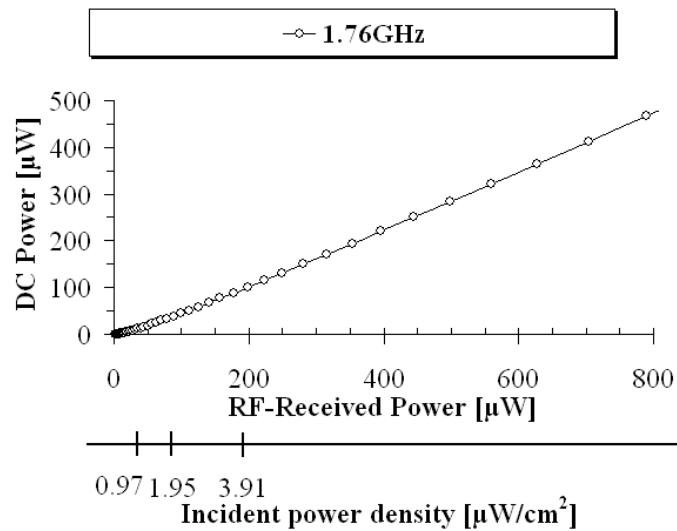
(b)

Figure 3.12: Output DC power as function of the input power **(a)** at 0.9GHz **(b)** 1.76GHz and **(c)** 2.45GHz

44
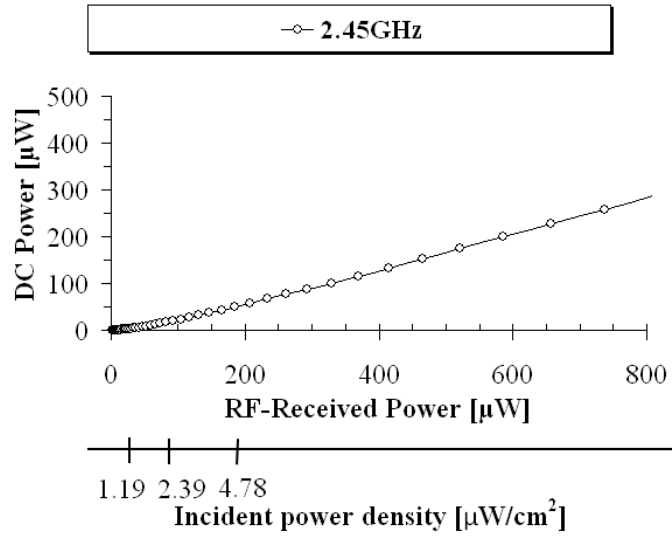
(c)

Figure 3.12: (continued) Output DC power as function of the input power **(a)** at 0.9GHz **(b)** 1.76GHz and **(c)** 2.45GHz

The global rectifier efficiency defined as;

$$\eta = \frac{\text{DC Output Power}}{\text{Incident RF Power}} \qquad\qquad \textbf{(3.1)}$$

Figure 3.13 shows a simulated result of the conversion efficiency with respect to the RF received power. In Figure 3.13, the maximum conversion efficiency 62% is achieved at 1.8mW at 0.9GHz and 1.76GHz and it increases rapidly with the input microwave power up to a maximum value. Conversion efficiency higher than 50% is obtained from 0.8 to 1.8mW RF received power at the rectifier input ports. When received power exceeds 2mW, the conversion efficiency decreases gradually with increasing input power. It is clear that more than 40% of the microwave input power is consumed in the diodes. Consequently, for achieving higher conversion efficiency, it is necessary to obtain diodes with reduced power consumption.
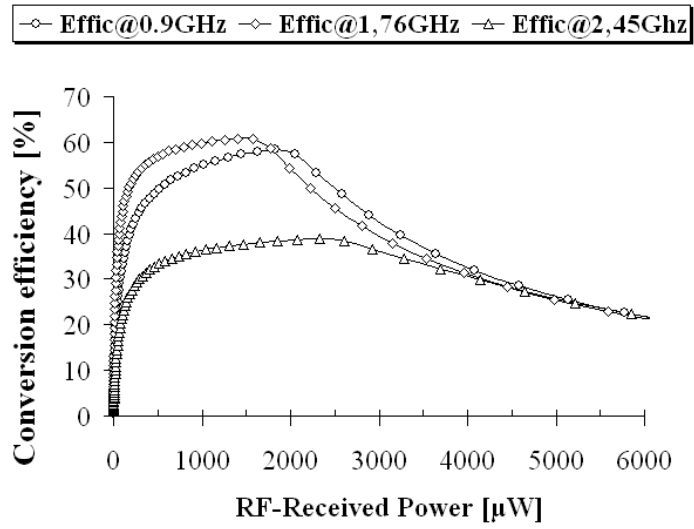
Figure 3.13: Power conversion efficiency as function of input power at the input ports of rectifier at the intended frequency bands

4. WEARABLE TEXTILES

In order to design an Aperture Coupled Patch Antenna with textiles, a selection of suitable textile materials are required. Conductive textiles are applied for the microstrip patch, the ground plane, and the feed line while non-conductive textiles are needed for the antenna substrate and feed substrate layers. Moreover, this two-layer antenna structure allows an independent selection of antenna substrate and feed substrate material in order to optimize the antenna characteristics [14].

4.1 Electro-textiles

In order to obtain better performance of the antenna, a conductive fabric needs to satisfy the requirements listed below.

• A low and stable electrical resistance ($\leq 1\,\Omega/\square$) of the fabric is desired to minimize losses.

• The (sheet) resistance must be homogeneous over the antenna area. In other words, the variance of the resistance must be small.

• The fabric should be flexible such that the antenna can be deformed [12].

In our research, we established that an electrical resistance of ($\leq 0.1\,\Omega/\square$) is a reasonable choice for conductive fabrics.

4.1.1 Conductive fibers

There are three methods of creating conductive fibers:

1) The filling of fibers with carbon or metal particles;

2) The coating of fibers with conductive polymers or metal;

3) The use of fibers that are completely made of conductive material [13].

The state-of-the-art conductive fibers are highly conductive metal wires and plated fibers, which are superior to other alternatives in terms of conductivity. Many alternatives in the construction of the fibers exist, however Nickel, Copper and Cobalt plated nylon fibers are the main selected fabric models in this research. The detailed picture of fabric antenna is shown in Figure 4.1.
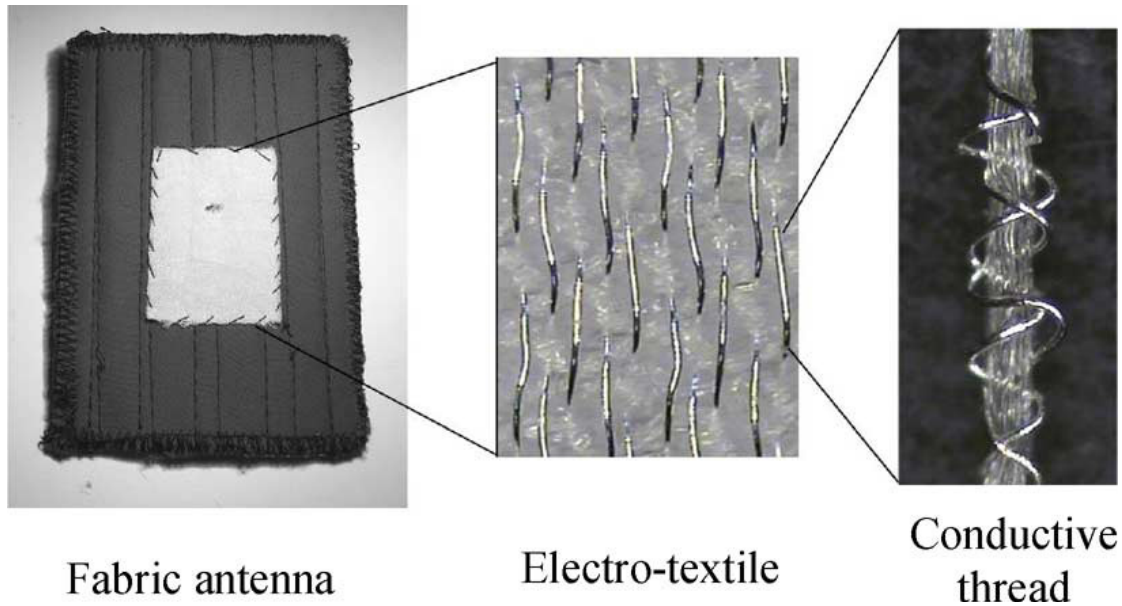
Figure 4.1: Fully fabric antenna constructed from electro-textiles [13]

4.1.2 Conductive threads

Conductive threads are created from single or multiple strands of conductive and nonconductive fibers. As shown in Figure 4.2, there are two categories of conductive threads: multifilament threads (see Figure 4.2 (a)–(d)) and monofilament threads (see Figure 4.2 (e)). Each has different electrical properties as well as wearability and reliability characteristics. The monofilament conductive thread shown in Figure 4.2 (e) is composed of single silver plated copper fiber (diameter 40μm). The X-static thread (see Figure 4.2 (a)) is formed by twisting many thin elastic silver plated nylon fibers together. The Litz wire (see Figure 4.2 (b)) contains 60 copper fibers, each of which has a diameter of 40μm. The threads in Figure 4.2 (c) and (d) are composite threads of insulating and metallic fibers. Both composite threads are created by spinning 40μm silver plated copper fibers around a nonconductive core which is composed of multiple

48

nonconductive fibers. The strong nonconductive fibers can protect the thin fragile conductive fibers from external tension, which makes the conductive threads more mechanically robust and still maintaining the electrical functionality. When elastic nonconductive core is used as in Fig 4.2 (d), the conductive thread becomes stretchable which is a desirable feature for wearability and the fabric takes on the feel of a traditional material [13].
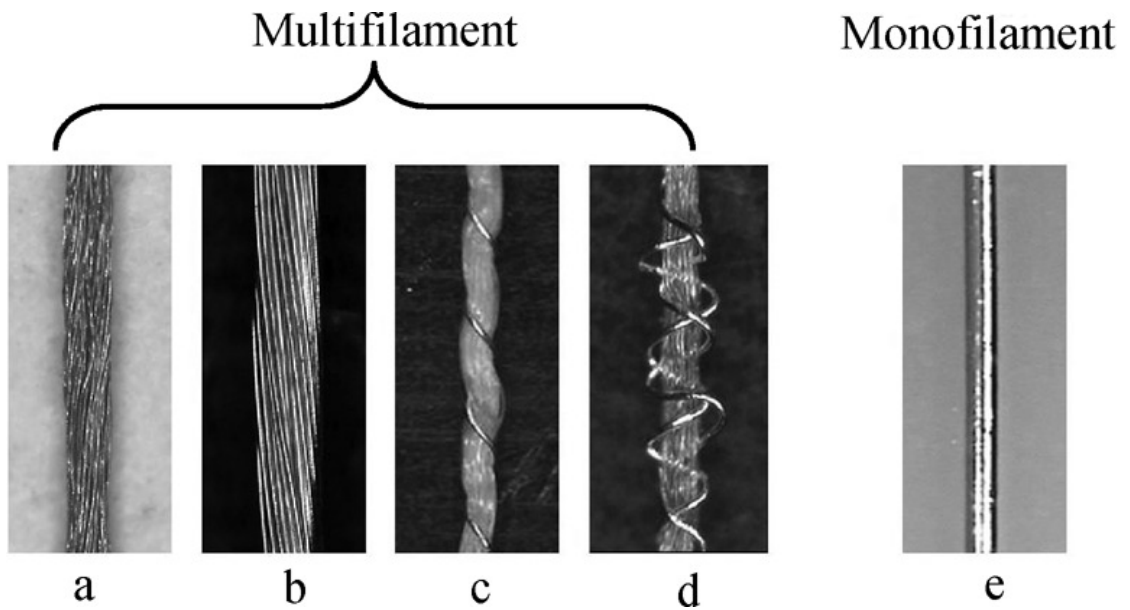
Figure 4.2: Various conductive threads [13]

4.1.3 Conductive Fabrics

Electro-textiles are mostly created by incorporating conductive threads into fabrics by means of weaving and knitting. The selection of the conductive threads and of the textile structure specifies the efficiency of the textile as an equivalent electro conductive material and guarantees its durability. In knitted fabrics, the threads meander through and create interlocking loops, while in woven fabrics the threads are straight in two orthogonal directions (see Figure 4.3 (a)-(b)). Traditionally, conductive threads are used in both directions in conductive woven fabrics. It is also mentioned in the research [13] that the application of woven fabrics which have conductive threads in only one direction and nonconductive threads in the other direction, this arrangement adds to the wearable feel of the fabric, while affecting the electrical parameters.

<center>(a)   (b)</center>
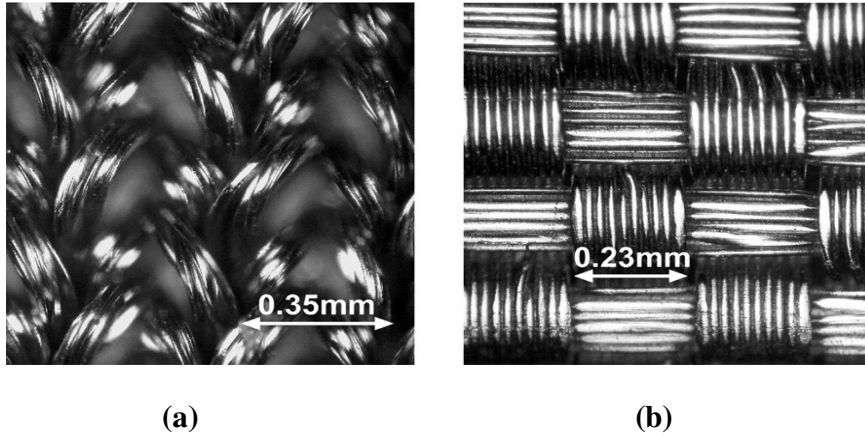
Figure 4.3: (a) Conductive, knitted and **(b)** woven Nora fabric [12]

4.1.4 Shape precision of the conductive fabrics

The woven antenna patch can only be shaped with the finite precision given by the thread thickness. In fact, the thread pitch virtually "discretizes" the possible sizes of the conductive patches. Assuming an antenna patch consists of N threads in one direction. The patch width then corresponds to N times thread pitch. Notice that the next possible width of the patch is either (N+1) times thread pitch or (N-1) times thread pitch [12].

4.2 Conductive Fabric Manufacturers

In the applications for the aperture coupled patch antenna, the most popular and effective conductive fabrics are Flectron, Shieldit and Zelt, please see references [14] and [18]. The manufacturer of these brands is Less EMF Inc. which offers electromagnetic, RF and microwave shielding for proper applications. Products are suitable for our desired purpose due to low dielectric resistivity ($\leq 0.1\Omega/\square$) and flexibility. Advance technology offers impressive options to consumers. On the web-site of the company many products are exhibited with appealing features. Please see the reference [34] in order to get more info on the products. As it can be seen in Figure 4.4, the conductive fabrics are flexible, and easy to cut and sew like ordinary fabric.

<center>50</center>
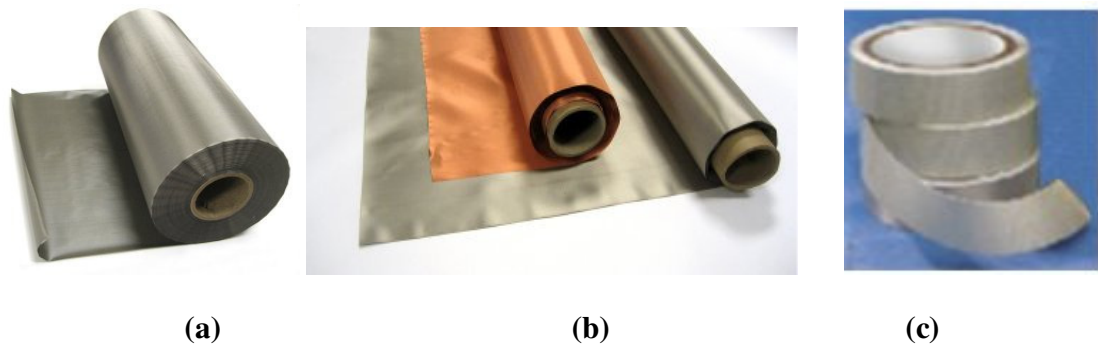
Figure 4.4: (a) Shieldit Super, **(b)** Flectron and **(c)** Ni/Cu/Co Fabric Tape [34]

In Figure 4.4 (a) Shieldit Super is based with a rugged plain weave nylon, plated with Nickel and Copper, then coated on one side with conductive acrylic which's resistivity is less than $0.1\Omega/\square$, plus a hot melt (203° - 338°F) adhesive with polyethylene barrier on the other side that provides excellent moisture resistance, and washability. It can be even iron on to cotton, wood, glass or paper, and also cut and sewn like ordinary fabric. The conductive and the adhesive sides are illustrated in Figure 4.5.
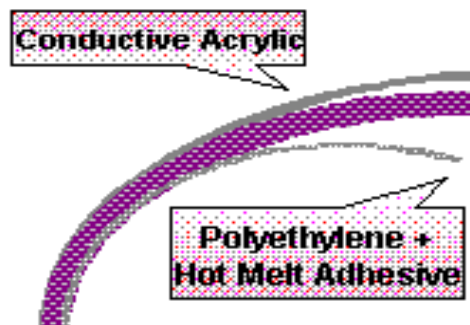
Figure 4.5: Shieldit Super's upper and lower sides [34]

In the reference [14], it is mentioned that for the antenna patch, the Shieldit fabric was preferred because it has an additional adhesive layer which makes it easier to attach the patch to the substrate layer. Shieldit is a plain weave nylon, plated with nickel and copper and therefore very conductive (less than $0.1\Omega/\square$). Moreover, it can be handled like an ordinary fabric.

The Flectron which is illustrated in Figure 4.4 (b) is the company's highest conductivity fabric. It is pointed out on the web-site that Flectron is a high quality copper plated nylon ripstop fabric with an amazingly low surface resistivity of less than $0.1\Omega/\square$. Light

weight with thickness of 0.006" (0.1524mm) and flexible, it is highly tear resistant and can be cut and sewn like ordinary fabric. On the other hand, Flectron fabric is not recommended for applications where laundering or dry cleaning will be needed. Material will tarnish with exposure to liquids and skin oils. It is emphasized in [35] that for the conducting parts Flectron is chosen because of its low surface resistivity and its large temperature range (-40C to 180C), which allows to solder the connector without burning holes in the electro-textile. Furthermore, in the research [14] which is on integration of aperture coupled patch antennas into textile systems, the microstrip feed line and the ground plane are made out of Flectron by the reasons that are mentioned before. One more fabric is worthwhile to mention with its properties of conductive adhesive and more robust to fray. As shown in Figure 4.4 (c), Ni/Cu/Co tape enables us to cut or slit quite narrow widths without losing electrical properties. By reference [36] it is possible to make a clear comparison of all kinds of conductive fabrics regarding their major characteristics.

4.3 Non-conductive Fabrics

The non-conductive fabric provides the dielectric between the antenna patch and the ground plane, also between the ground plane and the microstrip feed line. It requires constant thickness of few millimeters or less due to the antenna design and stable permittivity in order to prevent electrical properties of model from undesired modifications. Fleece and felt fabrics are generally employed in wearable antenna researches due to their low permittivity. In the research [35], it is mentioned that a Fleece fabric is used as antenna substrate with a thickness of 2.56mm, because of the inherent piled structure, the Fleece contains much air and therefore the permittivity is close to one, thus, low permittivity of the antenna substrate allows the design of antennas with a large gain and a high efficiency. Felt fabric is more appropriate as a feed line substrate due to its higher permittivity with respect to Fleece. The choice criteria of Felt as a feed line substrate are explained that because Felt is a denser textile material, it has a higher permittivity. In addition, the radiation losses are restricted by selecting a thinner material [14]. Tiantai Industrial Cloth Ltd. provides many alternatives to consumers who are dealing with Felt applications [37].

For higher dielectric constant applications such as between 3.5 and 6.5, Saint-Gobain Quartz offers a unique material Quartzel Fabric which is produced from quartz crystal fibers. Besides dielectric constant, Quartzel is employed in many different applications due to its very low loss tangent. Dielectric constant and loss tangent versus frequency is illustrated in Figure 4.6.
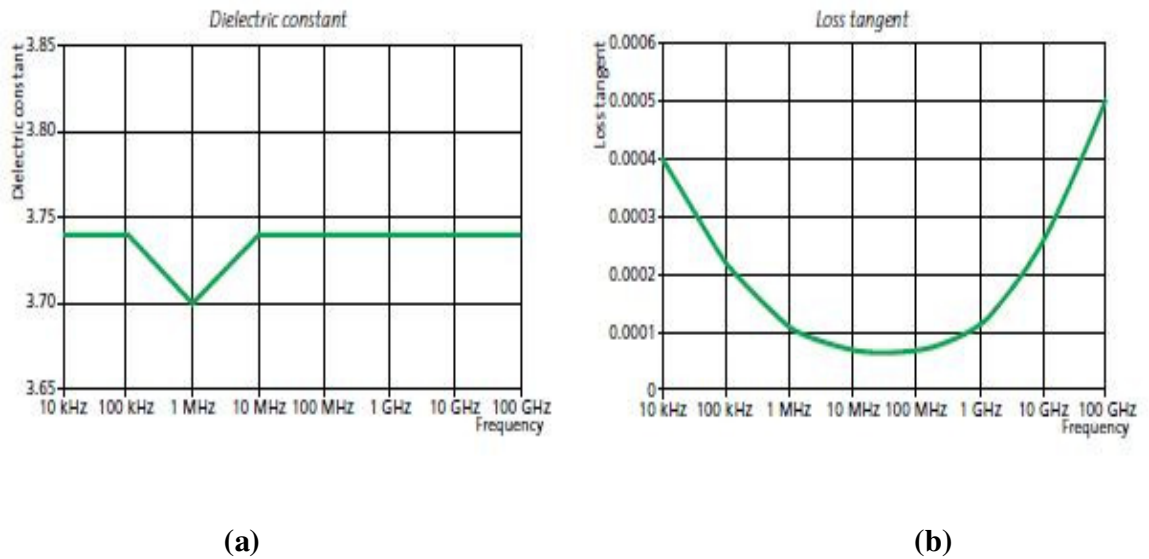

<div align="center">(a)</div> <div align="center">(b)</div>

Figure 4.6: (a) Dielectric constant and **(b)** loss tangent versus frequency [38]

As it can be seen in the figure (Figure 4.6 a-b), dielectric constant almost stays stable with the value of 3.74, while loss tangent differs from approximately 0.0001 to 0.0005 which is impressive for antenna applications in the frequency range 10kHz to 100GHz .

In Figure 4.7 a-b, comparative dielectric properties of fibers at 1MHz and 10GHz are shown. E Glass, D Glass and R/S Glass are materials made from extremely fine fibers of glass to be used as a reinforcing agent for many polymer products; the resulting composite material, properly known as fiber-reinforced polymer (FRP) or glass-reinforced plastic (GRP), is called "fiberglass" in popular usage while Aramid fibers which are used in aerospace and military applications, for ballistic rated body armor fabric, and as an asbestos substitute are a class of heat-resistant and strong synthetic fibers, on the other hand, Polyethylene is a thermoplastic commodity heavily used in consumer products, notably the plastic shopping bag [39]. As is seen, Quartzel Fabric is the best in term of loss tangent while Aramid is the worst. However, if intended

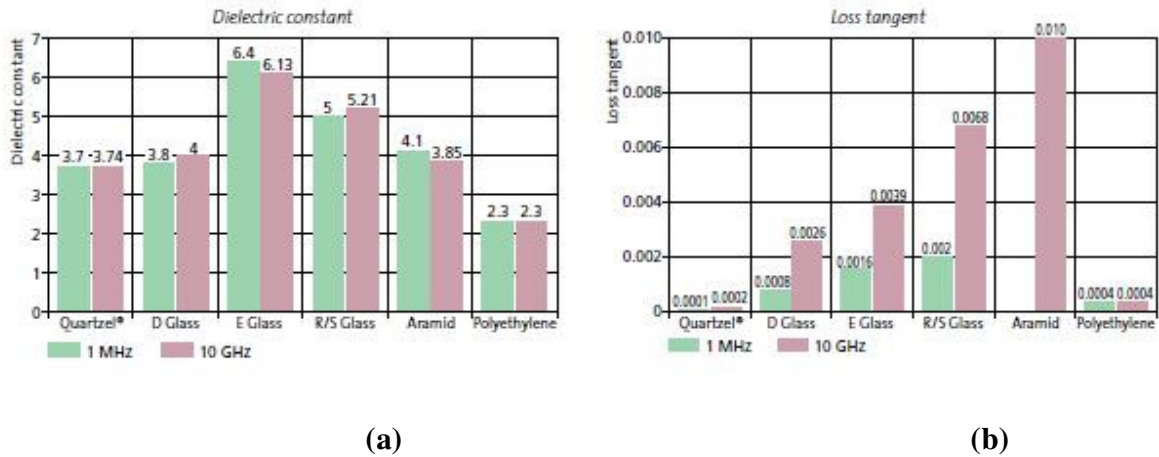dielectric constant is higher than 5, E Glass could be more convenient and also cheaper than Quartzel.

(a)   **(b)**

Figure 4.7: (a) Comparison of dielectric constants and **(b)** loss tangents [38]

It is worth to remark that the characteristics that are presented above are for virgin filaments. When materials are composed with another compound, e.g. resin, this usually affects the dielectric properties. In Table 4.1, the change of dielectric properties of different fibers with same resin can be seen.

Table 4.1: Comparison of different fibers with same resin [38]

	Frequency	Dielectric constant	Loss tangent
Quartzel	9.368GHz	**3.08**	**0.0022**
D glass		3.11	0.0037
Aramid		3.12	0.0049
E glass		3.95	0.0055
Quartzel	37.50GHz	**3.07**	**0.0024**
D glass		3.10	0.0045
Aramid		3.11	0.0057
E glass		3.86	0.0090

The similarities to normal fabrics in terms of flexibility and softness of Quartzel can be observed in Figure 4.8.
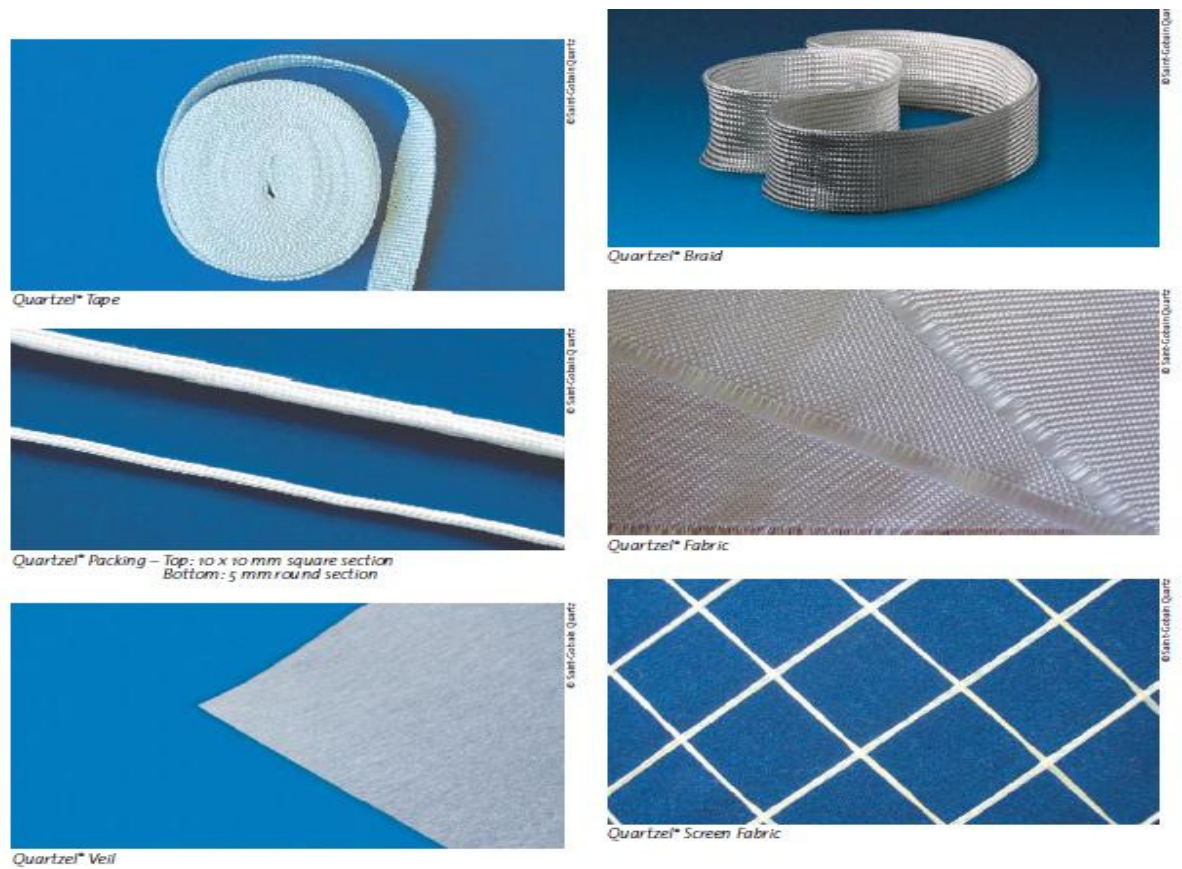
54

Figure 4.8: The pictures of Quartzel product in different types [38]

4.3.1 The permittivity extraction

Since the non-conductive material's dielectric properties are not known exactly due to their employment generally in different specific fields instead of the antenna applications, some methods are available in order to understand the dielectric properties of traditional non-conductive fabrics. In research on design of textile patch antenna [12], the technique that explained by *Grzyb et al*. in [40] was used to extract the permittivity of the textile substrates. This method utilizes scattering parameter measurements of two microstrip transmission lines of different lengths. Moreover, it is mentioned that "the relative permittivity of the Fleece fabric has been derived by comparing the measured and simulated resonance frequencies of a rectangular patch antenna and has been found to be 1.25." at the another research [35].

4.3.2 The composition of the conductive antenna structures with the dielectric substrates

In the antenna manufacturing process, the composition of the conductive antenna patch with the dielectric substrate is critical. First of all, the dimensions of the patch must be retained while being attached to the substrate. Second, the attachment procedure must not affect the electrical properties of the patch, e.g., the sheet resistance. For composition, the following four methods were evaluated by *Locher et al.* in [12].

1) Liquid textile adhesive (brand: Golden Fix);

2) Point-wise application of conductive adhesives;

3) Sewing;

4) Adhesive sheets, which are activated by ironing.

If the results are required to be presented in detail, application of the liquid textile adhesive 1) on conductive fabrics is impractical because the adhesive acts as insulator among the conductive yarns and electrical resistance shows inhomogeneity, and it could rise by a factor of ten at certain spots due to the uneven distribution. In the same way, second method is useless since mechanical stability was significantly worse. Similarly for sewing 3), attention needs to be paid preventing warpage during the sewing process. Second, the seam spacing must be smaller than 2cm in order to minimize wrinkling. This behavior is illustrated in Figure 4.9. A wrinkling corresponds to uneven distances between the antenna patch and the ground plane resulting in distortion of the antenna characteristic. A stitch passes through both the patch and the ground plane of the antenna. Shorts between antenna patch and ground plane can be observed because the sewing needle pulled small conductive fibers from the patch through the substrate and shorted them with the ground plane. The adhesive sheets 4) have the best performance. It evenly deposits as a thin layer on the conductive textile by ironing. Moreover, the adhesive only penetrates the surface of the conductive textile such that patch sheet resistance and substrate permittivity are not changed [12].
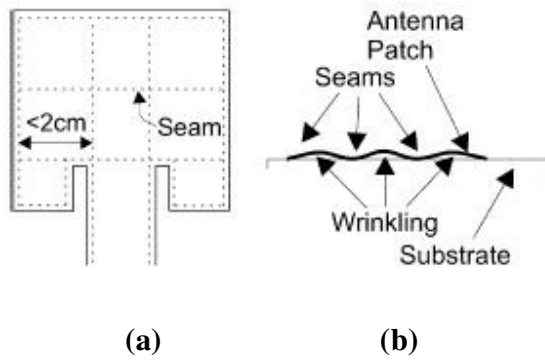
(a)   **(b)**

Figure 4.9: Sewed antenna **(a)** Sewed antenna patch with seam grid **(b)** Wrinkling of antenna patch between seams (cross section) [12]

4.3.3 Effects of bending

In realistic applications the antenna is integrated into parts of clothes that can be bent. Therefore, antennas should properly function even if they are bent. The reference [35] discusses the influence of bending on the return loss (S_{11}). The two prototypes were attached to plastic cylinders with two diameters: D=12cm and D=7.5cm. Although the antenna bent causes shift of the resonance frequency and change of bandwidth, in that research purposed band ISM remains covered (Figure 4.10).
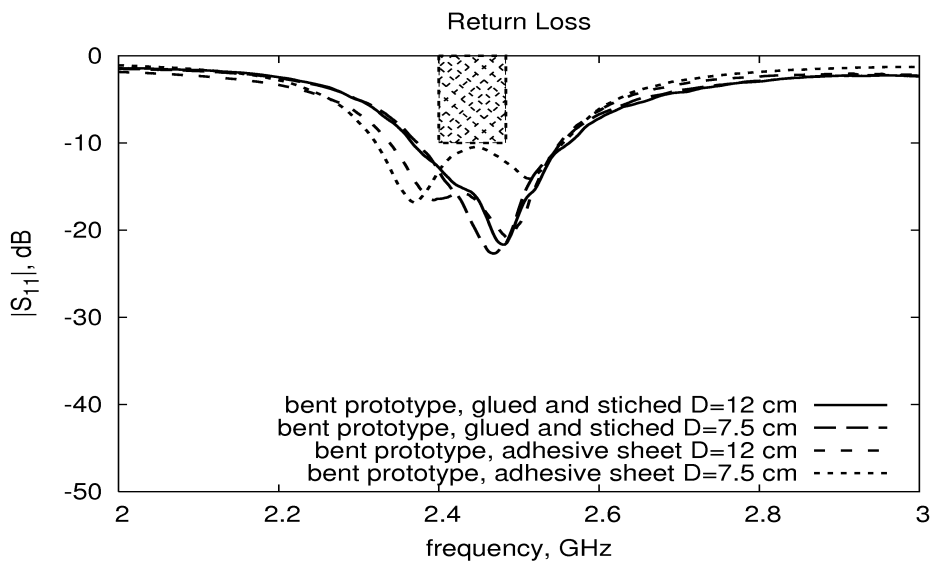

Figure 4.10: Influence of bending on the return loss (S11) of the prototypes [35]

57

In the same research, it was also investigated the return loss at different time instants in order to prove the stability of the antenna characteristics in time. The result for the first prototype which relies on a glue stick to attach the different layers to one another, and additionally stitched in order to obtain a uniform thickness is shown in Figure 4.11.
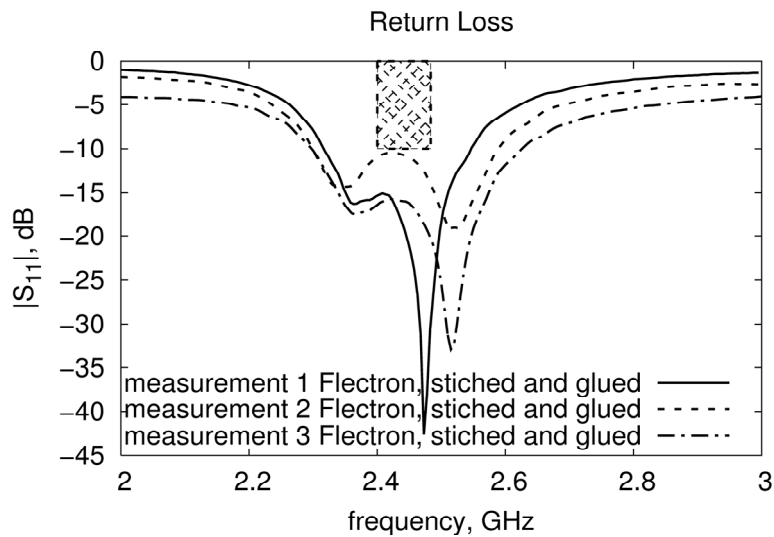

Figure 4.11: Return loss (S11) of the first prototype [35]

It is mentioned that measurement 1 was performed a few days after construction, measurement 2 a few weeks after construction, whereas measurement 3 was performed six months after construction. Although some variation in the measured return loss is seen, especially in the antenna bandwidth, the antenna provides complete coverage of the ISM band that is purposed by researchers. Similar conclusions can be drawn from Figure 4.12, where the evolution of the return loss in time is for the second prototype which assembled using the adhesive sheet. It can be seen that a slight shift in resonance frequency is noticeable between the different measurements, as well as some variation in the antenna bandwidth [35].
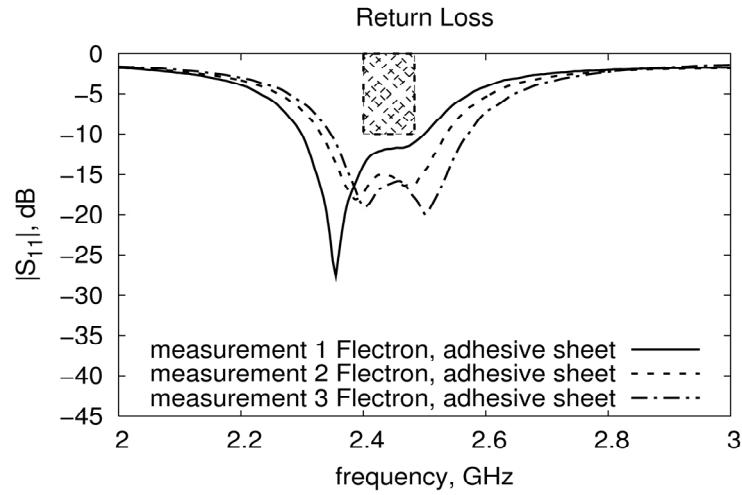
Figure 4.12: Return loss (S11) of the second prototype [35]

4.3.4 Influence of body

For the intended application, additionally the effect of human body on the antenna's return loss is presented. Therefore, the effect of the human body, represented by a substrate with $\in_r=53.3$ and $\sigma=01.52$ S/m located 8mm below the antenna ground plane, was investigated in the research [14]. As it can be seen in Figure 4.13 that, even in the vicinity of the human body, the antenna matching remains sufficient, although losses increase.

Figure 4.13: Return loss in vicinity of the body [14]

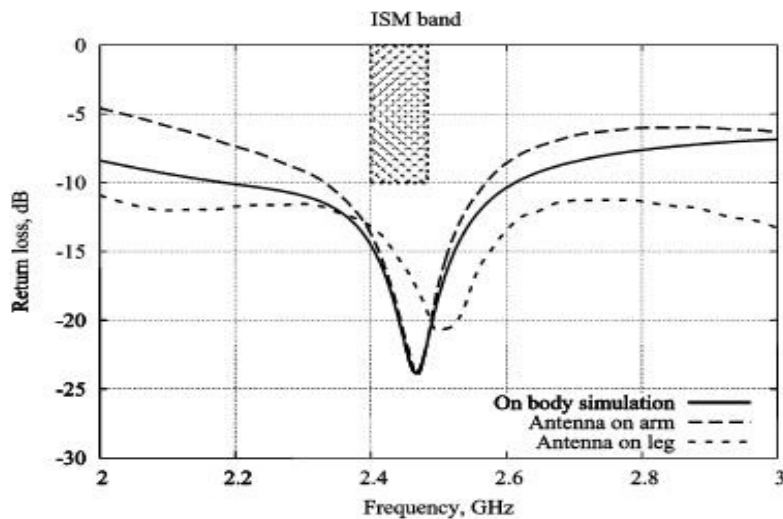In another research [35], the effect of human body to the antenna gain is presented. Therefore, an extra layer with $\in_r = 42$ and $\sigma = 0.99$S/m was used. Figure 4.14 shows that the presence of the human body only has a marginal influence on the antenna gain.
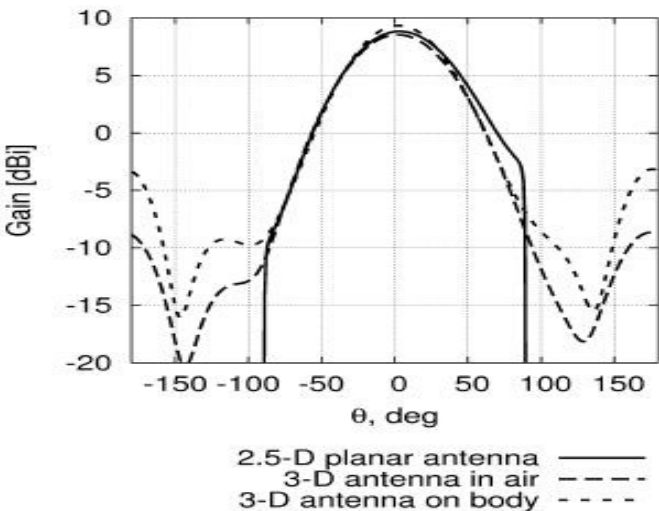

Figure 4.14: Influence of the body on the gain [35]

5. TEXTILE ANTENNA DESIGN

5.1 Material selection and characterization

The first step in the design of a textile antenna consists of choosing appropriate materials for the antenna and feed line substrates and the conductive parts. As an antenna substrate, we used a Fleece fabric with a thickness of 4mm and the dielectric constant of 1.25 instead of Polyhuretanic Foam, as found in the research [33]. As it is mentioned in the same research, due to the inherent piled structure, the Fleece contains much air and therefore the permittivity is close to one. Low permittivity of the antenna substrate allows the design of antennas with a large gain and a high efficiency. For the feed line substrate we used E-Glass material instead of Taconic because its dielectric constant, which is 6.13, is almost the same type of the latter. On the other hand, besides E-Glass material, Quartzel is used as a feed line substrate which has dielectric constant of 3.75 and a very low loss tangent of 0.0002.

For the conductive parts we chose Ni/Cu/Co coated nylon ripstop fabric, because of its low surface resistivity (less then 0.1 /sq) and its large temperature range (-10C to 80C), which enables us to solder the connector without burning holes in the electro-textile. It can be easily cut with scissors and used to create conductive pathways on surfaces or add shielding to cables and flexible conduits [34].

5.2 Antenna Measurements

The following results were obtained with the employment of E-Glass material as a feed line substrate. The simulations were conducted by using CST Microwave Studio 3-D field simulator. From figure 5.1, it can be noticed that the antenna simulation completely cover the GSM 900 and GSM 1800 bands, however, it does not include all the bandwidth for W-LAN, but the result is acceptable.

S-Parameter Magnitude in dB

Q 1	(0.87, -15.317)	
Q 2	(0.92, -12.64)	
Q 3	(1.73, -20.157)	
Q 4	(1.78, -10.993)	
Q 5	(2.4, -15.76)	
Q 6	(2.48, -4.8785)	

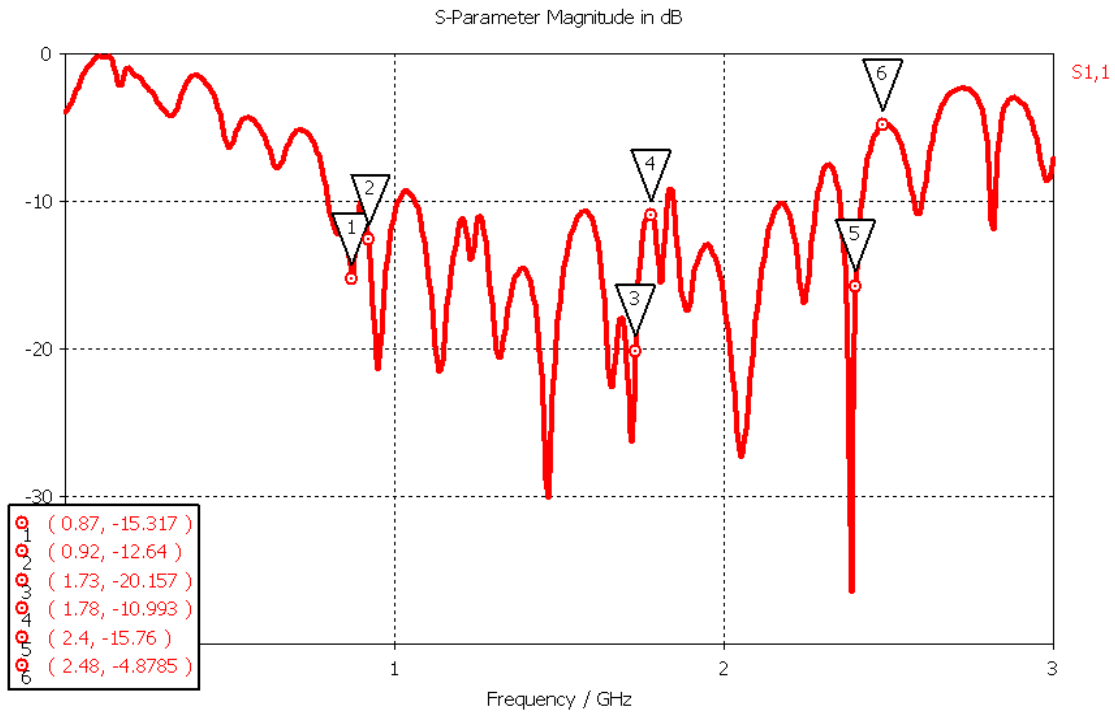**Figure 5.1:** Simulated return loss of the textile antenna by using E-Glass material

Figures 5.2 (a)-(b)-(c) show the simulated radiation pattern of the textile antenna in the E-plane at 0.89 GHZ, 1.74 GHz, and 2.45 GHz, respectively. Successful broadside radiation patterns are observed for each three bands. It can be seen that the electric field maximum value gradually decreases as frequency increases.
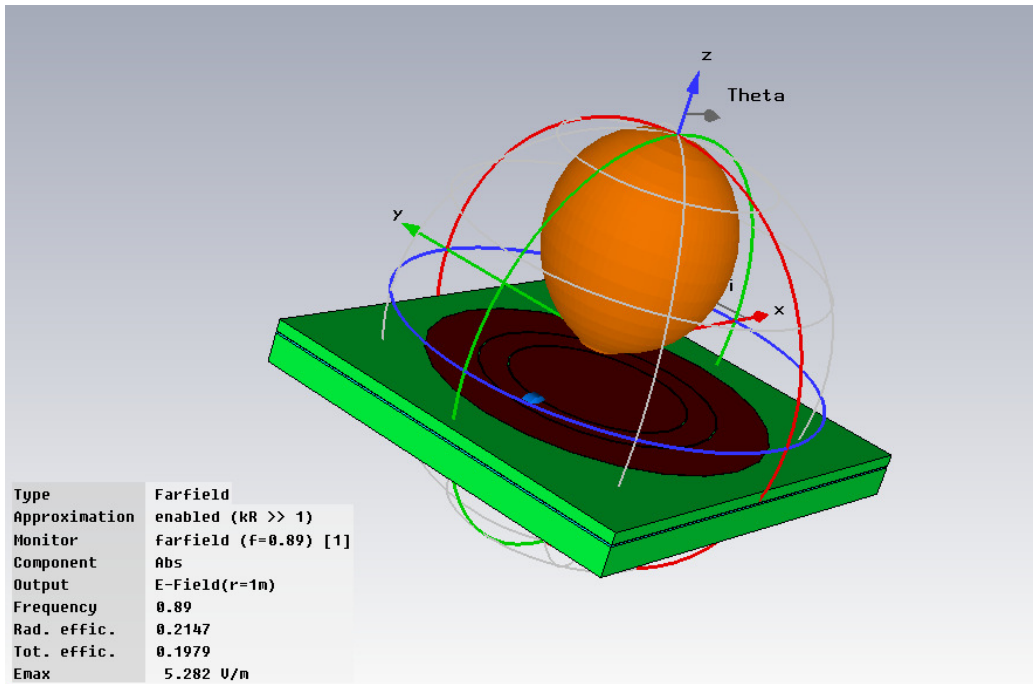
(a)
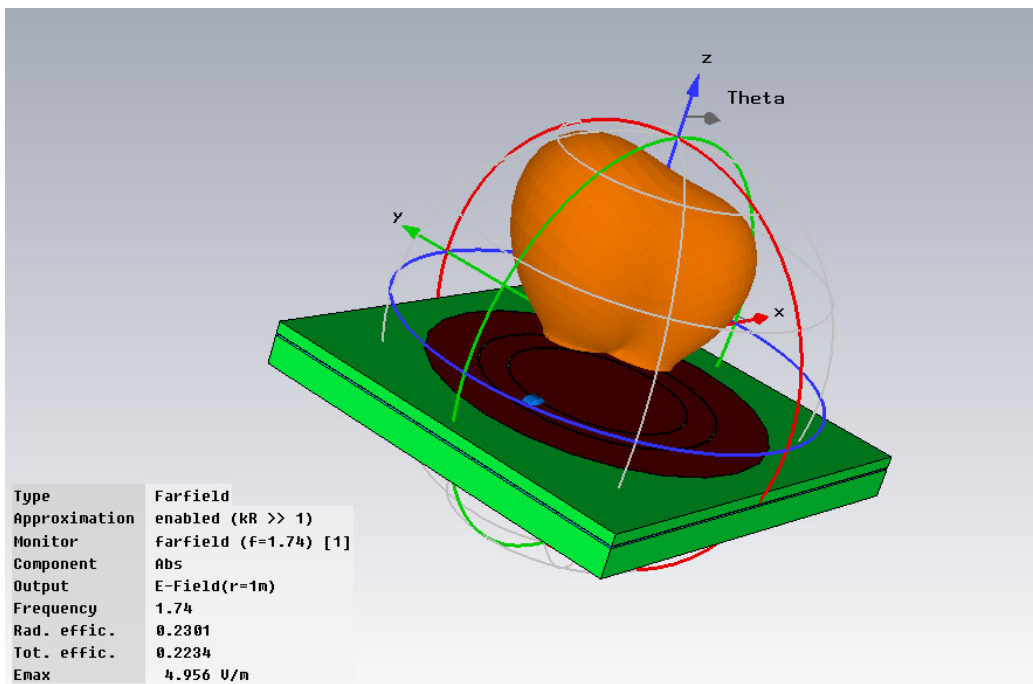
(b)

Figure 5.2: Simulated radiation pattern of the textile antenna by using E-Glass material at **(a)** 0.89GHz, **(b)** 1.74GHz and **(c)** 2.45GHz

Type	Farfield
Approximation	enabled (kR >> 1)
Monitor	farfield (f=2.45) [1]
Component	Abs
Output	E-Field(r=1m)
Frequency	2.45
Rad. effic.	0.1354
Tot. effic.	0.1005
Emax	4.325 V/m

(c)

Figure 5.2: (continued) Simulated radiation pattern of the textile antenna by using E-Glass material at **(a)** 0.89GHz, **(b)** 1.74GHz and **(c)** 2.45GHz

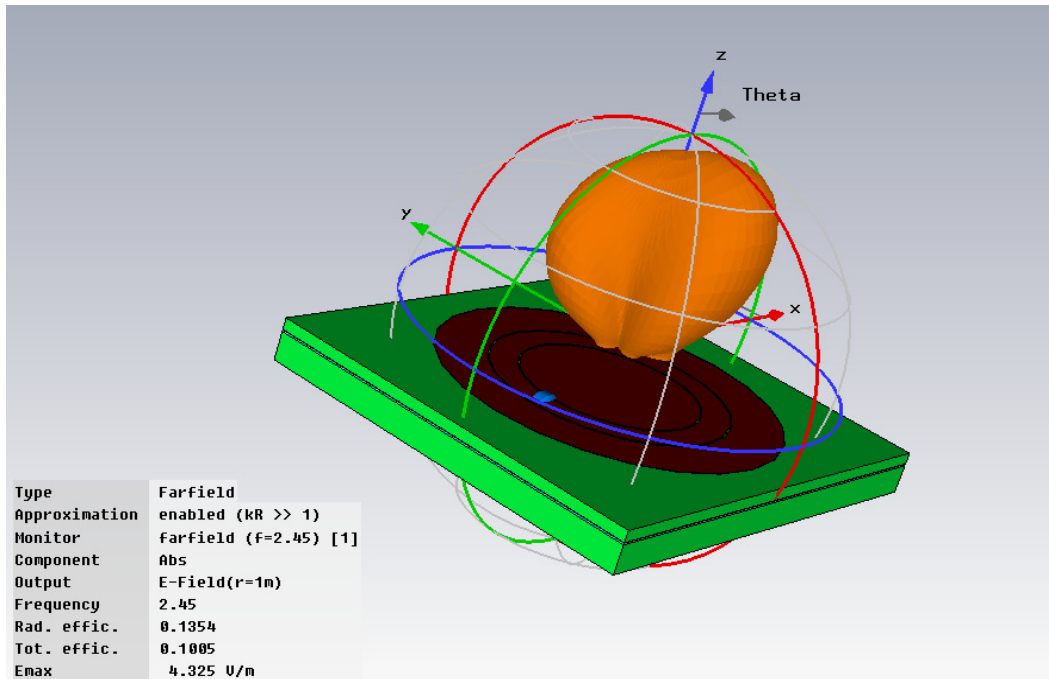Figure 5.3 indicates that the axial ratio, that should be lower than 6 in order to have circularly polarized antenna, is succeeded for the intended application.
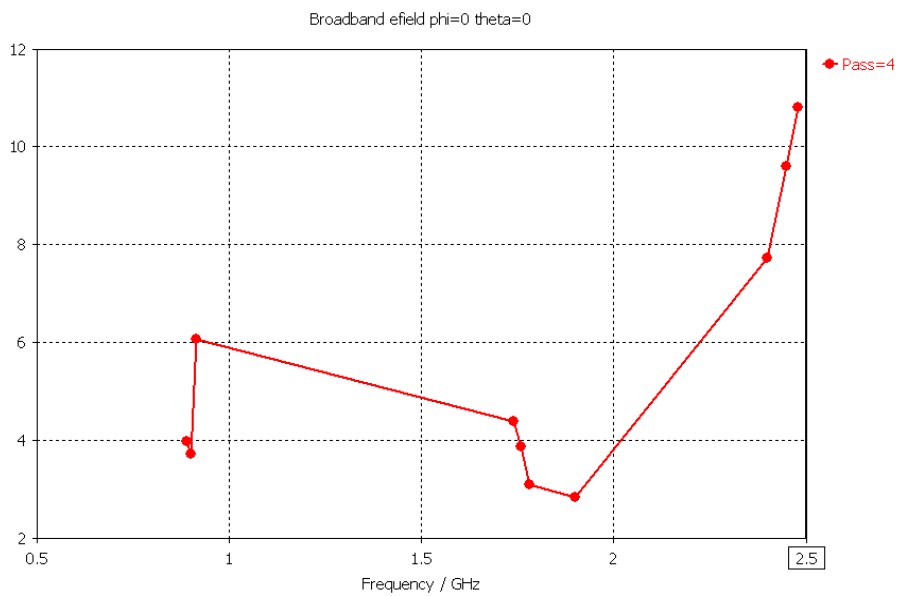

Figure 5.3: Simulated axial ratio of the textile antenna by using E-Glass material

64

The simulated antenna characteristics with Quartzel material are shown below. As it can be seen in Figure 5.4, W-LAN band is completely covered while the return loss of the textile antenna is sufficiently included for GSM 900 and GSM 1800 bands. As it is expected that E-Glass fabric gives better performance compared to Quartzel since the dielectric constant of E-Glass is closer to Taconic. Interestingly, improvement is observed at W-LAN band while the other two bands get worse. Nevertheless, the simulated return loss for Quartzel material is satisfying for frequency bands of interest.
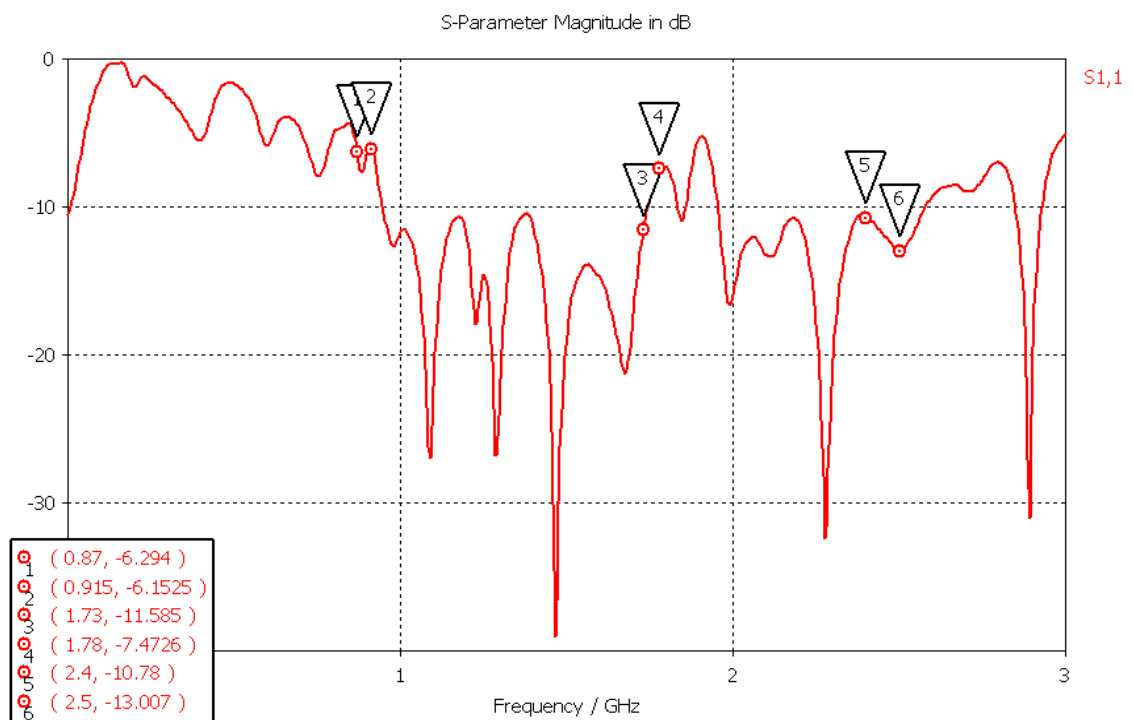
Figure 5.4: Simulated return loss of the textile antenna by using Quartzel material

The simulated radiation patterns at 0.89 GHz, 1.76GHz and 2.4 GHz are shown in Figure 5.5 (a)-(b)-(c). The best antenna radiation pattern is for GSM 1800 band while it is satisfactory for the remaining ones. Radiation patterns at the intended bands are weakened compared to E-Glass results (Figure 5.2) since the antenna resized in order to obtain the antenna impedance well-matched. Namely, feed line width and height of feed line substrate are optimized.

65
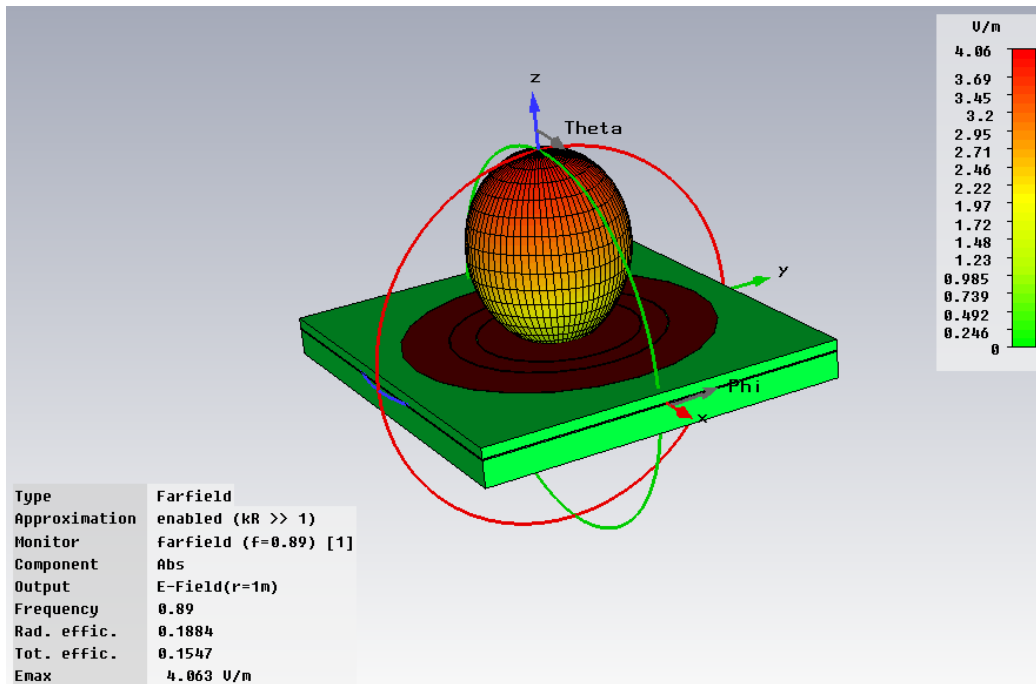
(a)
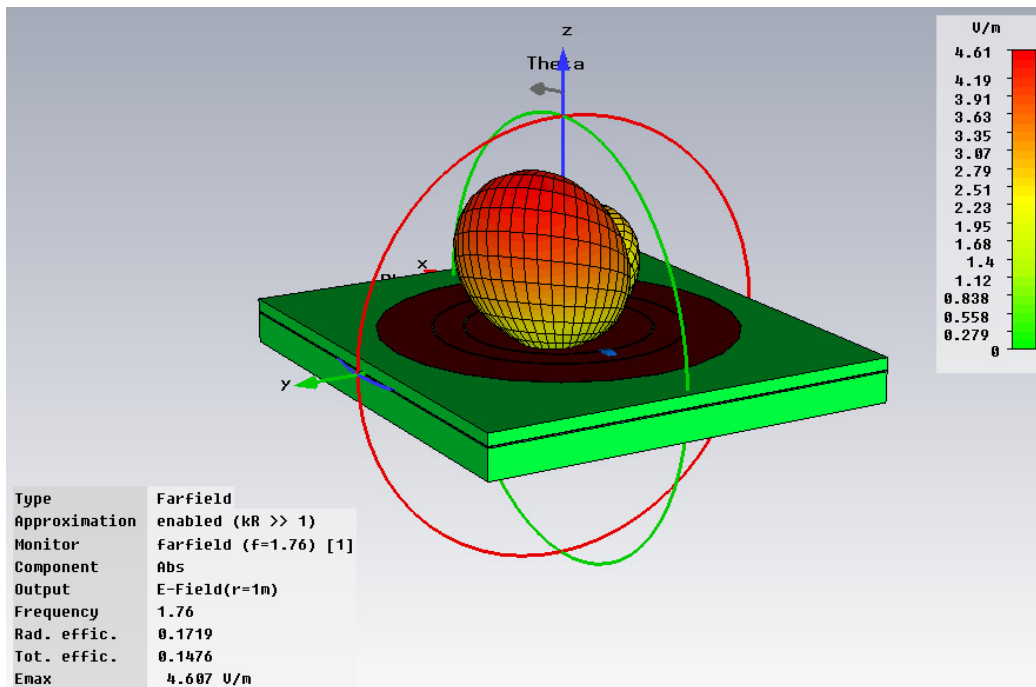
(b)

Figure 5.5: Simulated radiation pattern of the textile antenna by using Quartzel material at **(a)** 0.89GHz, **(b)** 1.76GHz and **(c)** 2.4GHz

Type	Farfield
Approximation	enabled (kR >> 1)
Monitor	farfield (f=2.4) [1]
Component	Abs
Output	E-Field(r=1m)
Frequency	2.4
Rad. effic.	0.1041
Tot. effic.	0.09544
Emax	3.781 V/m
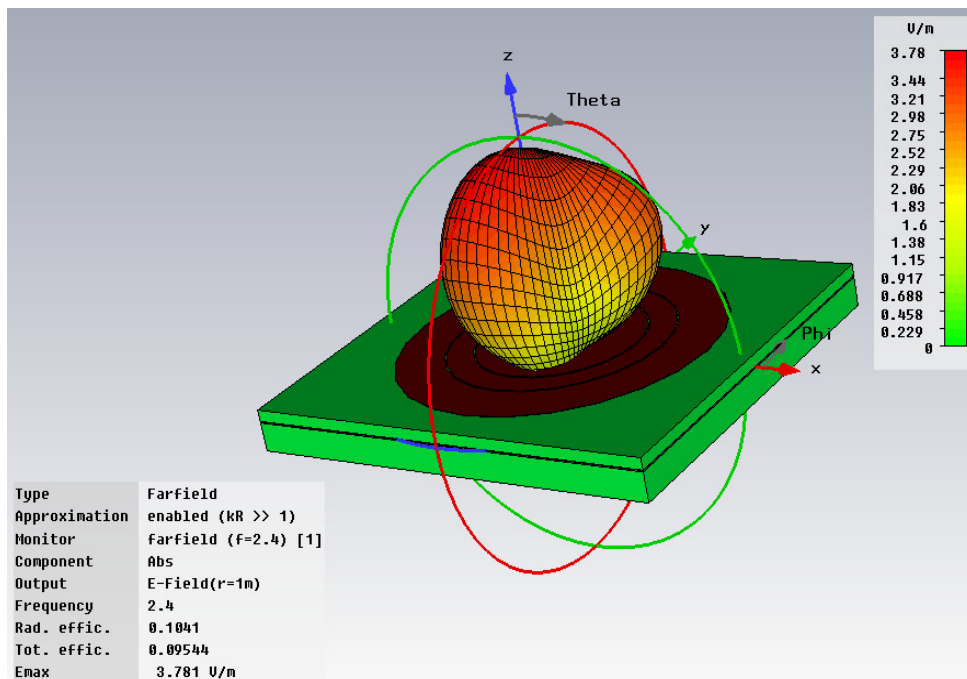
(c)

Figure 5.5: (continued) Simulated radiation pattern of the textile antenna by using Quartzel material at **(a)** 0.89GHz, **(b)** 1.76GHz and **(c)** 2.4GHz

In figure 5.6, it can be seen that the simulated axial ratio is lower than 6 for GSM 1800 and W-LAN bands, which means that the antenna is circularly polarized. As far as GSM 900 is concerned, the antenna is nearly circularly polarized. Again, due to the changes in dimension of the feed line, consequently, axial ratio performance differs from previous one (Figure 5.3). Better axial ratio is observed at W-LAN band while reduction is seen at GSM 900 band.

Figure 5.6: Simulated axial ratio of the textile antenna by using Quartzel material

5.3 Effects of Bending in vicinity of the Human Body

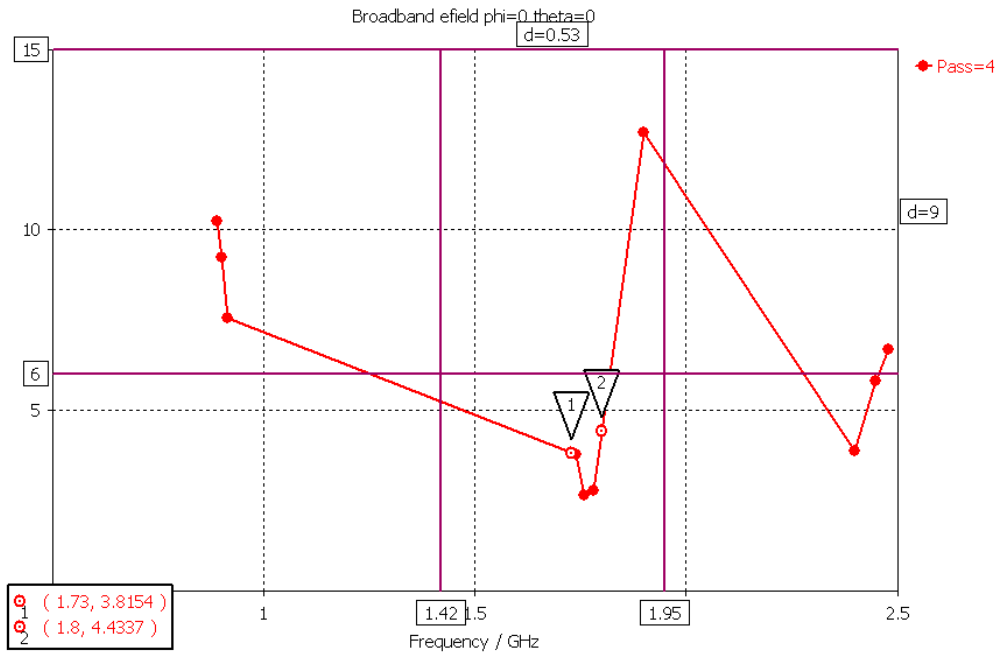Because of the intended application, we additionally studied the effect of bending in the vicinity of the human body on the antenna characteristics, namely; return loss, radiation pattern and axial ratio. The test setup, shown in Figure 5.7, includes cylinder with diameter of 150mm. This dimension is typical for the human chest. Antenna is bent around the cylinder. In order to see the effect of the human body, therefore, an extra layer with $\varepsilon_r = 53.3$ and $\sigma = 1.52$ S/m [14] is added, simulating the bended antenna around cylinder in the frequency range of 0 GHz-3.5 GHz. Furthermore, an additional shielding ground plane, which is made out of Ni/Cu/Co conductive fabric, is added at the lower part of the antenna in order to minimize back radiation to human body. The following results are conducted with the employment of E-Glass material as a feed line substrate, Fleece fabric as an antenna substrate and Ni/Cu/Co fabric for conductive parts. Cylinder is cut through x-y plane in order to reduce the simulation time. Therefore, the number of meshing size for simulation is reduced from 70 million to 7 million, thus, simulation time took almost 2 days otherwise it could take even 1 month.

68
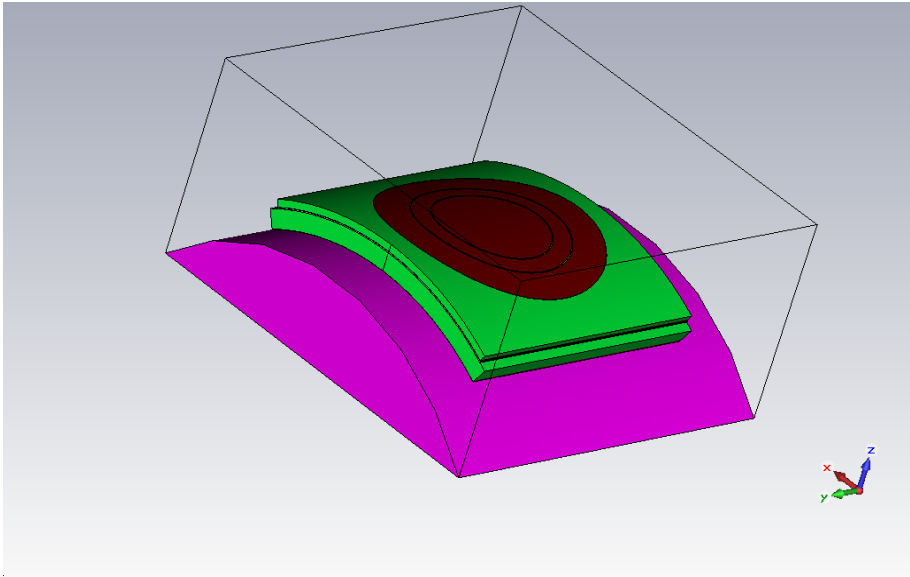
Figure 5.7: Bending antenna with radius of 150mm

Bending the antenna with 150mm diameter in vicinity of the human body, only marginally affects the return loss, as shown in Figure 5.8. The resonance frequencies show high immunity against bending. However, the center frequencies are shifted towards lower frequencies since the antenna is bent along dimension, which is enlarged by bending, determining the resonance frequency. Moreover, since the bending radius is quite large compared to other possible antenna locations on human body, for instance; arm or leg (typically 37.5mm 100mm and, respectively); deformation of the return loss is less. Bending of the antenna, compare to the flat antenna, worsens return loss performance at GSM 1800 and W-LAN bands while lower than –9.6dB is observed for GSM 900 band. By optimizing dimensions of the bended antenna, the resonance frequencies could shift towards frequency bands of interest in the future work.
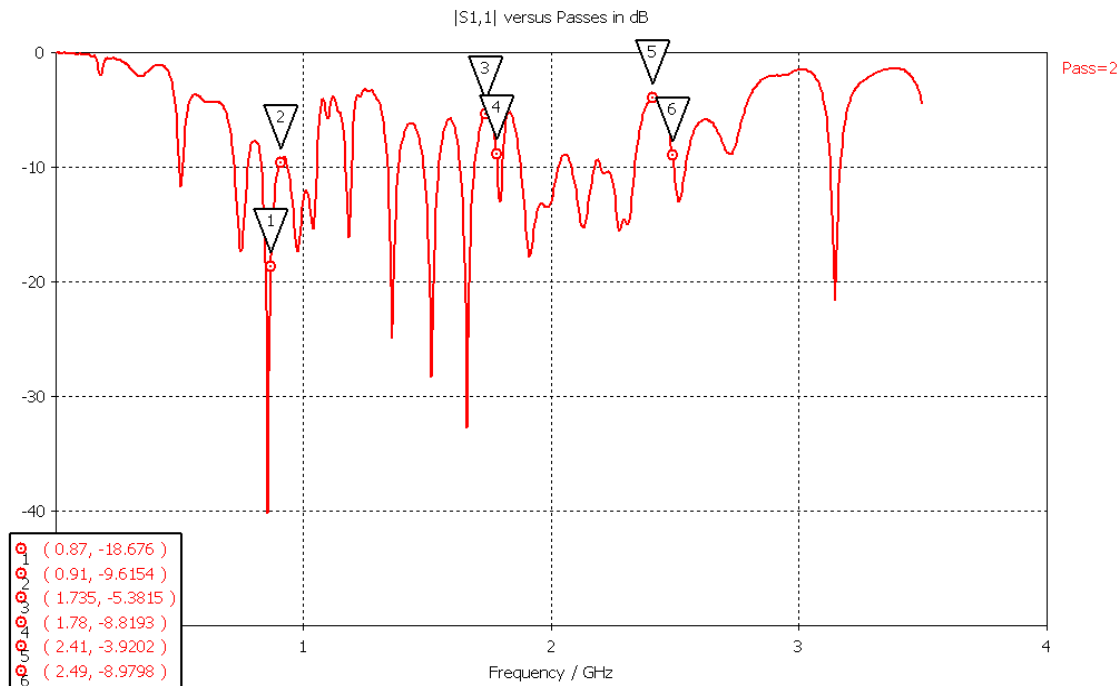
Figure 5.8: Simulated return loss of bending antenna in the vicinity human body

Bending the antenna minimally decreases the radiation pattern of the antenna, as shown in Figure 5.9 (a)-(b)-(c). Although return loss is much worse, bended antenna shows much more maximum radiation pattern compared to flat wearable one (Figure 5.2) at GSM 1800 and W-LAN bands. This result is, however, not surprising since as seen in Figure 5.9 (b)-(c), the radiation patterns are much narrower, that means an increasing in the maximum value of electric field, at these frequencies. Moreover, with reference to radiation pattern figure, it can be seen that back radiation to the human body is successfully blocked by using Ni/Cu/Co conductive fabric for shielding. In addition, it can be obviously seen in same figure, the bended antenna patterns are less directional as compared to its patterns in flat shape.
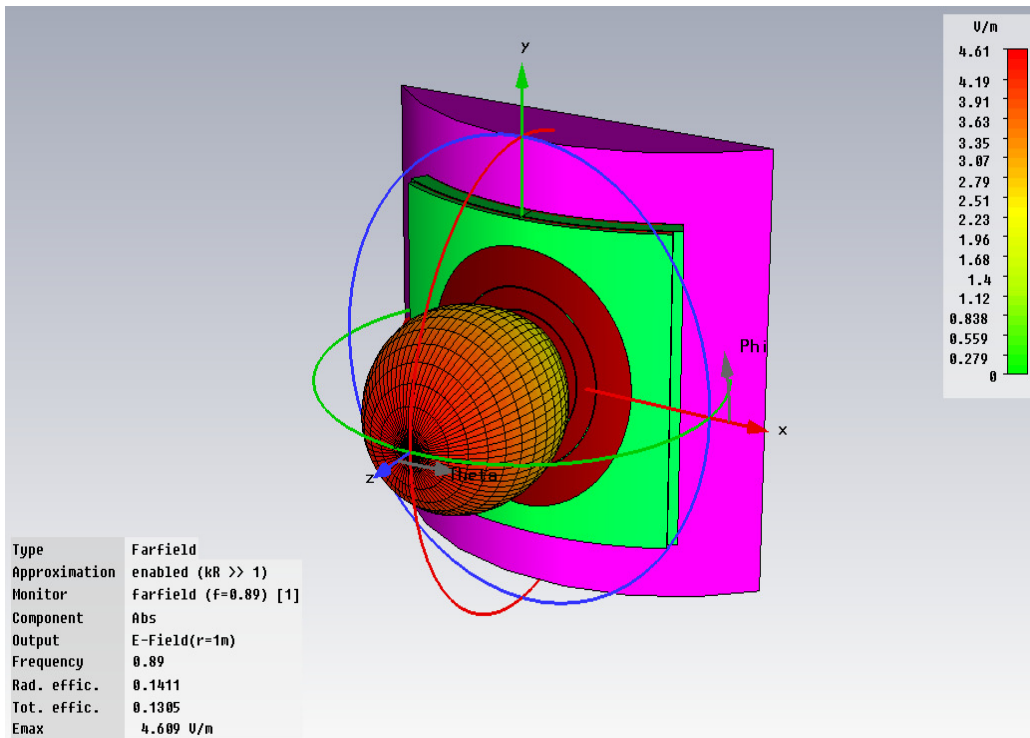
(a)
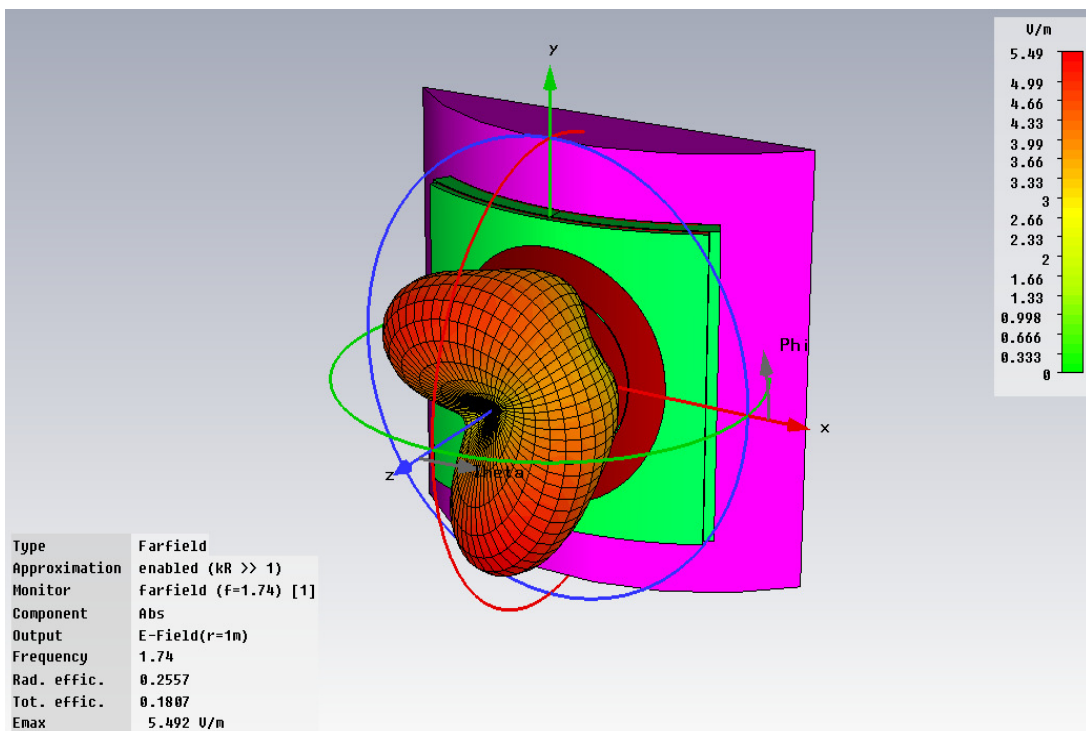
(b)

Figure 5.9: Simulated radiation patterns of bending at **(a)** 0.89 GHz, **(b)** 1.74 GHz and **(c)** 2.45 GHz

Type	Farfield
Approximation	enabled (kR >> 1)
Monitor	farfield (f=2.45) [1]
Component	Abs
Output	E-Field(r=1m)
Frequency	2.45
Rad. effic.	0.1173
Tot. effic.	0.07613
Emax	4.780 V/m
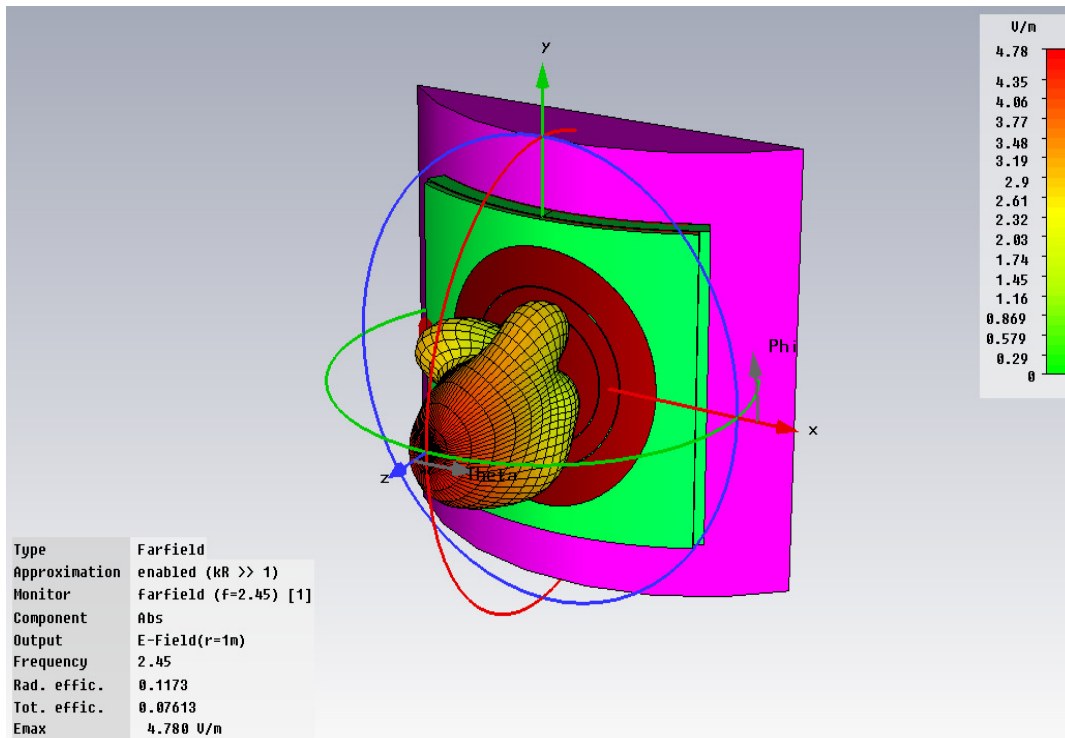
(c)

Figure 5.9: (continued) Simulated radiation patterns of bending at **(a)** 0.89 GHz, **(b)** 1.74 GHz and **(c)** 2.45 GHz

As it can be seen in Figure 5.10, the antenna bending does not destroy the antenna's circular polarization characteristic in this research. The bending antenna provides effective axial ratio in the frequency range of 0.8 GHz to 2.5 GHz. Any degradation of circular polarization performance is not observed, however, better axial ratio value for W-LAN band while worse for GSM 1800 band are obtained, compared to the flat wearable one (please see Figure 5.3).
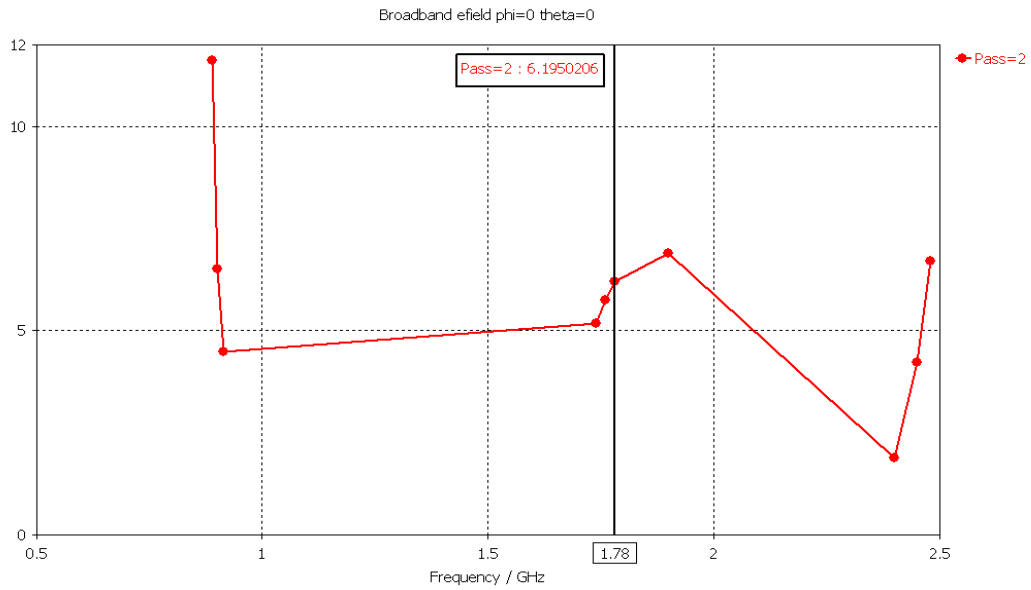
Figure 5.10: Simulated axial ratio of bending antenna in the vicinity human body

5.4 Bending Antenna in the Absence of Human Tissue

The following antenna simulations are run for bended antenna with conventional materials in the absence of human body. In order to see how the antenna is affected by human body, which is mentioned above, compared to absence of extra layer that represents human tissue, some antenna characteristics are presented. The bended antenna that is seen in Figure 5.11 is designed with completely conventional antenna materials and bended 150mm around cylinder. Then cylinder is extracted after construction.
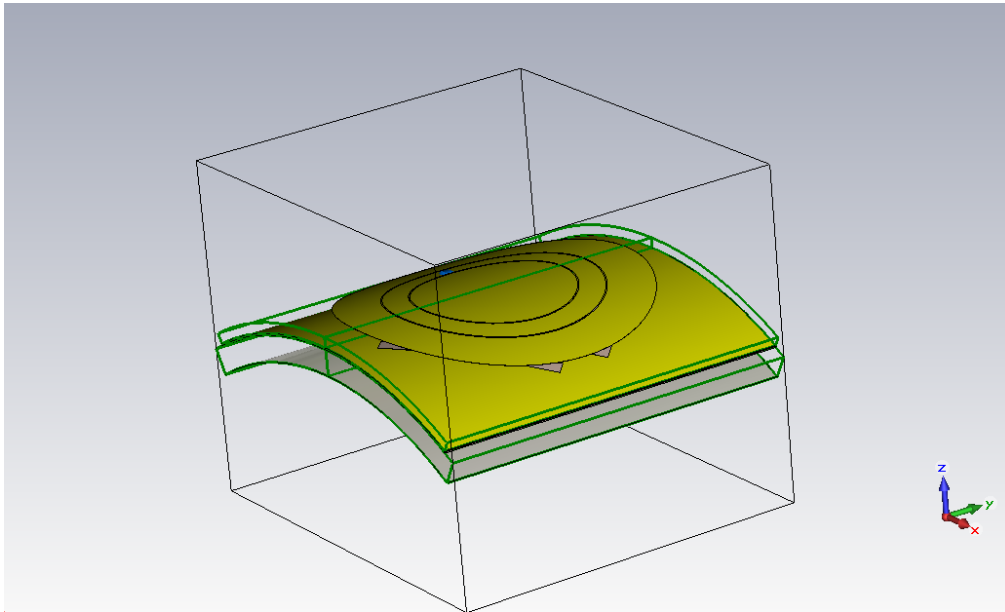
Figure 5.11: Bended antenna with conventional materials

As it can be seen in Figure 5.12, although one of the antennas is constructed with conventional materials while the other is made out of wearable fabrics (Figure 5.7), the return loss characteristics show similarities. For both antennas return loss performances are better at GSM 900 band and GSM 1800 band while it is weak at W-LAN band.

S-Parameter Magnitude in dB

S2,2

1 (0.87, -9.1201)
2 (0.92, -9.4987)
3 (1.73, -9.0461)
4 (1.78, -7.6657)
5 (2.41, -7.4728)
6 (2.49, -4)
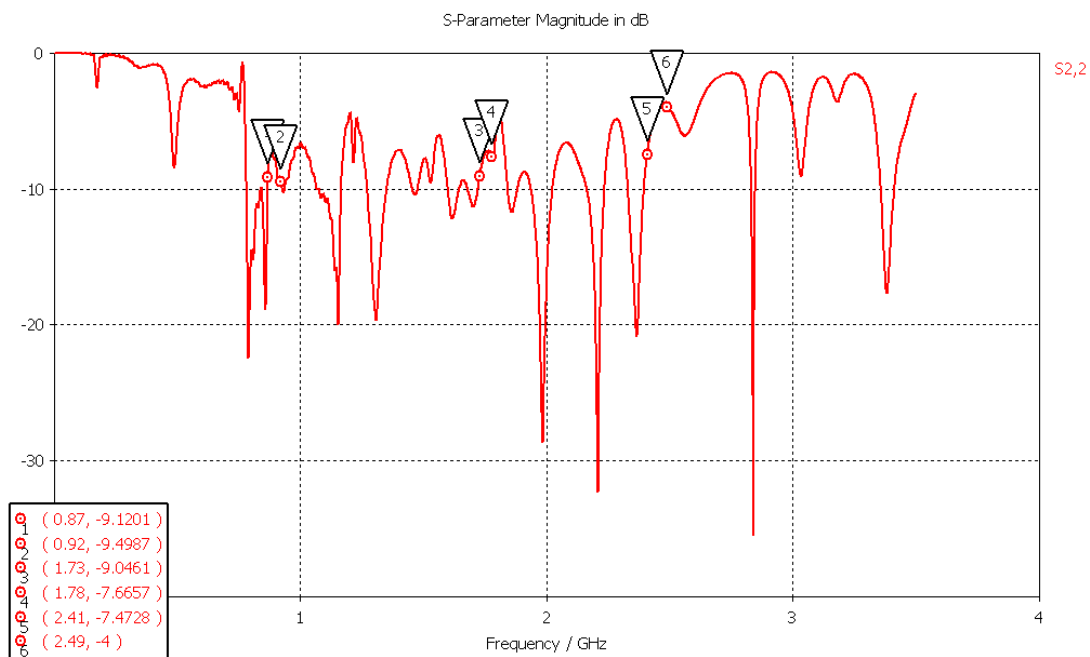
5.12: Simulated return loss of bending antenna in the absence of human body

As far as radiation pattern is considered, results show diverseness at upper GSM and W-LAN bands. As it can be seen in Figure 5.13, the maximum electric field is much stronger for the previous construction at GSM 1800 band, please see Figure 5.9 (b), while pattern is very effective for last construction at W-LAN band. These differences could appear either due to existence of human body or usage of different materials for antenna construction.
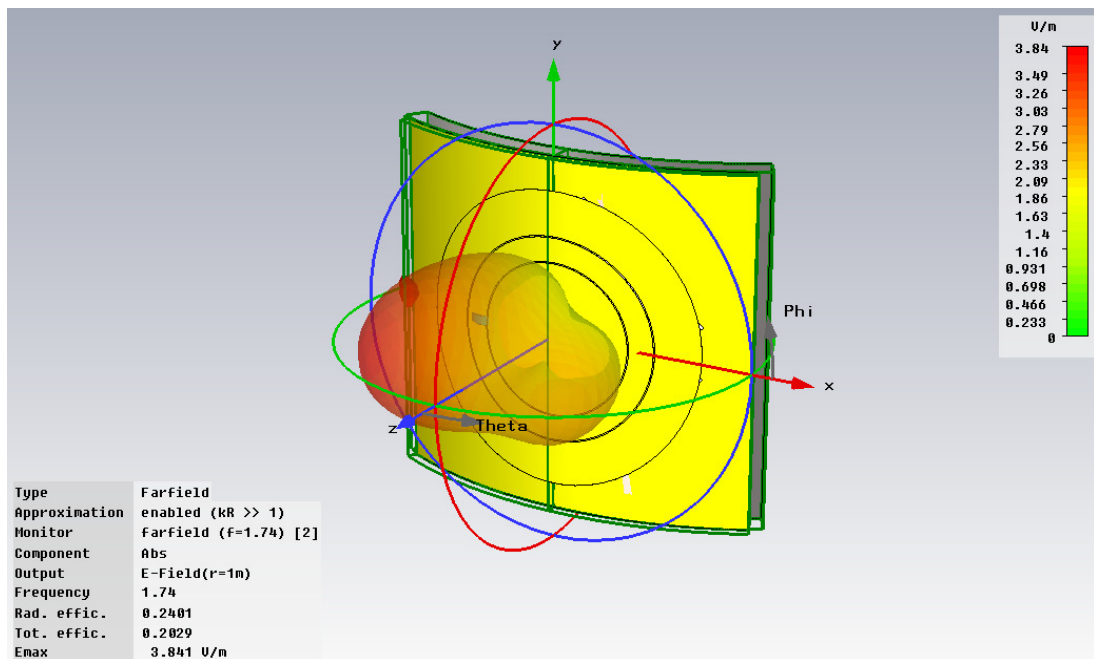
(a)

Figure 5.13: Simulated radiation patterns of bending antenna in the absence of human body at **(a)** 1.74 GHz and **(b)** 2.45 GHz

Type	Farfield
Approximation	enabled (kR >> 1)
Monitor	farfield (f=2.45) [2]
Component	Abs
Output	E-Field(r=1m)
Frequency	2.45
Rad. effic.	0.2123
Tot. effic.	0.1348
Emax	5.747 V/m
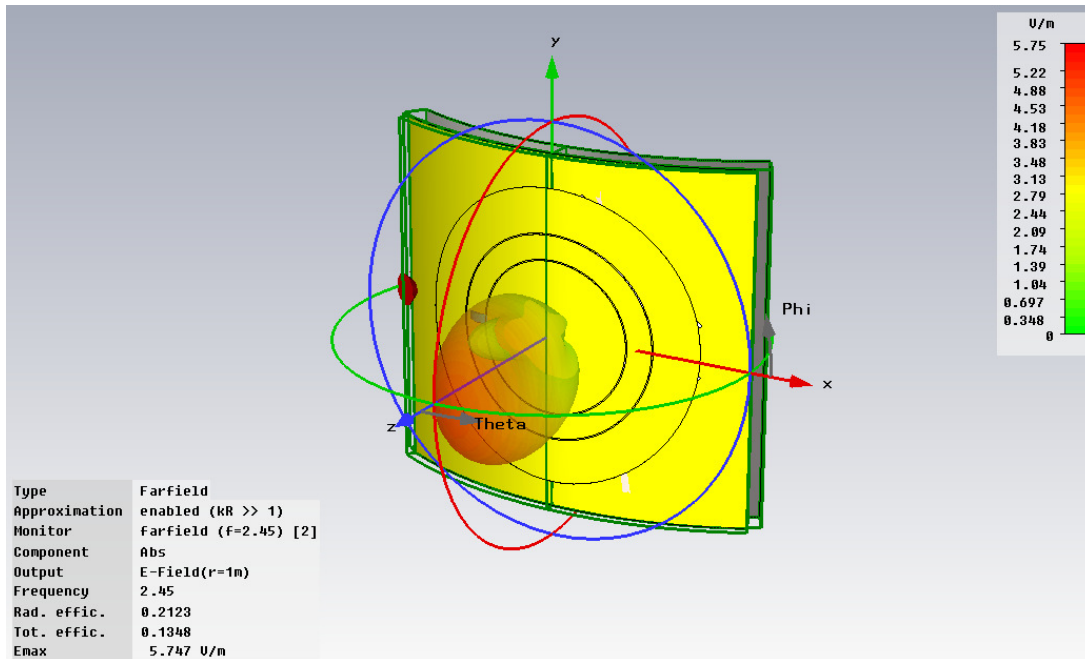
(b)

Figure 5.13: (continued) Simulated radiation patterns of bending antenna in the absence of human body at **(a)** 1.74 GHz and **(b)** 2.45 GHz

6. CONCLUSION

In order to harvest energy from the environment, an efficient antenna along with a circuit capable of converting AC power to DC power is needed. In this thesis, the circularly polarized multi-resonant antenna, which covers the frequency bands of GSM 900, GSM 1800 and W-LAN bands, and the rectifier circuit, that comprises Schottky diodes and capacitors, were employed [32]. Moreover, the antenna redesigned with wearable materials, which are entirely made out of textile materials such as conductive and nonconductive fabrics, in order to integrate the antenna into cloth, thus, making it mobile.

According to the simulation results of the first antenna, the antenna can properly operate and has good radiation patterns for the three purposed frequency bands. Moreover, it can provide circular polarization in the range of 0.8GHz – 2.5GHz. The thickness of the antenna is approximately 1.5cm; therefore it is easy to realize by using wearable applications. The materials used for simulation of the first antenna are Taconic as a feed line substrate, Copper for conductive parts and Polyhuretanic Foam as an antenna substrate.

A passively powered RF-DC conversion circuit operating at intended bandwidths is presented. The rectifier circuit is designed and can work for the signals which are higher than 200μW. It allows antenna to operate at very low input power levels. According to the simulation results, the rectifier has a maximum efficiency of 62%. For the power input between 0.8 mW and 1.8 mW, more than 50% conversion efficiency is obtained. On the other hand, when received power exceeds 2mW, the conversion efficiency decreases gradually with increasing input power.

At the last stage of the thesis, the antenna is redesigned by using wearable materials. For the conductive parts, Ni/Cu/Co coated nylon ripstop fabric is used instead of Copper. Since the antenna is composed of two non-conductive parts, namely; antenna substrate

and feed line substrate, Fleece fabric is used as an antenna substrate instead of Polyhuretanic Foam and for feed line substrate, two materials are used in turn; E-Glass and Quartzel instead of Taconic. In other words, two different materials are examined to have the best results. Moreover, the antenna is bended regarding to human chest profile and simulations are conducted in the vicinity of human body. For the intended application, which proposes a wearable design, the antenna provides sufficient antenna characteristics, namely; axial ratio, radiation pattern and return loss. It is also observed that E-Glass fabric gives better performance compared to Quartzel. This result is expected since the dielectric constant of E-Glass is closer to Taconic.

REFERENCES

[1] **Mateu, L. and Moll, F.,** "Review of Energy Harvesting Techniques and Applications for Microelectronics," Barcelona, Spain. Retrieved February 20, 2009, from http://pmos.upc.es/blues/publications/RevEnerHarvMicro.pdf

[2] "What is Energy Harvesting?" *Energy Harvesting Electronic Solutions for Wireless Sensor Networks&Control Systems.* Retrieved February 20, 2009, from http://www.energyharvesting.net/

[3] "Paybacks from energy harvesting" January 14, 2009. *Energy Harvesting and Storage.* Retrieved February 20, 2009, from http://www.idtechex.com/research/articles/paybacks_from_energy_harvesting_00001201.asp

[4] **Farmer, J. R.,** 2007. "A comparison of power harvesting techniques and related energy storage issues," Blacksburg, Virginia. Retrieved February 20, 2009, from http://scholar.lib.vt.edu/theses/available/etd-05212007-200815/unrestricted/Farmer_Thesis_05_15_2007_v2.pdf

[5] **Torres, E. O. and Rincon-Mora G. B.,** 2005**. "**Harvesting Ambient Energy will make embedded devices autonomous," Atlanta. Retrieved February 20, from http://www.embedded.com/showArticle.jhtml?articleID=170102227

[6] **Raju, M.,** 2008. "ULP meets energy harvesting: A game-changing combination for design engineers," *Energy Harvesting, Texas Instrument.* Retrieved February 20, 2009, from http://www.ti.com/corp/docs/landing/cc430/graphics/slyy018_20081031.pdf

[7] **Harrist, D. W.**, 2004. "Wireless Battery Charging System Using Radio Frequency Energy Harvesting," BS, University of Pittsburgh. Retrieved February 20, 2009, from http://etd.library.pitt.edu/ETD/available/etd-07212004-192328/unrestricted/Harrist_Thesis_072804.pdf

[8] **Hagerty, J. A., Helmbrecht, F. B., McChaplin W. H., Zane, R. and Popovic, Z. B.,** 2004. "Recycling Ambient Microwave Energy With Broad-Band Rectenna Arrays," *IEEE Trans. Microwave Theory Tech., vol. 52, no. 3, pp. 1014-1024.*

[9] **"**Wireless Local Area Networks (WLAN)" March 2006, page 2. Retrieved February 20, 2009, from http://foi.becta.org.uk/content_files/corporate/resources/technology_and_education_research/w_lans.pdf

[10] **Fiorini, P., Doms, I., Van Hoof, C. and Vullers, R.,** "Micropower Energy Scavenging," Leuven, Belgium, *Solid-State Circuits Conference, 2008. ESSCIRC 2008. 34th European 15-19 September 2008, pp: 4 – 9.*

[11] "NEC Unveils Wideband Wearable Antennas", October 2007. Retrieved March 13, 2009, from http://wirelesswatch.jp/2007/10/18/nec-unveils-wideband-wearable-antenna/

[12] **Locher, I., Klemm, M., Kirstein, T. and Tröster, G.,** 2006. "Design and Characterization of Purely Textile Patch Antennas," *IEEE Trans. Adv. Packaging, vol. 29, no. 4, pp. 777-778.*

[13] **Ouyang, Y. and Chappell, W. J.,** 2008. "High Frequency Properties of Electro-Textiles for Wearable Antenna Applications," *IEEE Trans. Antennas and Propagation, vol. 56, no. 2, pp. 381-389.*

[14] **Hertleer, C., F., Tronquo, A., Rogier, H., Vallozzi, L. and Van Langenhove, L.,** 2007. "Aperture-Coupled Patch Antenna for Integration Into Wearable Textile Systems," *IEEE Ant. Wireless Propagation Letters, vol. 6, pp. 392-395.*

[15] **Le, T., Mayaram, K. and Fiez, T.,** 2008. "Efficient Far-Field Radio Frequency Energy Harvesting for Passively Powered Sensor Networks," *IEEE Journal of Solid-State Circuits, vol. 43, no. 5, pp. 1287-1302.*

[16] **Kumar, G. and Ray, K. P.,** 2003. "Characteristics of MSAs," *Broadband Microstrip Antennas, pp. 3-4.*

[17] **Guo, Y.-X., Khoo, K.-W. and Ong, L. C.,** 2008. "Wideband Circularly Polarized Patch Antenna Using Broadband Baluns," *IEEE Trans. Ant. Propagation, vol. 56, no. 2, pp. 319-326.*

[18] **Hertleer, C., A., Rogier, H. and Van Langenhove, L.,** "Design of Textile Antennas for Smart Clothing," *7e FirW Doctoraatssymposium, 29 November 2006, Ghent University, Belgium.*

[19] **Hagerty, J. A. and Popovic, Z.,** 2001. "An Experimental and Theoretical Characterization of aA Broadband Arbitrarily-Polarized Rectenna Array," Universty of Colorado, USA, *Microwave Symposium Digest, 2001 IEEE MTT-S International, vol: 3, pp: 1855-1858, date: 2001.*

[20] **Wong, K. L.,** 2002. "Compact Circularly Polarized Microstrip Antennas," *Compact and Broadband Microstrip Antennas, pp. 162-220.*

[21] **Balanis, C.A.,** 1997. Antenna Theory Analysis and Design, John Wiley and Sons, Arizona State University.

[22] **Hagerty, J. A., Lopez, N. D., Popovic, B. and Popovic, Z.,** "Broadband Rectenna Arrays for Randomly Polarized Incident Wave," Universty of Colorado, USA. Retrieved March 15, 2009, from http://nemes.colorado.edu/microwave/papers/2000/EuMC_JHnlBP_00.pdf

[23] **Pozar, D.M.,** 1996. "A Review of Aperture Coupled Microstrip Antennas: History, Operation, Development, and Applications," Amherst, Massachusetts. Retrieved March 15, 2009, from http://www.ecs.umass.edu/ece/pozar/aperture.pdf

[24] **Schubert, T., Hart, H., Lanham, K. and Sass, M.,** 2008. "An Integrated Solution for Wireless Devices," *Electromagnetic Energy Harvesting,* University of San Diego. Retrieved March 15, 2009, from http://www.sandiego.edu/engineering/students/seniorProjects/fall_2008/RF%20Harvesting.pdf

[25] **Ungan, T. and Reindl, L. M.,** "Harvesting Low Ambient RF-Sources for Autonomous Measurement Systems," *IEEE International Instrumentation and Measurement Technology Conference Victoria, Vancouver Island, Canada, May 12 - 15, 2008.*

[26] **Walter, K., Werner, B.,** "Introduction to Schottky Rectifiers," *MicroNotes.* Retrieved March 20, 2009, from http://www.microsemi.com/micnotes/401.pdf

[27] Silicon Carbide Schottky Diodes - NEW 3G now available!. Retrieved March 20, 2009, from http://www.infineon.com/cms/en/product/channel.html?channel=ff80808112ab681d0112ab6a50b304a0

[28] **Barnett, R., Lazar, S. and Liu, J.,** "Design of Multistage Rectifiers with Low-Cost Impedance Matching for Passive RFID Tags," University of Texas, USA, *Radio Frequency Integrated Circuits (RFIC) Symposium, 2006 IEEE 11-13 June 2006, pp: 1- 4.*

[29] **De Vita, G. and Iannaccone, G.,** 2004. "Design Criteria fort he RF Section of UHF and Microwave Passive RFID Transponders," *Microwave Theory and Techniques, IEEE Transactions on, vol: 53, no: 9. (2005), pp: 2978-2990.*

[30] **Salonen, P. and Rahmat-Samii, Y.,** 2007. "Textile Antennas: Effects of Antenna Bending on Input Matching and Impedance Bandwidth," *Aerospace and Electronic Systems Magazine, IEEE, vol: 22, Issue 3, March 2007, pp: 10–14.*

[31] **Silver, J.P.,** "Micro-strip Patch Antenna Primer," *RF, RFIC and Microwave Theory, Design.* Retrieved March 20, 2009, from http://www.odyseus.nildram.co.uk/Systems_And_Devices_Files/Patch_Antenna.pdf

[32] **Rizzoli, V., Bichicchi, G., Costanzo, A., Donzelli, F., Masotti, D.,** 2009. "CAD of multi-resonator antenna for micro-power generation" DEIS University of Bologna, accepted for publication to *39th European Microwave Conference, September 2009, Rome, Italy.*

[33] **Yi, J., Ki, W. H., and Tsui, C. Y.,** 2007. "Analysis and Design Strategy of UHF Micro-Power CMOS Rectifiers for Micro-Sensor and RFID Applications," *IEEE Trans. on Circuits and Systems, vol. 54, no. 1, pp. 153-166.*

[34] EMF Shielding & Conductive Fabrics. Retrieved April 3, 2009, from http://www.lessemf.com/fabric.html

[35] **Tronquo, A., Rogier1, H., Hertleer, C., and Van Langenhove, L.,** "Applying Textile Materials for the Design of Antennas for Wireless Body Area Networks," Gent, Belgium, *Antennas and Propagation, 2006. EuCAP 2006. First European Conference on, 6-10 November 2006, pp: 1-5.*

[36] EMF Shielding and Conductive Fabric Selection Guide. Retrieved April 3, 2009, from http://www.lessemf.com/fabric_guide.html

[37] Filter Cloth Exporter: Tiantai Industrial Cloth Co.,Ltd Retrieved April 3, 2009, from http://www.filterclothes.com/cp/class/0.html

[38] "Fused Quartz Textiles Brochure and Technical Data" Retrieved April 3, 2009, from http://www.quartz.saint-gobain.com/Media/Documents/S000000000000001011/Quartzel%20Brochure%20&%20Technical%20Data.pdf

[39] "Material Science", *Making Films Function Around the Globe and Beyond.* Retrieved April 3, 2009, from http://www.dunmore.de/material-science.html

[40] **Grzyb, J., Ruiz, I., and Tröster, G.,** "An investigation of the material and process parameters for thin-film MCM-D and MCM-L Technologies up to 100 GHz," in *Proc. 53rd Electron. Compon. Technol. Conf. (ECTC2003), New Orleans, LA, May 2003, pp. 478–486.*

CURRICULUM VITA

Cem Özlem was born in 1983 in Kırdjali, Bulgaria. He finished his primary and secondary school educations in Ankara. He graduated from Ankara Kocatepe Mimar Kemal High School achieving the highest grade of the first rank. He received his bachelor degree in Electronics Engineering from Istanbul Technical University in 2007. Afterwards, he started his M.Sc. in Telecommunication Engineering in ITU in September 2007. In September 2008, he started his masters thesis in the DEIS University of Bologna, as an exchange student.
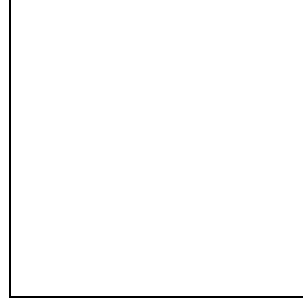
Candidate's full name: **Cem Özlem**

Place and date of birth: **Kırdjali/Bulgaria 01.09.1983**

Permanent Address: **Via Ernesto Masi, 41. Bologna-Italy**

Universities and
Colleges attended: **Istanbul Technical University, University of Bologna**